UNIVERSITY OF CALIFORNIA
SANTA CRUZ

OPENCARM: OPEN SOURCE CAMERA ARRAY MICROSCOPY FOR BIOLOGY

A dissertation submitted in partial satisfaction of the
requirements for the degree of

DOCTOR OF PHILOSOPHY

in

COMPUTER ENGINEERING

by

Pierre V. Baudin

March 2023

The Dissertation of Pierre V. Baudin
is approved:

Dr. Mircea Teodorescu, Chair

Dr. Colleen Josephson

Dr. David Haussler

Peter Biehl
Vice Provost and Dean of Graduate Studies

Table of Contents

List of Figures

OpenCArM: open source camera array microscopy for Biology

Pierre Baudin

Abstract

The need for experimental replicates means biology research labs are often growing many cell cultures in parallel. Monitoring the health of these cultures as they grow is important for avoiding costly interruptions in the research pipeline. Common approaches involve removing culture plates from incubator environments to view them under a microscope. This manipulation can stress cells and end up being disruptive to healthy growth environments. To facilitate non-disruptive automated cell culture monitoring, an open source framework for the design and deployment of parallel multi-channel microscopes was developed.

Open Camera Array Microscopy (or openCArM) supports the design of multi-well parallel imaging systems composed of independent autonomous camera units. The framework defines module types that can be assembled together and configured for a given use case. One such configuration (the "Picroscope") performs in-incubator, longitudinal imaging studies on 24 well cell culture plates. "Picroscope" devices have been used in experiments with samples ranging from *Xenopus Tropicalis* frog embryos to human cortex brain organoids.

openCArM systems have a modular design that allows them to be built around other cell biology automation devices. Experiments have been run using the "Picroscope" combined with the "Autoculture" system, an automated cell culture feeding platform. To support these devices, a connected lab equipment management system was developed to provide experiment tracking, data analysis and equipment control.

openCArM devices can be made out of low cost 3D printed materials and off-the-shelf imaging hardware, representing a significant step forward for the

accessibility of cell culture automation systems.

Chapter 1

Introduction

1.1 Motivation

Replicability is a fundamental principle of science. An experimental result that can't be replicated is not a valid scientific finding. Authors of academic papers are expected to provide all of the information needed to replicate the results they report. Even so, there is a real replicability problem facing the scientific community [Baker, 2016a, Sayre and Riegelman, 2018, Baker, 2016b]. While this problem exists in all fields of science, we are focusing here on the field of Biology. A 2016 survey of researchers working in the biological sciences found that over 70% reported trying and failing to replicate results found in the literature. Equally concerning, over 60% of respondents reported trying and failing to replicate their own results [Baker, 2016a]. This so called "crisis of reproducibility" is a serious issue. New scientific knowledge always builds on existing knowledge, if the scientific literature is full of invalid results, then it building anything on top of it is impossible.

Despite these concerning numbers, these replicability issues are unlikely to be the results of widespread scientific fraud. Biological experiments are complex and despite the availability of detailed protocols, differences between lab facilities and

their teams introduce many vectors of uncontrolled variation. For example, in cell culture experiments, differences in how often temperature and gas regulated incubators are opened or how much time a sample spends out of the incubator for routine manipulation can cause varying amounts of stress on the culture. This can affect the metabolism of the cells and cause unpredictable effects on the experimental results.

Reducing this uncontrolled variation is a key to improving the replicability of biological experiments. One proposed way to do this is to increase the amount of automation in the experimental process [Miles and Lee, 2018]. Any automation that reduces the amount of human intervention in the experimental process is likely to reduce the amount of uncontrolled variation.

Modern biological experimentation requires cultured cells. To gather strong data, experiments often need many replicates. For this reason, labs are often growing hundreds of cell cultures at a time. Monitoring the health of cell cultures is most commonly a manual process involving technicians removing cell plates from incubator environments to image them with conventional microscopes. This manipulation can stress cells and end up being disruptive to healthy growth environments.

Automating the capture of visual data from cell cultures means more data can be gathered without the need for human intervention. This reduces the amount of uncontrolled variation in the experimental process. While commercial solutions exist for longitudinal live cell monitoring (explored later in section 2.2), they are expensive and inflexible.

However, the past several years have seen a massive increase in the availability of high quality open source camera hardware. Additonally, open source image analysis software like Fiji [Schindelin et al., 2012] and CellProfiler [Stirling et al., 2021] are

mature and widely used by scientists in the field. Factoring in the widespread availability of low cost fabrication tools like 3D printers, there is an opportunity here. **Can we build a general use framework for integrating these technologies into new customizable longitudinal microscopy systems?**

1.2 Contribution to the field

The goal of this work was to create a low cost, flexible, and open source solution for longitudinal live cell imaging. We published two papers describing a device made primarily of 3D printed components that allows simulaneous longitudinal imaging of every well in a 24 well culture plate non-instrusively inside an incubator. We call this device the "Picroscope" [Baudin et al., 2021, Ly et al., 2021]

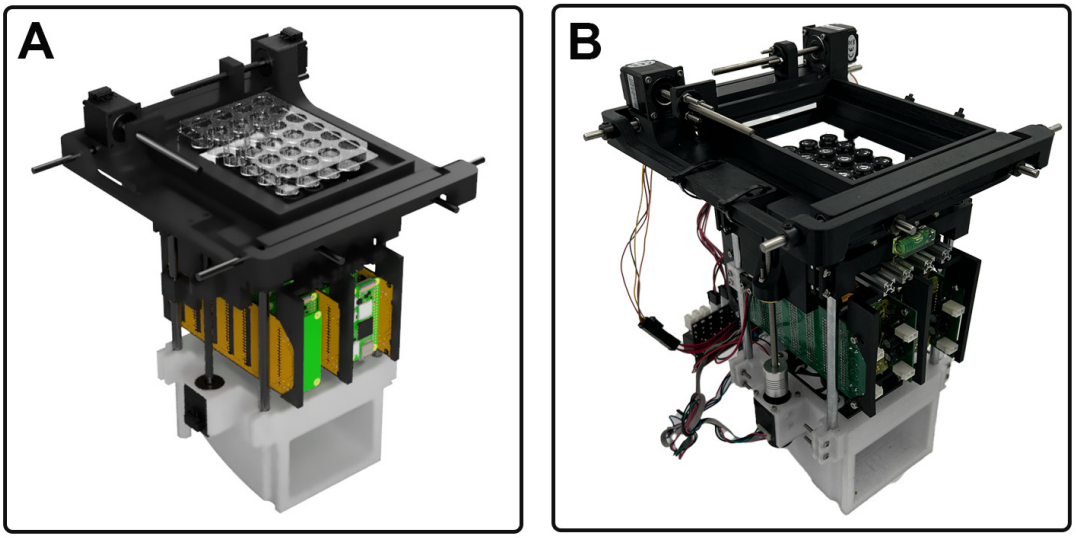

Figure 1.1: Picroscope A: 3D CAD render made in Autodesk Fusion 360, B: built version

The picroscope is an assembly of independent modules, these modules can be assembled into different configurations with different hardware depending on the goals of the designer. The conceptual architecture of this system as well as

the software needed to implement it is what we call **openCArM**, standing for open-source camera array microscopy. OpenCArM devices have been used in studies on stem cell derived cerebral organoids [Seiler et al., 2022, Ly et al., 2021] as well as in educational project-based-learning modules for students in high school and college [Baudin et al., 2022].

openCArM enables designers to create custom solutions for longitudinal live cell imaging or replicate existing open source devices like the Picroscope. The openCArM simplifies the acquisition of large amounts of biological imaging data as well as the organization and access of this data in the cloud. The remote control and monitoring offered by openCArM based systems has applications in professional lab environments as well as school classrooms. Public repositories for the systems mentioned in this document are shown in appendix A.3

Parts of this Document were previously published in the following articles: [Baudin et al., 2021, Baudin et al., 2022, Baudin and Teodorescu, 2023, Ly et al., 2021, Seiler et al., 2022, Parks et al., 2022]

Chapter 2

Background

Parts of this Chapter were previously published in the Journals Heliyon, Elsevier Internet of Things, and Communications Biology [Baudin et al., 2022, Baudin et al., 2021, Ly et al., 2021]

2.1 Remote Lab Operation

The COVID-19 pandemic changed the work landscape throughout the world. Widespread lockdowns during the height of the pandemic required many jobs to transition to a remote format. Bench scientists were unequally affected by this transition, experiencing a substantial reduction in their ability to produce work compared to computational scientists [Myers et al., 2020]. This situation is likely to have long-lasting consequences on science careers, particularly for junior investigators. This has motivated the development of new approaches for remote experimentation. These advancements will have lasting benefits long after the pandemic is over.

Techniques for remote operation of lab equipment exist on a wide spectrum of cost and complexity, from fully automated labs utilizing expensive

robotic systems [Lippi and Da Rin, 2019, Schmidt et al., 2008], to Do-it-Yourself (DIY) 3D printed microscopes with basic Internet access [Aidukas et al., 2019a, Maia Chagas et al., 2017]. The further development of low cost solutions for remote lab control will bring more options within the reach of institutions with limited means [Baden et al., 2015]. This would allow under resourced labs to reap many of the benefits of the "lab of the future"[Miles and Lee, 2018]. Many cost reductions have been made possible by innovations in the Internet of Things (IoT) space[Ornes, 2016], ranging from software frameworks to low cost network capable devices[Chaczko and Braun, 2017, Foundation and Contributors, 2022, Lima et al., 2019, Patel and Devaki, 2019].

The landscape of low cost lab automation solutions features many contributions from the "maker" community. These enthusiasts are creating designs to manufacture lab equipment with consumer accessible tools [May, 2019, Meyer, 2012, Baden et al., 2015]. Several open source microscope designs have been proposed using 3D printing and low cost computing platforms like the Raspberry Pi [Aidukas et al., 2019a, Maia Chagas et al., 2017]. The Raspberry Pi is small low cost computer that runs a fully featured linux based operating system. Starting as low as 5$, the Raspberry Pi substantially reduces the cost of computer clusters. Clusters used to be considered a major investment only used for intense computation tasks. With Raspberry Pi, it's affordable to build a dedicated cluster for almost any application. [Abrahamsson et al., 2013, Saffran et al., 2016, Cox et al., 2014].

OpenCArM systems utilize Raspberry Pi clusters to enable remote device control. Providing a robust and low-cost solution for remote interaction with the lab.

2.2 Microscopy

There are various physical ways to capture images of small things, the most common of which involves capturing light that directly interacts with the objects of interest. This broad type of microscopy is referred to simply as light based microscopy [Thorn, 2016] reviews the prominent techniques in light based microscopy for biology. These techniques are broadly divided into the categories of brightfield and fluorescence. Brightfield microscopy techniques typically involve illuminating the sample and capturing an image from the sample's effect on the light transmitting through it. Brightfield is the most simple form of microscopy and while it can be very useful for things like measuring the size and growth of a cell culture, limitations prevent it from being useful in a number of areas where more complex microscopy tools shine.

2.2.1 Fluorescence Microscopy

Fluorescence microscopy involves illuminating a sample with an excitation light that causes elements of the sample to emit light in a different frequency, the excitation light is filtered out and the image is generated just from light emitted from the sample. Fluorescence microscopy techniques allow us to highlight specific cell types in a culture and view how they grow and propagate. This can allow more information to be gleaned from an image sample than traditional bright field approaches.

Fluorescent imaging requires a fluorescent sample. Fluorescence in a sample can come from dyes added or from proteins expressed by cells in the sample. The strength of the fluorescent signal determines the sensitivity of the equipment required to image it. Fluorescent dyes typically result in a stronger signal than fluorescent proteins [Süel, 2011], allowing fluorescent imaging to be performed

with very simple equipment, as is done in [Maia Chagas et al., 2017]. Fluorescent proteins expressed by genetically modified cells are a comparatively small signal, this means that we have to work harder to effectively capture the signal. This means using camera optics capable of capturing more light, and using filters capable of more effectively removing excitation light from the signal.

2.2.2 Live Cell Longitudinal Monitoring

Advances in microscopy have allowed scientists to perform longer term observations of cellular processes and organisms' development and behaviors. Longitudinal imaging has been pivotal to uncovering cellular mechanisms behind biological processes [Specht et al., 2017]. Several options exist on the market to perform longitudinal imaging of biological materials. These range from super-resolution microscopes that allow the imaging of individual biomolecules [Godin et al., 2014, Miller et al., 2010] to conventional benchtop microscopes, which are common in academic research[Selinummi et al., 2009, Hernández Vera et al., 2016, Savas et al., 2018, Miller et al., 2010, Wincott et al., 2021], industrial [Yao et al., 2020, Zamxaka et al., 2004] and teaching laboratories[Ferreira et al., 2019].

Live cell imaging refers to techniques for recording image data of live cell cultures with minimal disturbance. Several live cell imaging techniques are explained in. [Frigault et al., 2009]. Primary concerns when doing live cell imaging include, photodamage and photobleaching, and environmental factors such as temperature and ph of media. Typically, live cell microscopy involves a compromise between image quality and interruption of the cells natural behavior.

Photodamage refers to the process wherein light damages cells or bleaches fluorophores. Of particular concern is ultraviolet and infrared light. Ultraviolet

damages DNA and focused infrared causes localized heating which in turn causes damage to amino acids. Even light used to excite fluorescence causes some level of phototoxicity. Additionally, fluorophores get "bleached" by the excitation light. For these reasons, optimal imaging systems designs should prioritize maximum clarity with minimum required light. Light detectors used should be appropriately optimized to capture the wavelengths of light associated with the fluorescent proteins you intend to image.

The analysis done in [Frigault et al., 2009] showed that longer exposure times with dimmer excitation light cause less damage than shorter exposures with more intense light. The efficiency of light collection can be optimized by selecting good filters, high numerical aperture (NA) objectives, and by selecting efficient image sensors. For bright field imaging, we should illuminate with the highest frequency that doesn't cause photodamage along with an objective with a maximized NA. This gives us the ability to resolve the smallest features possible. For fluoresence, the λ in question is the emission frequency of the fluorophore.

These equations demonstrate that numerical aperture is a very important consideration for effective live cell imaging, and that we would like to maximize this parameter as much as is feasible.

Efficient image collection through the objective is not the only light collection parameter to optimize. Selecting an efficient sensor for our task is important as well. CMOS sensors are cheap and widely available, a tradeoff being that their Quantum Efficiency (the measure of what % of light is captures) typically lands in the <60% range. CMOS sensors have been shows to be sufficient for bright field microscopy. High res charge coupled sensors, or CCDs, tend to have a considerably higher Quantum Efficiency, making them more effective for fluorescence.

2.2.3 Camera Array Microscopes

Camera array microscopes are a class of microscope that uses a grid of cameras to capture data. Some designs use computational image fusion approaches to combine multiple images of the same area to get a higher resolution result [Aidukas et al., 2019b], while others focus more on parallel capture of data from distinct areas of interest [Chan et al., 2019, Chan and Yang, 2020]. One system, the Ramona MCAM, is capable of doing both [Thomson et al., 2022]. While these systems show impressive results with both computational image fusion and parallel capture, they are custom designed form factors that would require significant modification to be used in other physical configurations. A flexible system that can accommodate a wide range of camera array sizes and configurations would be a valuable addition to the field.

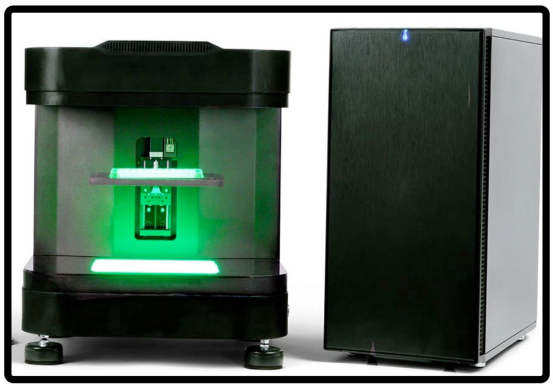

Ramona MCAM

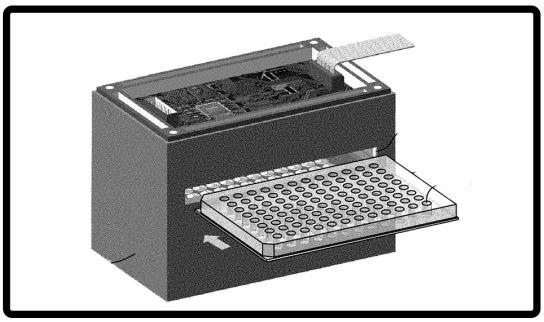

Parallel Image Aquisition System
(Patent # US10754140B2)

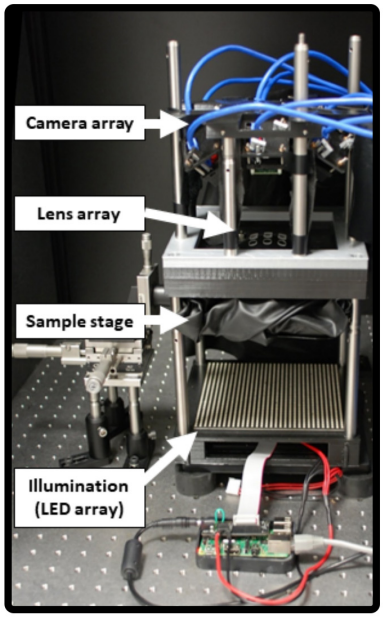

Multi-Camera FPM Microscope
(Aidukas et. al.)

Figure 2.1: Camera Array Microscopes Ramona MCAM is a commercially available camera array microscope, Also shown are the [Aidukas et al., 2019b] device and the [Chan et al., 2019] device.

OpenCArM is such a system, enabling the creation of highly configurable camera array microscopes capable of brightfield or fluoresence microscopy.

OpenCArM was developed within a neurobiology research group called the Braingeneers; tools developed with openCArM were designed to interface with systems made by other teams within the group who have been working on different areas of in-vitro neuroscience including stimulating and recording activity from cell cultures.

2.3 Neuroscience and Cell Culture

Cell culturing is a process deeply involved with many aspects of the field of neuroscience. Having access to cultured cells is crucial for many areas of research. Brain cells grown in the lab enable us to do things like model aspects of early brain development [Muguruma and Sasai, 2012] or look at the way neurons pass signals to each other [Araque et al., 2001]. Gene editing tools like CRISPR allow researchers to intentionally mutate cells in order to investigate the effects of those genes on the brain [Savell et al., 2019].

2.3.1 Electrophysiology

Electrophysiology is the study of electrical activity in biological systems. It is useful for studying neuronal networks, since individual neurons pass signals to each other primarily through electrical impulses. Electrophysiological experiment tasks consist of either recording or stimulating a biological sample. Tools for electrophysiolgy typically consist of various forms of bio-compatible electrodes. The electrodes are connected to a recording or stimulation device.

In vivo applications in humans

In vivo, implantable electrophysiology devices like the Utah Intracortical Electrode Array [Maynard et al., 1997] have been used to facillitate brain computer interaction for patients with paralysis [Hochberg et al., 2006, Hochberg et al., 2012, Simeral et al., 2011]. Implantable neurostimulation devices have also found success for the treatment of tremors in Parkinson's patients [Schuepbach et al., 2013]. Non-invasive stimulation methods have also found medical uses for the treatment of depression [Health, 2021], and research shows the potential of non invasive stimulation to enhance memory [Ezzyat et al., 2017]

In vitro applications

While these results are impressive, in vivo human experimentation with invasive electrophysiolgy devices is very difficult to do. The inherent risks involved with surgery mean that any research done with these devices must first pass through many stages of animal research and it can take years before a new idea is ready for human trials. In vitro experimentation is considerably simpler and faster, but it is not without its own challenges. 2D cell cultures differ greatly from the complex 3D brain structures they are meant to model. 3D organoids are a promising solution to this problem, and they are being used to study the electrophysiology of early brain development [Trujillo et al., 2019].

2.3.2 Optogenetics

Optogenetics is a technique that uses light to interact with cells that are genetically engineered to react to light [Fenno et al., 2011]. Similar to electrophysiology, optogenetics can be used to stimulate and record neural activity. However, optogenetics has the advantage of being non-invasive. It has been used to study the activity of neurons in organoids [Shiri et al., 2019]. While electrophysiology requires dedicated tooling, optogenetics can be done with the same tools already used for imaging cell cultures.

Section 2.2 describes the landscape of hardware that can be used to gather images from biological experiments. However, effectively gleaning insights from the data we capture is a problem that goes beyond the hardware. Managing and analysing large data sets from high scale parallel cell culture experiments requires it's own set of tools.

2.4 High Throughput Biology

A major benefit of in-vitro biological research is the relative ease with which samples can be grown or obtained compared to in vivo work. It is possible for labs to grow many samples in parallel, allowing every experimental condition to be run with numerous replicates. [Sarrafha et al., 2021]. This has been made possible by the development and proliferation of robotic systems that can automate many types of biological experiments or clinical screening procedures [Hart, 2013, Dörr et al., 2016].

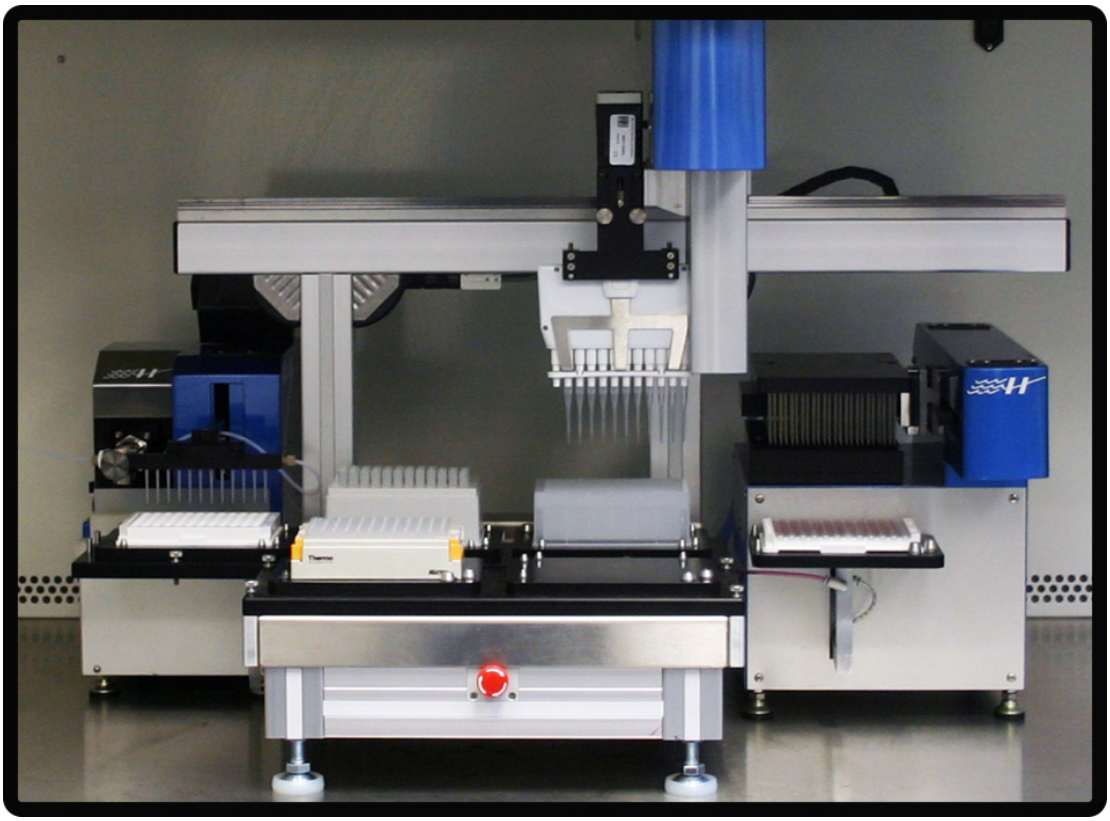

Figure 2.2: Hudson Robotics ELISA Automation Hudson Robotics makes robotic systems for high throughput analysis, this is a benchtop system they produce for automating Enzyme Linked ImmunoSorbent Assays (ELISAs) ELISA assays are used to detect the presence of a specific protein or other biomolecule in a sample and are commonly used in clinical diagnostics.

System automation of this type leads to better reliability and repeatability, which strengthens potential insights and provides new big data challenges. The wide use of automated high throughput data collection has generated many big data sets. This has motivated the development of software frameworks for analyzing these data in automated or semi-automated ways. [Ollion et al., 2013]

2.4.1 Data Analysis in the Cloud

In many research areas, data is being captured faster than researchers are able to analyze it, there has been exponential growth in the data available for analysis. [Fan et al., 2014]. Creating workflows and pipelines that allow us to efficiently process these datasets is crucial. To this end, it's desirable to leverage the vast computational resources of cloud systems. A container based framework for creating these workflows in the cloud is proposed in [Schulz et al., 2016]. Packaging software in containers allows us to run the same software on different cloud systems with no changes to the code. And using a container orchestration system like Kubernetes allows us to run many containerized "jobs" making efficient use of computational resources.

2.5 Conclusion

The following chapters will explore many facets of the openCArM platform and showcase results from various applications of topenCArM systems. we will show the hardware and software components that allow the device to function, as well as the data analysis tools developed to draw insights from captured data. Finally we will discuss the impacts of the technology and future directions for the project.

Chapter 3

openCArM Hardware Modules

Parts of this Chapter were previously published by Elsevier Internet of Things and Communications Biology [Baudin et al., 2021] [Ly et al., 2021]

In this chapter we will discuss the hardware tools that enable openCArM devices to work, as well as the custom hardware that was developed for openCArM based systems.

3.1 Background

3.1.1 Open Source Microscopes

The use of open-source technology, including 3D printers, laser cutters, and low-cost computer hardware, has democratized access to rapid prototyping tools and dramatically increased the repertoire of biomedical equipment available to laboratories around the world[Willis, 2018, Barber and Mostajo-Radji, 2020]. Through rapid prototyping and the use of open source platforms, the technology can be replicated and quickly improved[Coakley et al., 2014, Ambrose et al., 2020]. 3D printer technology has been applied to several fields in biomedicine,

including biotechnology [Gross et al., 2014], bioengineering[Baden et al., 2015, Alessandri et al., 2017], and medical applications including fabrication of tissues and organs, casts, implants, and prostheses [Ventola, 2014]. Existing 3D printed microscopes range in complexity from simple low cost systems with pre-loaded imaging modules [Beattie et al., 2020a] to portable confocal microscopes capable of imaging individual molecules[Brown et al., 2019] and even 3D printed microfluidic bioreactors[Khan et al., 2021].

The majority of low-cost 3D printed microscopes are not intended for longitudinal imaging of simultaneous biological cultures (e.g., multi-well, multi-week biological experiments). They usually have a single imaging unit[Maia Chagas et al., 2017, Kim et al., 2012, Diederich et al., 2020, Hernández Vera et al., 2016, Wang et al., 2017, Zhang et al., 2015, Zhang et al., 2013, Baden et al., 2015, Collins et al., 2020, Cybulski et al., 2014, Kim et al., 2016a, Aidukas et al., 2019a] or perform confocal imaging[Brown et al., 2019] . Other systems have taken advantage of one camera attached to a gantry system to perform imaging of multiple experimental replicates[Bohm, 2018, Merces et al., 2021, Gürkan and Gürkan, 2019]. Few 3D-printed microscopes have been developed that perform multi-well imaging with medium throughput [Merces et al., 2021, Kim et al., 2016b]. Several biological applications exist that would greatly benefit from multi-well, multi-week simultaneous imaging, as it allows for concurrent interrogation of different experimental conditions and the inclusion of biological replicates. These include cell culture applications, in which 2D and 3D culture models can be tracked over multi-week periods, as well as developmental and behavioral biology experiments in which multi-week tracking could be performed on whole organisms.

OpenFlexure

Special mention should be given to the openFlexure project [Collins et al., 2020], who developed a highly configurable 3D printed microscope around which a substantial community has formed. Along with their core microscope system they also developed and published two complementary systems for fine positioning of samples and optics, these being the Delta Stage [McDermott et al., 2022] and the Block Stage [Meng et al., 2020]. These devices are shown in figure 3.1

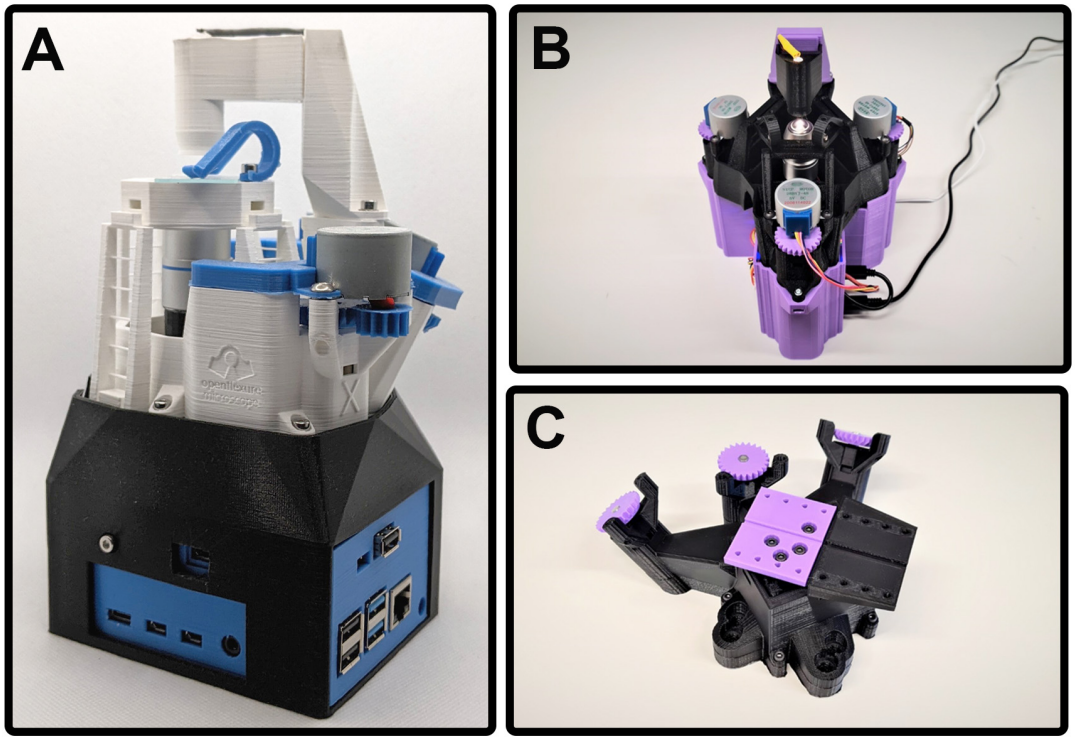

Figure 3.1: OpenFlexure Systems A: OpenFlexure Microscope, B: Delta Stage, C: Block Stage. Images taken from `openflexure.org`

In addition to making their designs and build instructions available, they have supported a community of scientists, engineers, and other DIY microscopy enthusiasts who share knowledge and ideas in their forums. Any designers of 3D printed microscope systems would benefit greatly from the knowledge shared in

these forums.

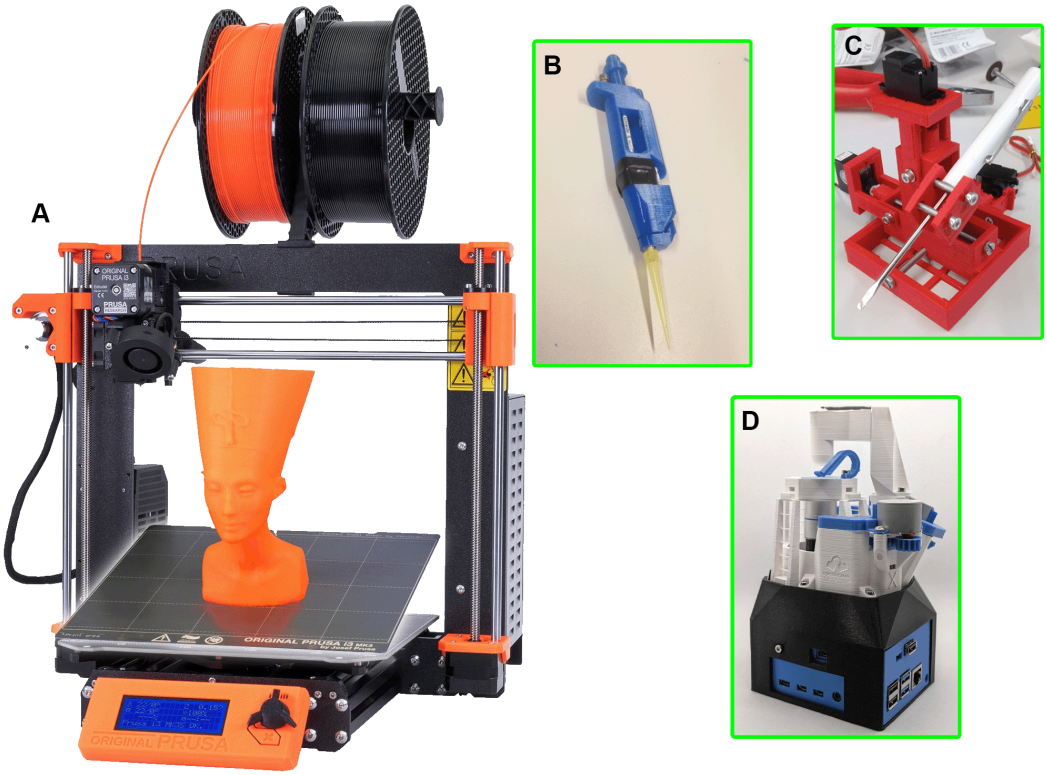

Figure 3.2: 3D Printed Labware A: Prusa MK3 FDM 3D printer, a common desktop 3D printer, B: 3D printed micropipette from [Baden et al., 2015], C: 3 axis micromanipulator from [Baden et al., 2015], D: openFlexure 3D printed microscope system [Collins et al., 2020]

3.1.2 Optics

When designing a microscope system using off-the-shelf image sensors there are several categories of lens optics that can be used (figure 3.3). M12 lenses are compact and can be put installed at a level of density that allows cameras to have the same spacing as a 24 well plate. C/CS mount lenses on the other hand, are larger and therefore require more space. The upside of this trade off is that the larger sensor makes high sensitivity applications like fluoresence microscopy possible. However, the ideal for microscopy applications would be to use an

objective that is specifically designed for those applications. Microscope optics come in several common standards, the most common of which is RMS (Royal Microscopical Society). The difficulty with adapting RMS microscope objectives to a C/CS mount camera is the required tube length. Without a tube lens to reduce this length, the height of a microscope system with RMS optics would take up too much space in an incubator.

Figure 3.3: Options for Lens Optics M12 lenses are compact and low profile, C/CS mount optics are compatible with larger image sensors, RMS microscope optics have high zoom but require complex mounting systems.

Using a tube lens allows us to have a lower profile imaging system. We designed a custom optical tube that can join plan achromat RMS microscope objectives to a C/CS mount camera.

3.2 Imaging Hardware Modules

A camera module consists of one Raspberry Pi connected to an image sensor and objective. The module can be made with several different hardware depending on the desired application.

3.2.1 Compact Camera Unit

For applications that require many cameras to be packed into a small area, we have used the compact Raspberry Pi "spy camera". This camera unit contains all needed electronics embedded into the ribbon cable, allowing us to pack many of these cameras close together without concern for colliding PCBs.

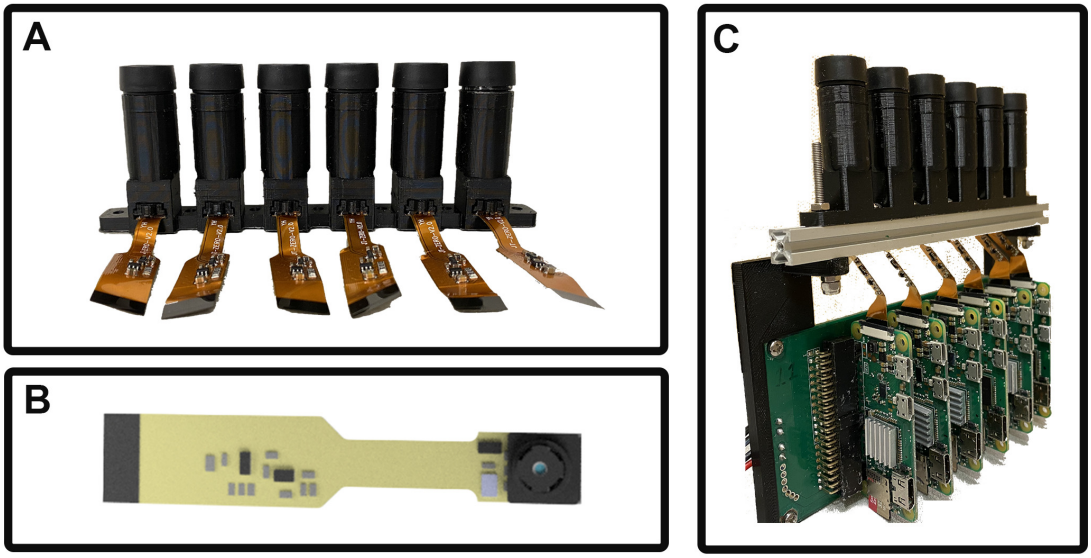

Figure 3.4: Compact Camera Module The spy camera based compact camera module can be packed into the form factor of a standard 24 well culture plate. A: a row of 6 cameras, B: a rendering of the spy camera in it's off the shelf form. C: one row of cameras mounted with their corresponding Pi Zeros.

3.2.2 Fluorescence Camera Unit

Attempts to do fluoresence microscopy with the compact spy camera units found some limited success. However, the limitations of the hardware meant that these camera units were not viable for the level of detail desired for the cell cultures being developed in our group.

For this reason, we developed a new imaging module using the more powerful Raspberry Pi High Quality Camera. This camera features a considerably larger sensor and a C-mount compatible lens attachment. This allows us to easily mount high quality microscope objectives to this system. The camera is also capable of capturing long exposure images without the the considerable firmware overhead this required in the spy camera based units. These camera units can be packed into the form-factor of a standard 6-well cell culture plate, allowing parallel imaging in a manner similar to the 24 well Picroscope.

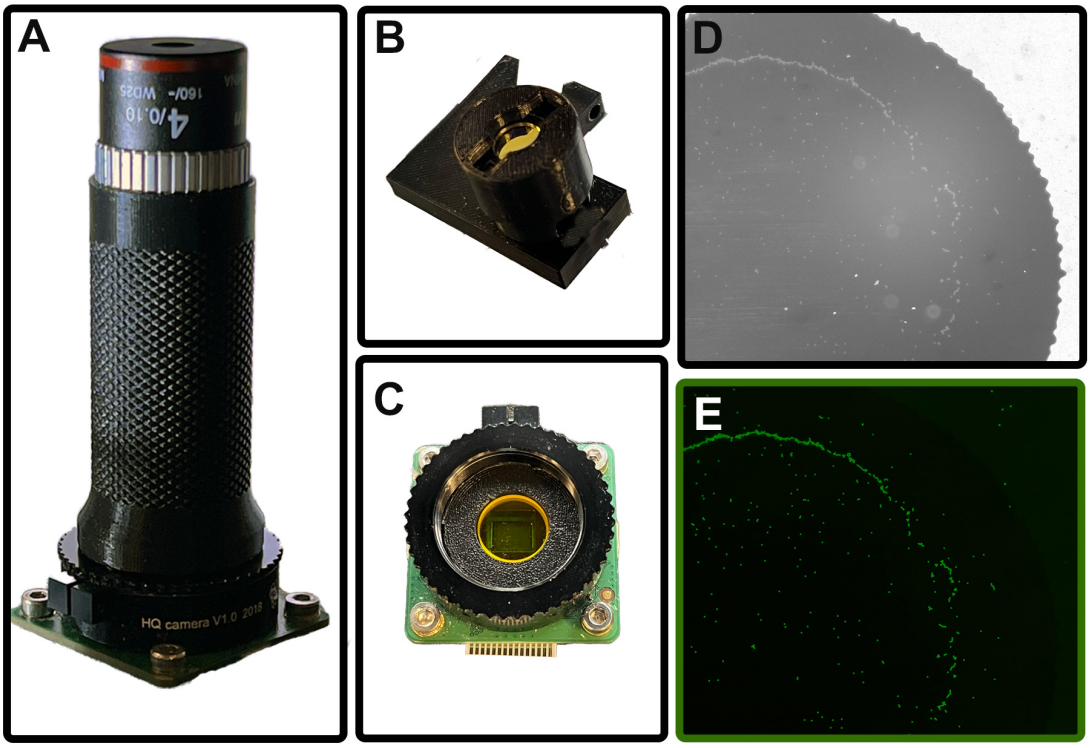

Figure 3.5: Fluorescence Camera Module The high quality camera based fluorescence camera module can be packed into the form factor of a standard 6 well culture plate. **A**: Single HQ camera unit with attached objective, **B**: GFP Excitation light, **C**: GFP emission filter placed in optical path immediately above image sensor, **D**: Brightfield image of GFP calibration slide. **E**: Fluorescence image of GFP calibration slide with 15μm beads.

A key factor making this design possible is our custom microscope objective mount seen in figure 3.6. Commonly used RMS threaded finite conjugate objectives typically have a back focal length of 15cm, using a tube lens to lower the required height of the microscope objective allows us to have an imaging unit that remains compact while still providing high quality results. The Openflexure documentation [Richard et al.,] documents a straightforward method to calculate tube lens placement based on image sensor size.

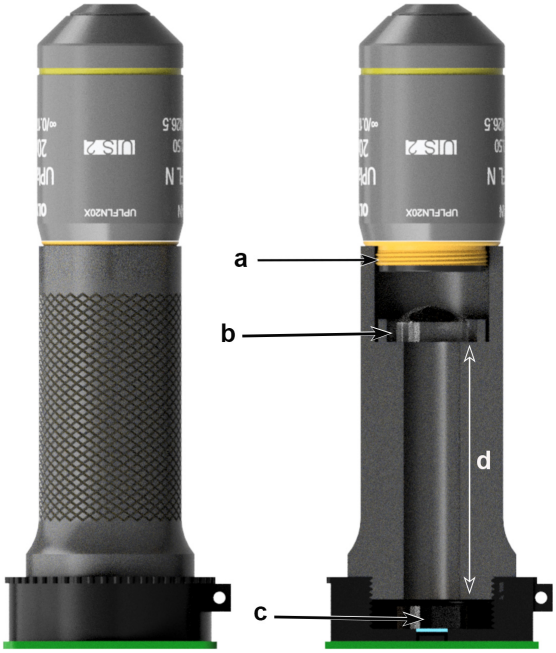

Figure 3.6: Fluorescence unit optics, **a:** standard RMS thread allows compatibility with many different off-the-shelf microscope objectives, **b:** tube lens allows for shorter optical tube, **c:** fluoresence emission filter sits atop sensor within the optical tube, **d:** tube lens position calculated based on our camera system as shown in appendix A.1

3.3 Focus Adjustment and Z-Stacks

For a 24 well Picroscope type system, individually adjusting focus is not possible. Instead, each camera has the same focal point and we move them up and down to find focus. The cameras are mounted on a moving elevator stage and are each attached to a Raspberry Pi Zero W. The Pis are mounted on a custom printed circuit board (PCB) for power distribution. The elevator stage is controlled by 2 stepper motors with encoder based feedback control to ensure they remain level. Encoders allow the system to measure the travel of each stepper, allowing it detect jammed states and compensate for skipped steps. Early iterations of the device lacked the encoder based feedback and as a result, experiments were sometimes

halted due to a jammed elevator stage. Implementing feedback control into the elevator stage movement has greatly increased the robustness of the system.

The movement of the elevator stage allows us to easily adjust focus. This control gives us the ability to collect z-stack imaging sweeps. Z-stacks are a set of pictures taken from various elevations, they are a common data type for biological microscopy. Z-stacks allow us to track cellular outgrowths on different planes, giving depth data to our results. The concept is illustrated in figure 3.7.

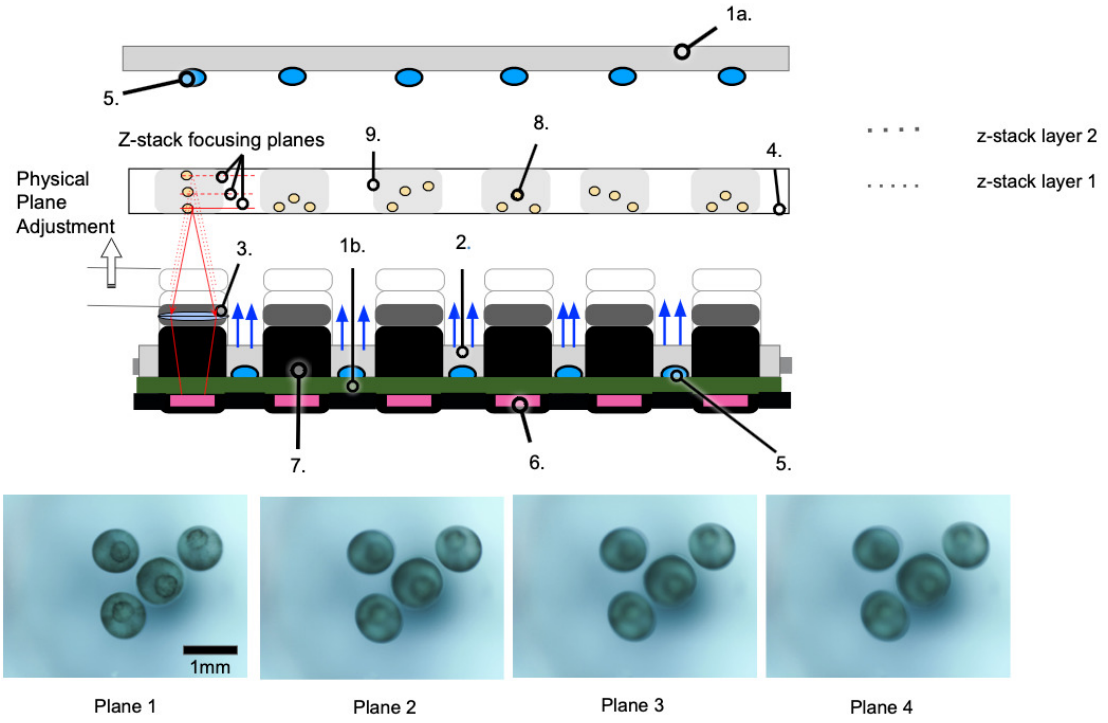

Figure 3.7: Schematic representation of the z-stack function 1.a = Over-the-plate illumination board, 1.b = Under-the-plate illumination board, 2 = Acrylic Light Diffuser, 3 = Lenses, 4 = Cell Culture Plate, 5 = LEDs, 6 = Raspberry Spy Cameras, 7 = 3D Printed Camera Bodies, 8 = Biological Sample (e.g., Frog Embryos), 9 = Individual Culture Well. The photos at the bottom were taken at four planes 0.3 mm apart

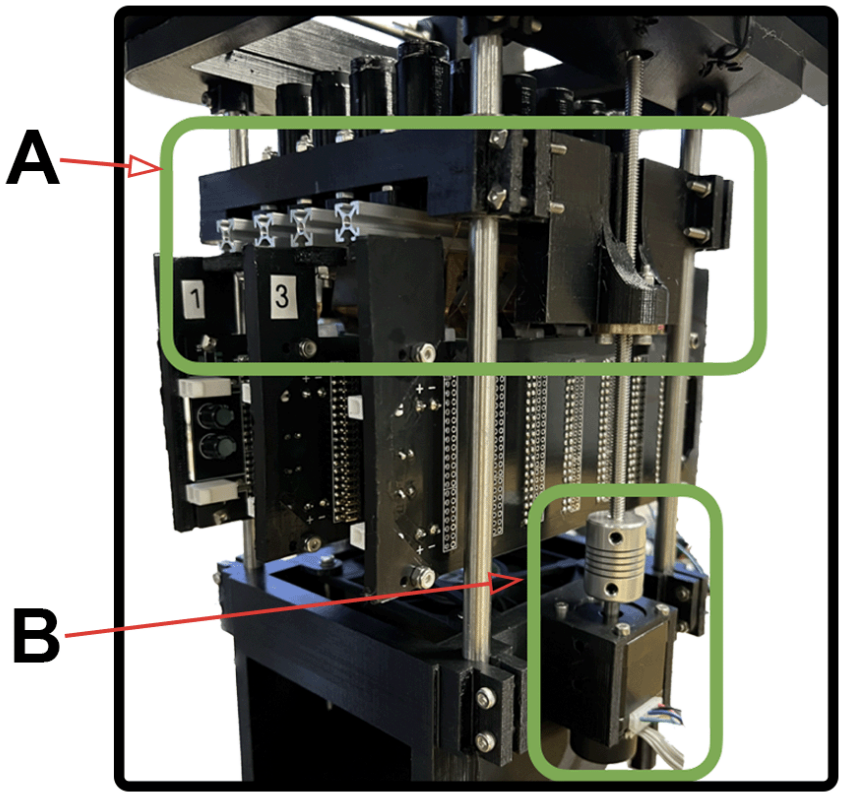

Figure 3.8: Elevator Stage A: the elevator stage holds the rows of cameras and Raspberry Pi zeros. B: Stepper motors with encoder based position feedback ensure the stage remains level and does not jam

Planar translation across the XY plane is also possible with our system and is explored further in section 3.4.

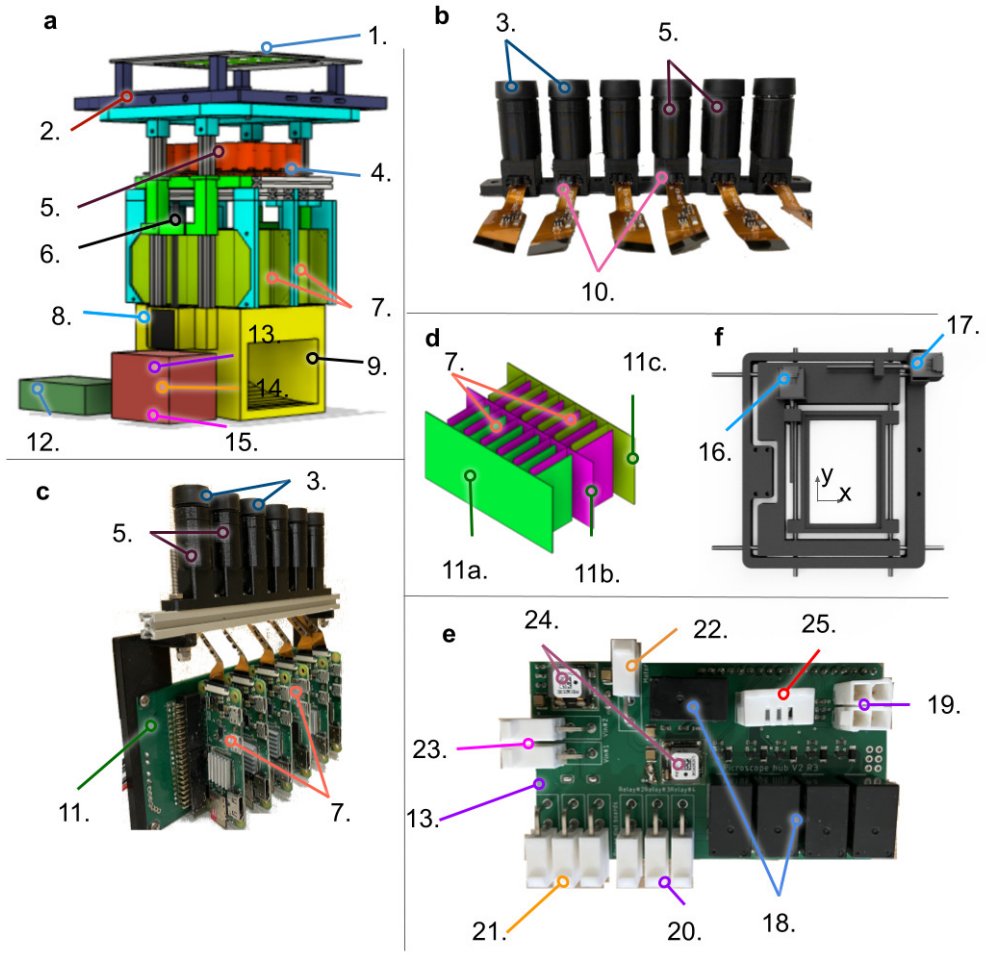

Figure 3.9: The Picroscope. **a** Physical representation of the imaging system. **b** one line of independent cameras. **c** An integrated rack of cameras and Raspberry Pi board computers. **d** The interlacing strategy of four independent racks of power distribution boards. **e** The Raspberry Pi Hub and Arduino Uno, Motor driver and custom relay board **f**The XY adjustment stage. 1 = Over-the-plate illumination board, 2 = 3D printed Cell Culture Plate Holder & XY stage, 3 = Lenses, 4 = Illumination Board from below, 5 = 3D Printed Camera Bodies, 6 = 3D Printed Elevator, 7 = Raspberry Pi Zero W, 8 = Motors, 9 = Base, 10 = Raspberry Spy Cameras, 11 = Interface Board a. row 1, b. rows 2 and 3 c. row 4, 12 = Pi Hub – Raspberry Pi 4, 13 = Custom Relay Board, 14 = Adafruit Motor/Stepper/Servo Shield for Arduino v2, 15 = Arduino Uno, 16 = Y-Axis stepper motor, 17 = X-Axis stepper motor, 18 = Relays, 19 = Limit switches connectors, 20 = Power distribution board connectors, 21 = Light board connectors, 22 = Motor power connector, 23 = 12 V power source, 24 = Voltage regulators, 25 = Temperature & Humidity sensor.

3.4 XY Translation Stage

One of the primary trade-offs to consider when designing a microscopy platform is zoom level vs. field of view (FOV). In some applications, this is an adjustable parameter. Mult-lens optical systems often allow users to adjust FOV and zoom based on what they want to image. On a platform meant to image many samples in parallel, individually controlling zoom for each sample in an automated fashion would be a considerable design challenge. For the Picroscope, we opted to have a fixed optical zoom level. The level of zoom was chosen so that we can resolve cell scale features while still having enough FOV to view broader morphological changes in large samples. However, this approach often puts us in situations where some wells of a plate would have interesting features in view while others will not. To address this issue, we designed a plate holder that uses stepper motors to adjust the position of the sample plate, allowing for translational sweeps of the entire sample area.

This XY translation stage holds a standard 24-well cell culture plate and uses stepper motors to control the plate's position. The design is comprised of 3D printed elements, linear bearings, linear rods, and motors. With this stage, the culture plate can be translated up to 15mm in one direction and 20mm in the other. This adjustment range gives us the ability to view any part of the well.

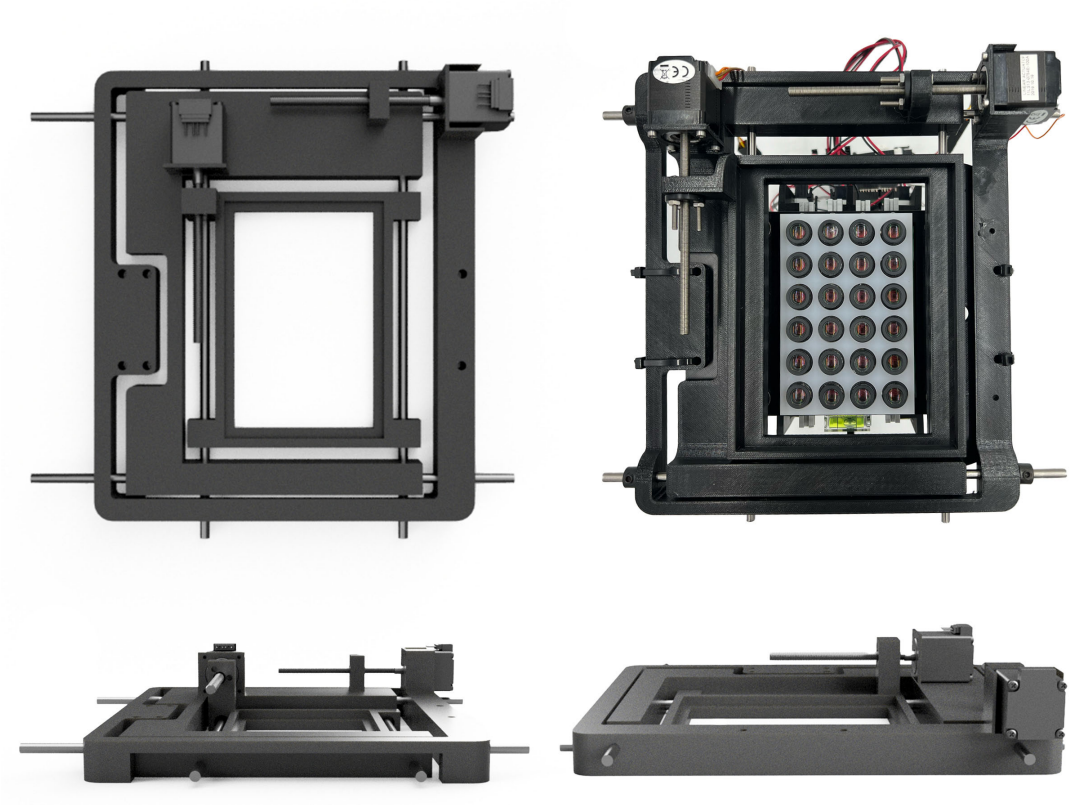

Figure 3.10: XY Plate Translation Stage XY positioning stage allows the position of the culture plate to be controlled so that areas of interest can be brought into the cameras field of view

3.5 Lights, Sensing and Power Control Stack

For handling low level direct motor control and toggling of power to lights and Raspberry Pis. We use an Arduino based stack of boards seen in figure 3.9e and on the left in figure 3.11. This bit of hardware also reads from limit switches and a temperature and humidity sensor to detect faults and shut down the system if it detects conditions that may harm the samples. For sample illumination we use a custom designed array of 3W white LEDs shows in figure 3.11 on the right

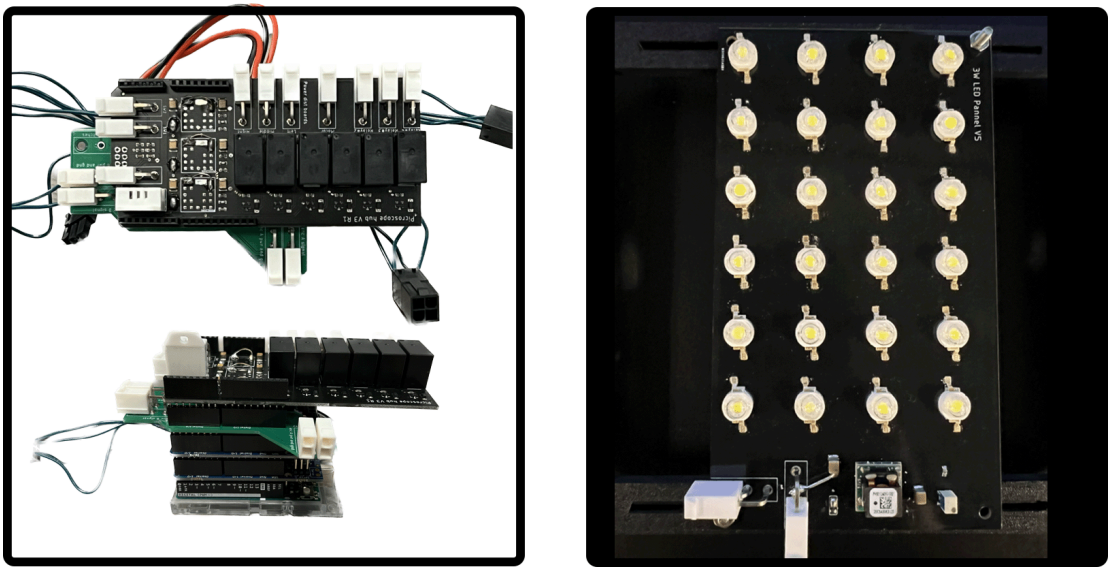

Figure 3.11: Sensing and Power Control + Lights Left: sensing and power control stack, Right: custom designed array of 3W white LEDs

Chapter 4

openCArM Software for Device Operation

4.1 Background

openCArM relies on a number of background technologies that allow it to function. This section will provide a brief overview of these technologies and their applications to openCArM.

4.1.1 The Internet of Things

The Internet of Things, (or IoT) is a technology paradigm wherein higher order systems can be viewed as networks of individual devices connected to each other through the internet. It's a paradigm that allows for flexibility and complexity arising from the development and combination of simple connected subsystems. Developments in consumer available technology for IoT have simplified the design and deployment of vast networks of devices, offering new approaches for sensing and control.

4.1.2 IoT for Biological Applications

The most visible implementations of IoT today are in the realm of consumer electronics. Lighting, thermostats, washing machines, microwave ovens, and even toasters are among the common household devices that now have "smart" varients that connect to the internet to allow their owners to control them from digital assistants or their phones. Much less broadly known, are the applications of IoT for industrial or biotechnology uses.

The Internet of Bio-Nano Things

The Internet of Bio-Nano Things is a concept laid out in [Kuscu and Unluturk, 2021]. They describe a paradigm in which new nanoscale devices enable sensing in difficult to reach areas. This could enable minimally invasive monitoring of health metrics deep in the human body. The authors describe a number of potential applications for this technology, including closed-loop sensor based drug delivery, artificial restoration of communication pathways between different organs, and bioremediation based environmental cleanup in situations like oil spills. IoT sensing applications for cell culture bypass many of the inherent challenges of placing sensors deep in the body. However, many insights from this work can be applied to in vitro biological applications.

IoT in Industrial Biotechnology

The utility of IoT in microalgea biorefineries is investigated in [Wang et al., 2022]. Microalgea biorefineries are industrial facilities made to grow and convert microalgea into various usable products including biofuels and bio-plastics. The chemical processes undergone in these facilities are biological in nature and therefore sensor applications in this field have parallels to the kind of

sensing that would be helpful in large scale cell culture. Data from devices can be used for monitoring growth and projecting future growth of microalgea, as well as monitoring the growth environment to avoid contamination and optimize growth conditions.

IoT Camera Clusters

Multi camera sensor networks are in common use for surveillance technology [Santamaria et al., 2019, Muhammad et al., 2018, Plageras et al., 2016, Abas et al., 2018]. While single camera remote operable systems for microscopy exist [Zamani et al., 2020, Cai et al., 2020], an IoT based camera cluster for parallel microscopy is a novel application.

4.1.3 Industrial IoT and Digital Twins

The adoption of IoT technologies in industrial applications has been broadly described in the literature as Industry 4.0 [Lasi et al., 2014]. Industry 4.0 involves the integration of various level of "smart" sensing and control into industrial processes. Using data from large networks of sensors, the state of a manufacturing facility can be more accurately determined. Work in this field has lead to the rise of the concept of the digital twin [Grieves, 2015]. A digital twin is a virtual representation of a physical object, system or process. Fundamentally, digital twins are models of their physical equivalent that are continually updated with data from from their physical counterparts. Digital twins provide an abstraction that allow process engineers to interact with things at the system level rather than needing to parse data from individual sensors and control individual actuators. This is a flexible model that allows for the integration of more sensors at a later time, adding more data in this way improves the accuracy of the digital twin.

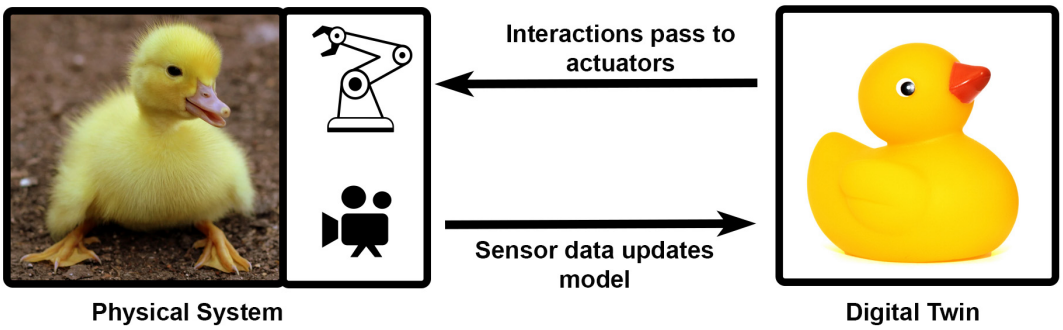

Figure 4.1: Digital Twin digital twins are continuously updating models of physical systems that can be used to abstract sensors and modes of interaction with the modeled system

The concept of a digital twin can be applied to cell culture. Samples can have digital twins that reflect the modes of possible interaction allowed by the devices used to grow them. The devices themselves can also have digital twins, as well as the entire cell culture facility.

4.1.4 What does openCArM need?

openCArM hardware has four key software needs that must be addressed for it to be a functional tool. These needs are:

1. Device Provisioning
2. Messaging
3. Data Storage
4. A User Interface

4.2 Device Provisioning

A system like the *Picroscope* involves many camera units. It's critical that each unit understands it's place in the greater whole. Each camera module needs to know it's position in the grid, as well as which actual camera array it belongs to. Raspberry pi's boot off of an sd card that must be flashed with an operating system to use. For openCArM devices, two key firmware loads were created, each of which can be flashed to an SD card and loaded onto a raspberry pi. However, if every camera pi truly had the exact same load on it then it would be impossible to tell which camera was which. To solve this problem, a provisioning system was created that allows each camera to be uniquely identified and configured. The basic process for a 24 well system is as follows, first 24 cameras are flashed with the camera node firmware. Then a configuration file in each of their /boot/ partitions needs to be modified to indicate it's position in the array and which hub it responds to. The array position is used to determine the mDNS hostname of the raspberry pi zero. This hostname change from a config file is a useful peice of functionality that had to be implemented for this application. Noting that this might be useful for others, the key aspects of this hostname change were put up on github at `https://github.com/pvbaudin/RPi-Change-Hostname`.

4.3 Messaging

In order for commands to be sent between modules, there needs to be a messaging system in place. The MQTT (Message Queue Telemetry Transport) protocol is a lightweight publish/subscribe based system that is well suited for this purpose. MQTT is a standard that is widely supported by many different hardware and software platforms. MQTT involves the use of a message broker to

handle sending the messages where they need to go. The broker is a central server that can be accessed by any device that is connected to the same network. The broker is responsible for routing messages to the correct devices. MQTT brokers can be self-hosted or cloud hosted. For openCArM, a self-hosted broker was used.

4.4 Data Storage

openCArM devices need to be able to store data locally. This is important because it allows for the system to continue to function even when internet connection is lost and only local networking is available. However, when internet is available, the data needs to be uploaded somewhere in order for it to be useful for others. For this purpose we use S3 (Simple Storage Service) buckets. S3 is a storage service primarily provided by AWS, but open source implementations of the standard exist as well. In our research group, we use a self-hosted S3 implementation called MinIO running on computation resources from the Pacific Research Platform (or PRP [Smarr et al., 2018])

4.5 User Interface

4.5.1 Control Console

We developed a device control console website (figure 4.2) to provide the needed functionality of enabling users to directly send commands to the devices connected to the IoT framework. In the case of imaging devices, the control console allows users to launch imaging experiments, adjust focus, toggle lights, and activate the live view functionality of any of the cameras. This gives users a high degree of control over the imaging process, allowing them to fine-tune the settings to

capture the best possible data. The live view feature is particularly useful for adjusting focus or XY plate position, as it provides users with a real-time visual representation of the sample they are imaging. This allows users to make quick adjustments to the device's settings, ensuring that it will capture the best data possible.

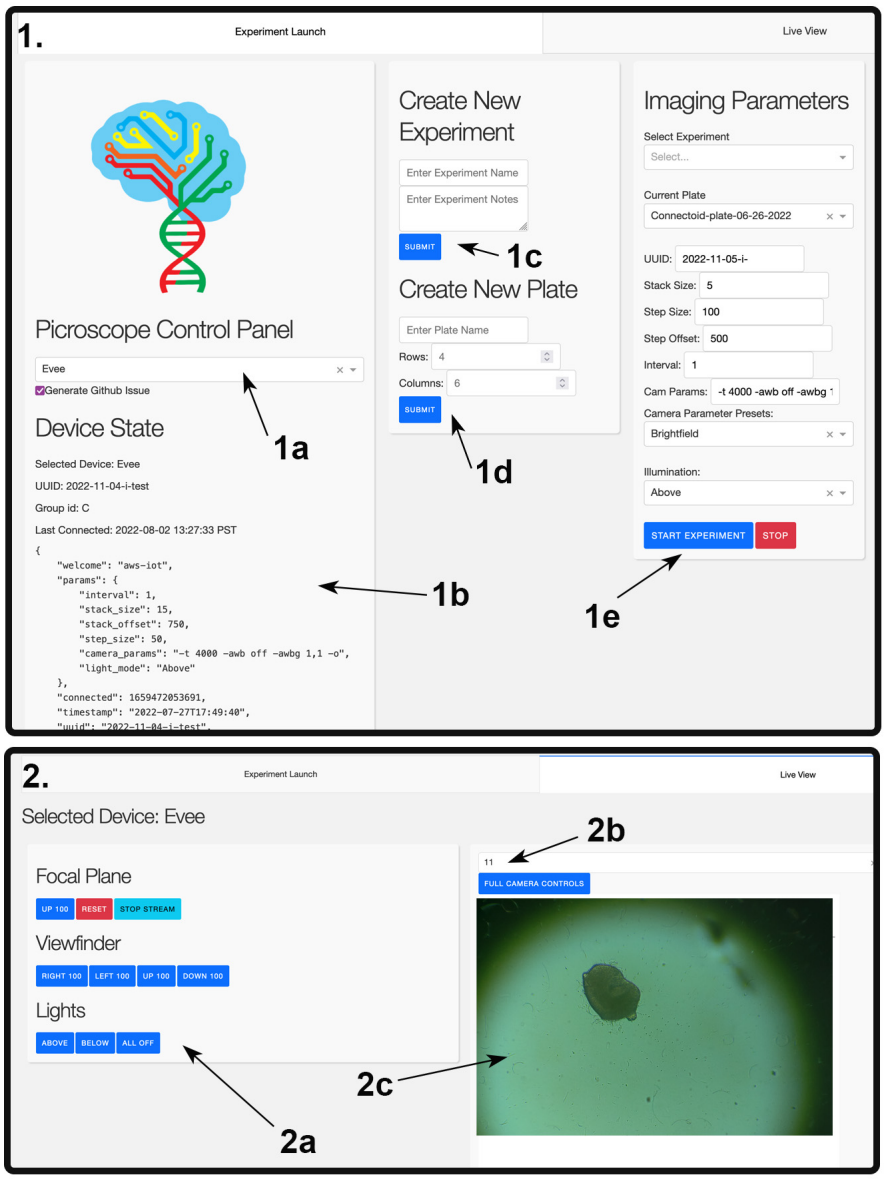

Figure 4.2: Imaging Device Control Console 1: Experiment Setup View, the device selection dropdown menu (1a) populates the Device State field (1b) with data from the Things database, Here you can define new experiments (1c) and plates (1d), these objects generate entries in the database, The Imaging Parameters section (1e) is where we set parameters like z-stack size and image capture interval; 2: Live View, Here we can see a live view of any of the cameras in the system and adjust focus or XY plate position. The panel at (2a) allows users to toggle lights and adjust plate position to capture the best possible data. The camera dropdown menu (2b) allows users to select which camera to view. and 2c shows the live view of the selected camera.

4.5.2 Livestream Server

While the core functionality of openCArM based microscopes is to capture longitudinal z-stack data on long timescales, there are scenarios where it is necessary for the user to see a live view through the cameras. This is necessary for setting focus or adjusting the position of the cell plate. In order to facilitate this, a system was developed to allow any user to request a low latency real time image stream from any camera. By using the open source Raspberry Pi camera web interface [silvanmelchior, 2023] each camera unit has a highly configurable MJPEG stream that can be accessed over the local network. Each camera unit is configured to have its livestream toggled through MQTT messages. Making these streams accessible through the internet is done using two Docker containers.

1. Running on a RPi 4 "Hub" device, the container serves as a reverse proxy for the camera units, receiving the live video streams from the cameras and forwarding them to another container running on a cloud server.

2. Running on a cloud server, this container connects to the Docker container on the "Hub" through a VPN and receives the live video streams. The container runs another reverse proxy which makes the streams available to the control console website.

Having the livestream system set up in this way makes it fast and easy to set up new systems while maintaining security. By using a containerized VPN, the live video streams are isolated from the rest of the host system and cloud server. The VPN is configured using the open source tinc VPN [Sliepen, 2010] which is a mesh VPN that allows for secure communication between nodes. The VPN is configured to only allow communication between the "Hub" and the cloud server. The cloud server container is configured to only allow communication from the

control console website. This configuration is shown in figure 4.3.

Besides being used for microscopes, one can easily imagine this system being used for other applications including DIY home security systems. For that reason this work is open sourced and available on github at `https://github.com/pvbaudin/raspberry-pi-livestream-tunnel`

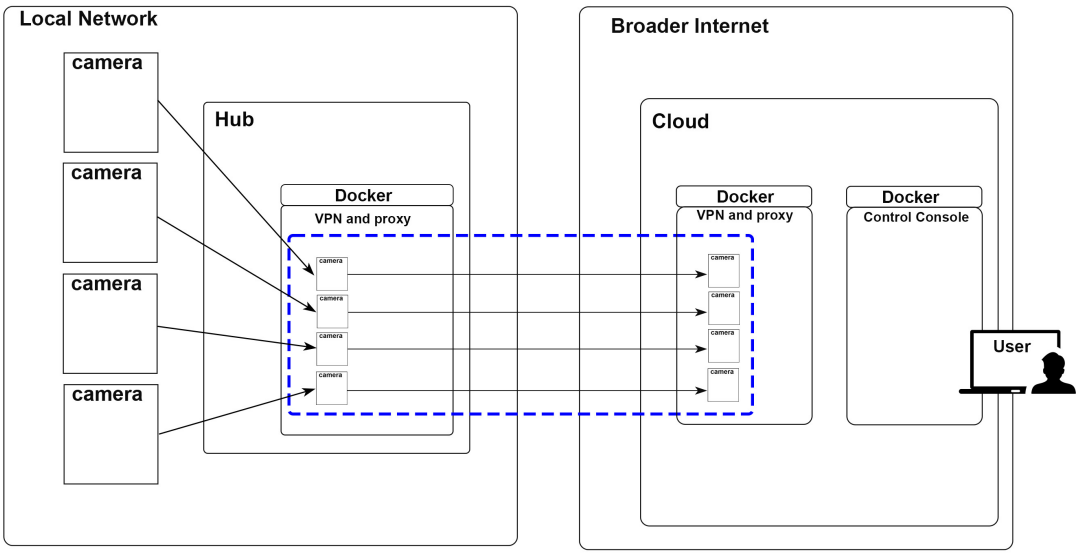

Figure 4.3: Livestream Network Structure Containerized VPN and reverse proxy system for securely streaming live video from Raspberry Pi cameras to a web interface.

4.6 Conclusion

The development of remote capability for openCArM devices this device offered many unique challenges from a design perspective. When the system is reliant on the internet for reporting what is going on with a cell culture, loss of contact can mean many different things. These can range from a short term internet outage to a catastrophic system failure. Loss of contact in this way presents major issues if one were to deploy the system in an unmanned remote location. We attempt

to address this issue by anticipating the various failure modes and setting up external monitoring systems that can alert us if they occur and in some cases take automatic action.

In the event of a system failure, it is critically important to ensure that the issue doesn't lead to a loss of the biology experiment on top of it. Implementing failsafes for potential hardware issues is important. Early iterations of the Picroscope caused incubator environments to overheat and cook the cell cultures. It can be quite frustrating for a researcher to spend time growing and plating a culture, only for an instrument to cook it. This scenario led to the implementation of a overheat safety shutoff system, a temperature and humidity sensor was added to the Picroscope. On the software side, a user can select and modify the safety shutoff temperature remotely and if that threshold is reached, all power to the system is shut off. The hub pi remains powered as it is located outside of the incubator environment. The hub remaining active allows the user to remotely reset the system if it has been deemed safe to continue.

In the event of a more minor issue, such as an internet outage, the system is designed to continue operating with only the local wireless network. In this state, users can no longer change experiment parameters, but the system will continue capturing data and storing it locally on the hub pi until the internet comes back, at which point all data gathered during the outage will be uploaded to the server

While we've described the efforts taken to ensure the system does not cause interference with experiments, it should be noted that the regular operation of this system can actually save experiments that are going wrong for other reasons. Using a Picroscope to monitor a culture remotely means that the user can notice issues with the cells sooner and be more likely to be able to take corrective action.

Chapter 5

Data Handling and Analysis

Parts of this Chapter were previously published in the Journal Elsevier Internet of Things [Parks et al., 2022]

5.1 Background

5.1.1 Cloud Computing

As data analysis tasks have trended towards larger and larger data sets, the need for more powerful computational resources has grown. Cloud computing is a model for providing these resources [Qian et al., 2009]. In this model, the resources are provided by a cloud provider, who is responsible for maintaining the hardware and software infrastructure. Users interact with the cloud either through command line interfaces (CLIs), application programming interfaces (APIs), or through web interfaces given by the cloud providers. In this model, users can execute long running tasks, and then retrieve the results when they are finished. One of the key technologies that make this model usable is containerization.

Containerization

Containerization is meant to address the many factors that can cause a piece of code to run differently in one system vs another. For instance, software dependency conflicts are a common issue when running multiple pieces of software on one system [Abate et al., 2012]. Often times, two pieces of software will require different versions of the same library, or a system update on one piece of software will break another. Managing these dependencies has been an important aspect of software development for decades. Containerization addresses this issue by packaging software with all of its dependencies within a virtualization layer and providing isolation between different containers. At the cost of increased overhead, this allows the software to be run on any system that supports the containerization technology and allows many containers to be run on the same system with minimal potential for conflicts [Watada et al., 2019]. This is great for programmers as they can configure and test the software within a container on their own system before deploying the container into a cloud system to operate on the full data set.

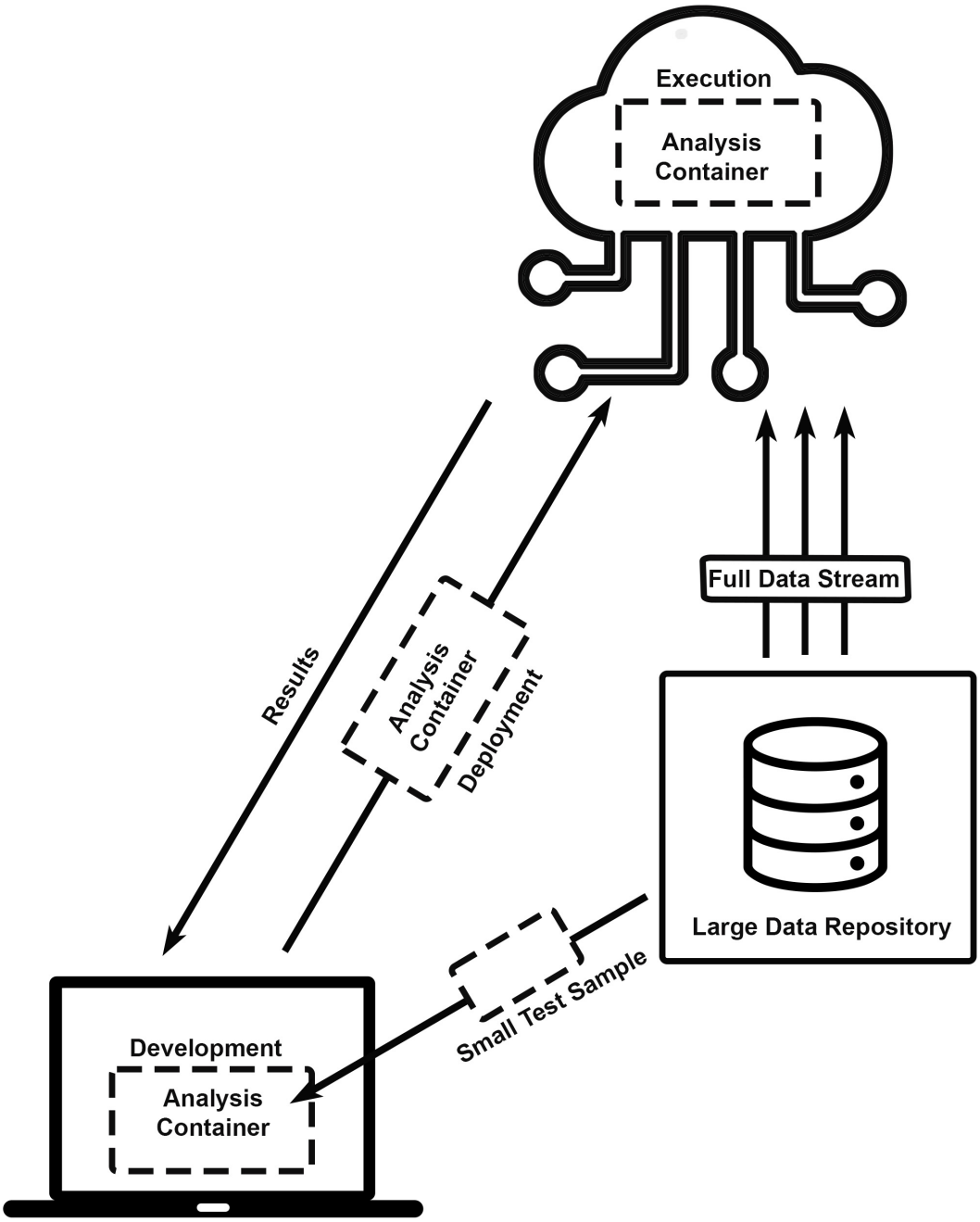

Figure 5.1: Containerization developing data analysis software in a containerized environment allows for easy deployment to cloud systems.

Docker and Singlularity

Docker is a popular containerization technology that is widely used in cloud computing [Merkel, 2014]. Docker containers are created by writing a Dockerfile that specifies the software and dependencies that should be included in the container. The Dockerfile is then used to build the container image. The container image is a file that contains all of the software and dependencies needed to run the software. The image can then be run on any system that supports Docker. Singularity is a containerization technology that is designed to be used on high performance computing (commonly abbreviated to HPC) systems [Kurtzer et al., 2017]. Singularity containers are created by writing a Singularity recipe file that specifies the software and dependencies that should be included in the container. The recipe file is then used to build the container image. The container image is a file that contains all of the software and dependencies needed to run the software. The image can then be run on any system that supports Singularity.

For institutions with access to high performance computing systems, Singularity is a more performant choice, however Docker is more widely supported by cloud providers and has a large base of contributing developers who are constantly improving the software.

5.2 Shadows Database

We use an SQLite database to track and store data related to the various devices and objects within the system. The database is managed using Strapi, an open-source headless content management system that provides a flexible and powerful way to define and manage the data structures used by the system.

This framework allows us to track objects at various levels of abstraction.

There are "users" who are the scientists and technicians who are authorized to work with the equipment. There are "interaction objects" such as microscopes or the autoculture systems, which are physical devices that can be controlled and monitored through the internet. There are also "plates", which contain "wells" which in turn contain "samples". These are logical objects that represent the experimental samples being used in the research, and they can be related to the physical devices and other data in the system. The ability to track data in this hierarchical structure allows the Braingeneers to analyze their results in powerful ways. For example, they can easily track the progress of a particular sample over time, or compare the results from different samples or devices. Additionally, the use of SQLite and Strapi allows the team to easily query and manipulate the data, making it simple to extract insights and generate reports.

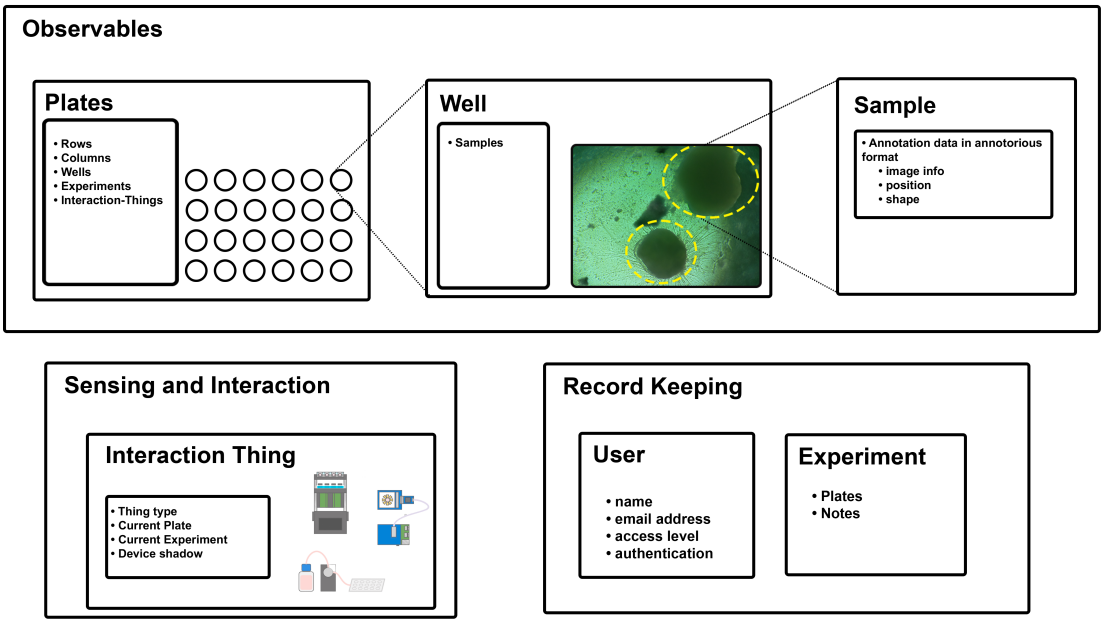

Figure 5.2: Shadows Database The Shadows database tracks objects at various levels of abstraction. Similar to the concept of the digital twin shown in figure 4.1, device state is tracked, and the state of experiment objects is tracked as well, experiment notes and users are stored as well

5.3 Braingeneers DataHub

The Braingeneers DataHub website is a front-end interface that gives authorized users access to view and interact with the data collected through this framework. The website is built using VueJS, a popular open-source JavaScript library for building user interfaces. The website is hosted on a cloud server, and is accessible through a web browser. The website is designed to be intuitive and easy to use, and it provides a variety of tools for viewing and analyzing the data. The website is shown in figure 5.3.

One of the most powerful features of the website is the image viewer. In the image viewer, users can navigate through timeseries z-stack image data. This allows them to see the changes that occur in the sample at different layers over time, helping them gain a deeper understanding of the sample's behavior. Additionally, using an open-source image annotation plugin called annotorious, users can tag samples of interest. This allows to more easily track specific samples of interest as they change over time.

The image viewer also allows users to generate and view timelapse videos of any well at any z-level, allowing them to see how the sample changes over time in a dynamic and easy-to-understand format. The timelapse videos can be generated at different z-levels, so users can see how the sample changes at different depths. This feature provides a powerful way to quickly understand the overall behavior of the sample, and can help identify patterns that may not be visible in individual images.

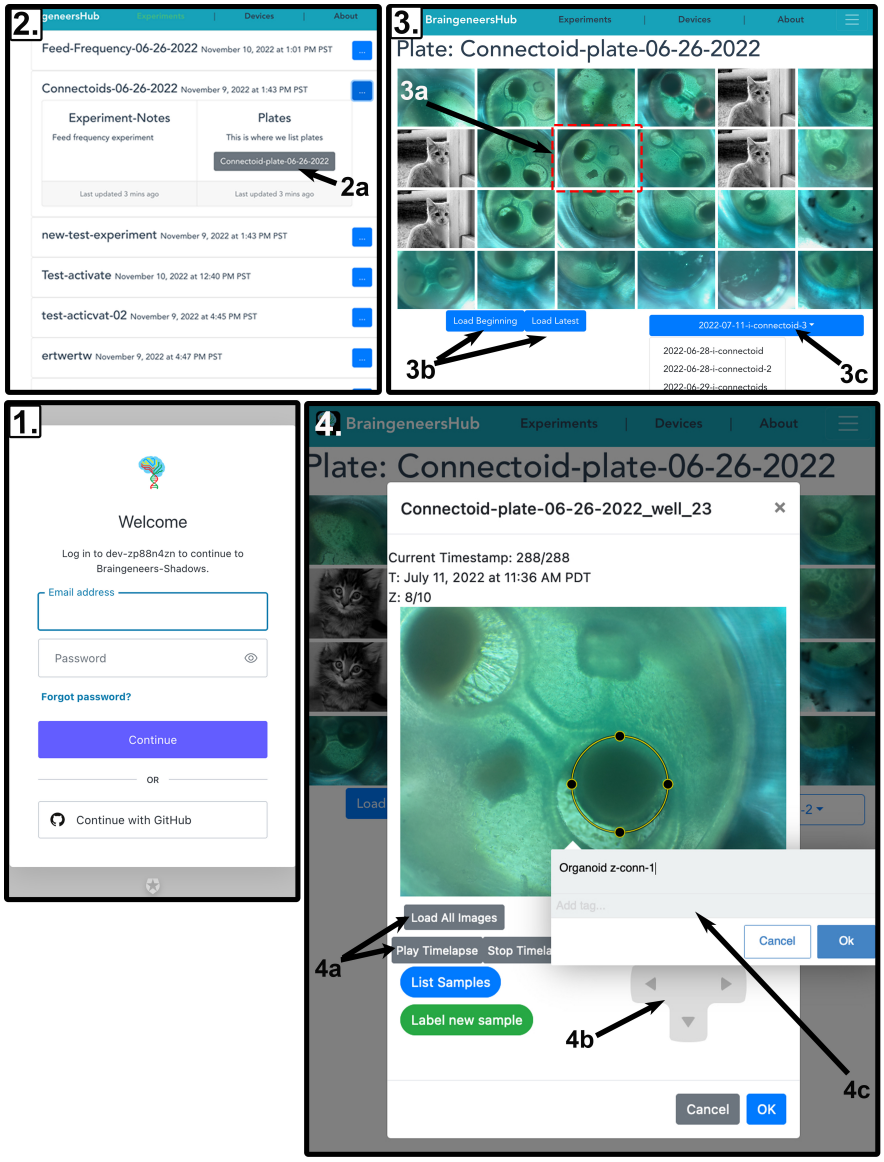

Figure 5.3: Braingeneers DataHub Website 1: Access control handled with Auth0 authentication; 2: The experiment selection screen, selecting an experiment opens a collapsable view where notes and plates (2a) are shown; 3: The plate view, showing all wells for a given plate, clicking a well (3a) opens the single well view (4), controls for loading thumbnails for the beginning and end of the dataset are given (3b), 3c shows a dropdown menu for all image sets associated with a plate; 4: Single well view, 4a loads a timeseries for a given layer and plays a timelapse, 4b allows navigation through z-stack layers and timesteps, 4c is the sample tagger where annotations can be added to the image and identified as samples of interest.

5.4 Image Analysis Features

5.4.1 Extended Depth of Field

In addition to being viewable through our web interface, the pictures on the PRP can be fed into scripts for generating focal plane stacked composite images with FIJI [Schindelin et al., 2012] using the Extended Depth of Field plugin [Forster et al., 2004]. This plugin allows us to generate a single image containing the best focused features from each layer of the z-stack. We can also use a script to generate timelapse videos from experiments. Generating timelapse videos with focus stacked frames allows for easy visual analysis of longitudinal changes in 3 dimensional samples.

The containerization of these programs with Docker allows us to run them in an automated fashion and easily deploy them with cloud service providers. [Merkel, 2014]

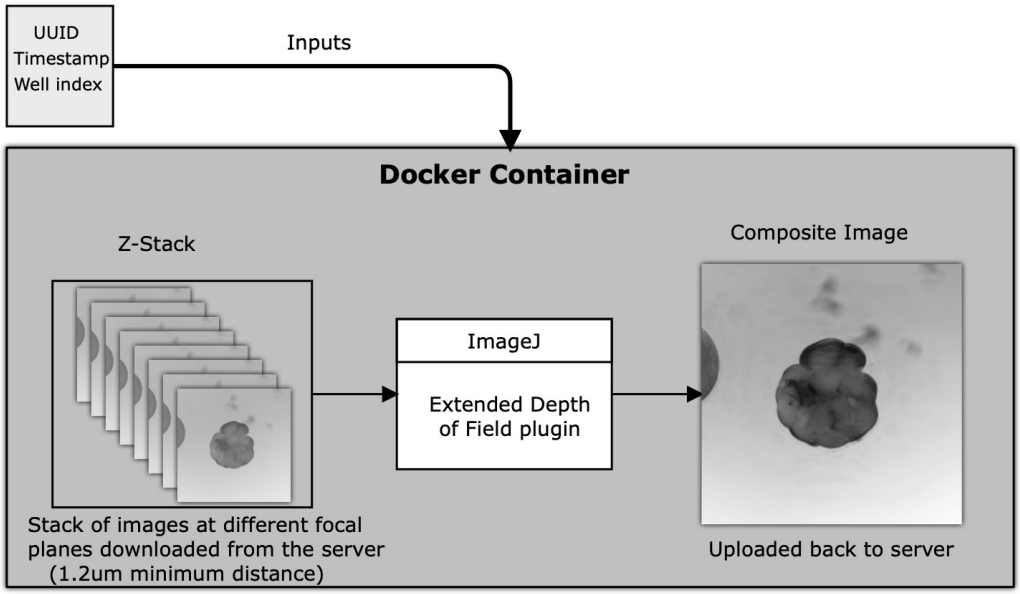

Figure 5.4: Extended Depth of Field: Docker Containers are used to generate composite images with FIJI

5.4.2 Binary Threshold based Growth Tracking

For experiment samples that grow in a single centralized structure, a simple method can be used to track their growth over time. Binary thresholding takes all pixel values above a certain threshold and sets them to 1, and all pixel values below the threshold are set to 0. This allows us to easily count the number of pixels in the image that are above the threshold. This method is shown in figure 5.5

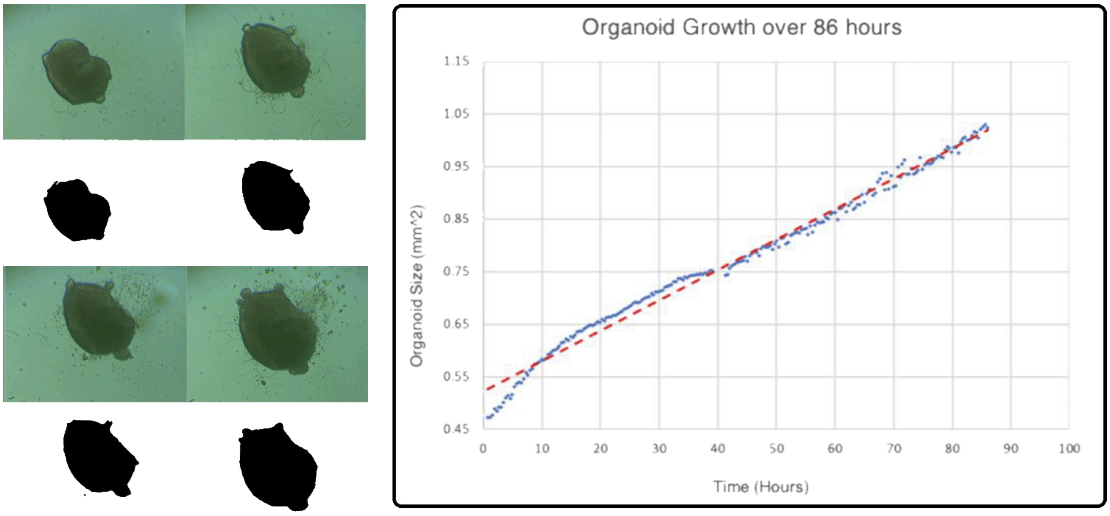

Figure 5.5: Growth Tracking: computationally simple growth tracking of cerebral organoid cell culture with binary thresholding

5.4.3 3D Reconstruction of Organoids

Since our imaging system captures z-stack data, we have depth information for any features that are visible on a given layer. This means we can generate 3D models. This is similar to the extended depth of field image compositing presented earlier and is detailed in figure 5.6

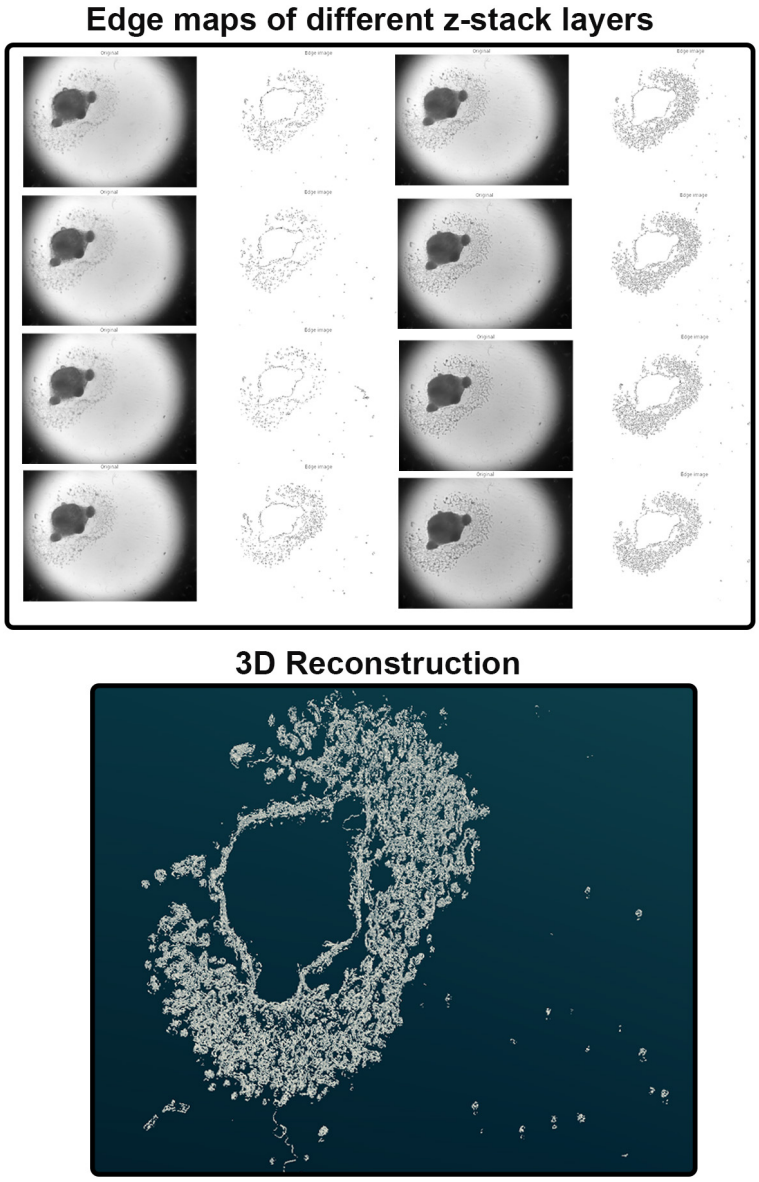

Figure 5.6: 3D Structure of Outgrowths Modelled from Edge Maps Edge maps are captured from the in-focus elements of each z-stack layer. Marching cubes algorithm used to assemble 3D model from these layers.

This 3D modeling approach allows us to track morphological changes in the culture. Morphological change is a useful metric for many experiments. Brightfield z-stack imaging is primarily useful for tracking the size of the opaque center of an organoid and for tracking transleucent outgrowths.

Chapter 6

System Architecture

6.1 System Architecture

To support the Braingeneers lab work, a custom IoT framework was developed. The framework includes several key components that work together to provide a robust and versatile system for device tracking, data collection, and analysis.

Figure 6.1 shows the core structure of this framework. We have numerous network connected devices that are used to collect data or control experiments. These include imaging devices like those described in this thesis, as well as other devices for electrophysiological recording and stimulation of cultures, or the autoculture microfluidic feeding system. Data from these devices is gathered and stored in the shadows database (section 5.2) for smaller items like experiment notes and metadata, while larger items are stored on the Pacific Research Platform (PRP) in an s3 object store. This data is then available for analysis through docker containerized tools and for visualizaton through a web-based interface. The Braingeneers can use this framework to track and analyze their experiments, and to share their results with collaborators.

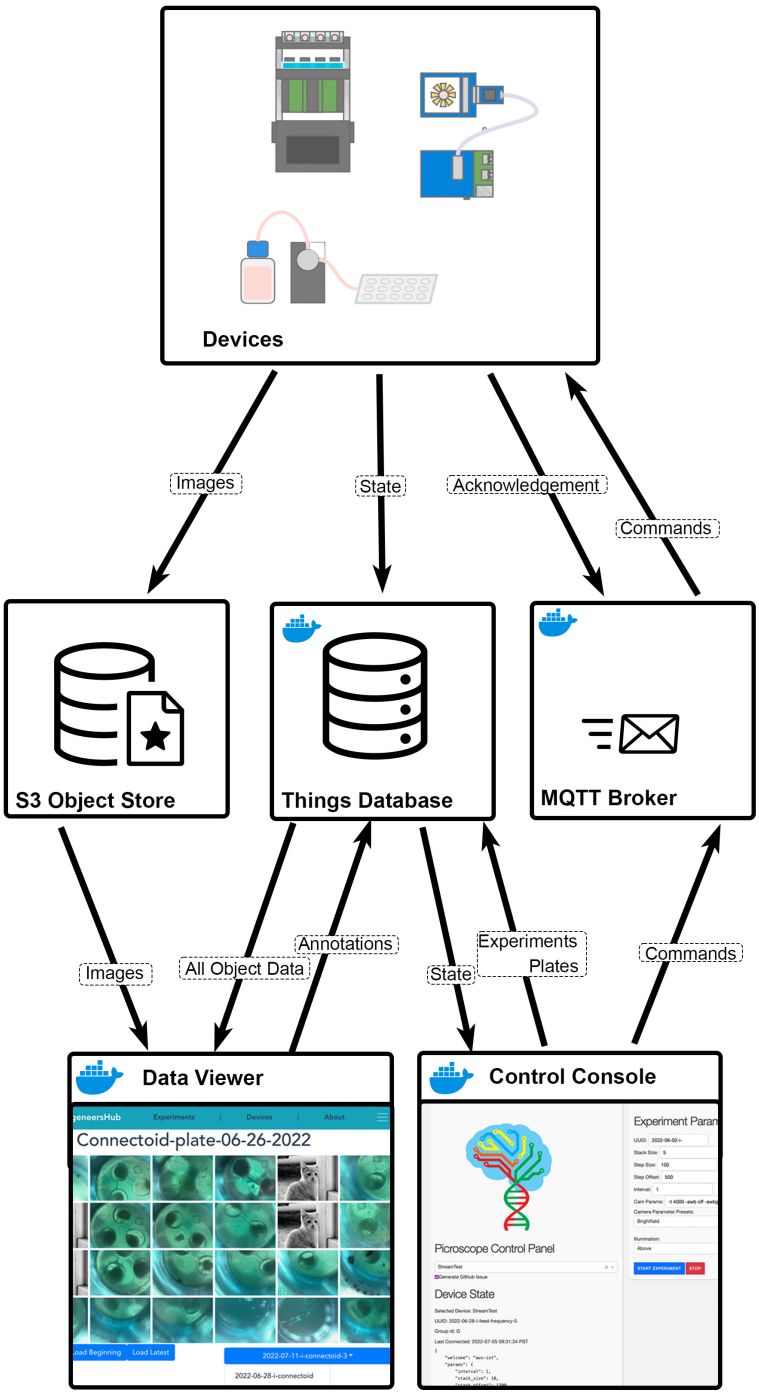

Figure 6.1: Device Communication Devices send and receive messages through MQTT message broker, devices take action based on received commands and send state to the things database through REST API calls, substantial data generated by devices is stored in the PRP s3 object store.

6.2 Internal Device Artchitecture

6.2.1 Hub Module

Hub modules serve as the communication bridge between cloud services and local hardware. The Hub receives high level commands including experiment parameters and translates this into the required system behavior. Necessary commands are passed to the hardware control stack (section 6.2.2) and to the camera units (section 6.2.3) to trigger image captures and initialize data transfers. Hub modules are responsible for gathering image data from camera modules and uploading them to the s3 object store.

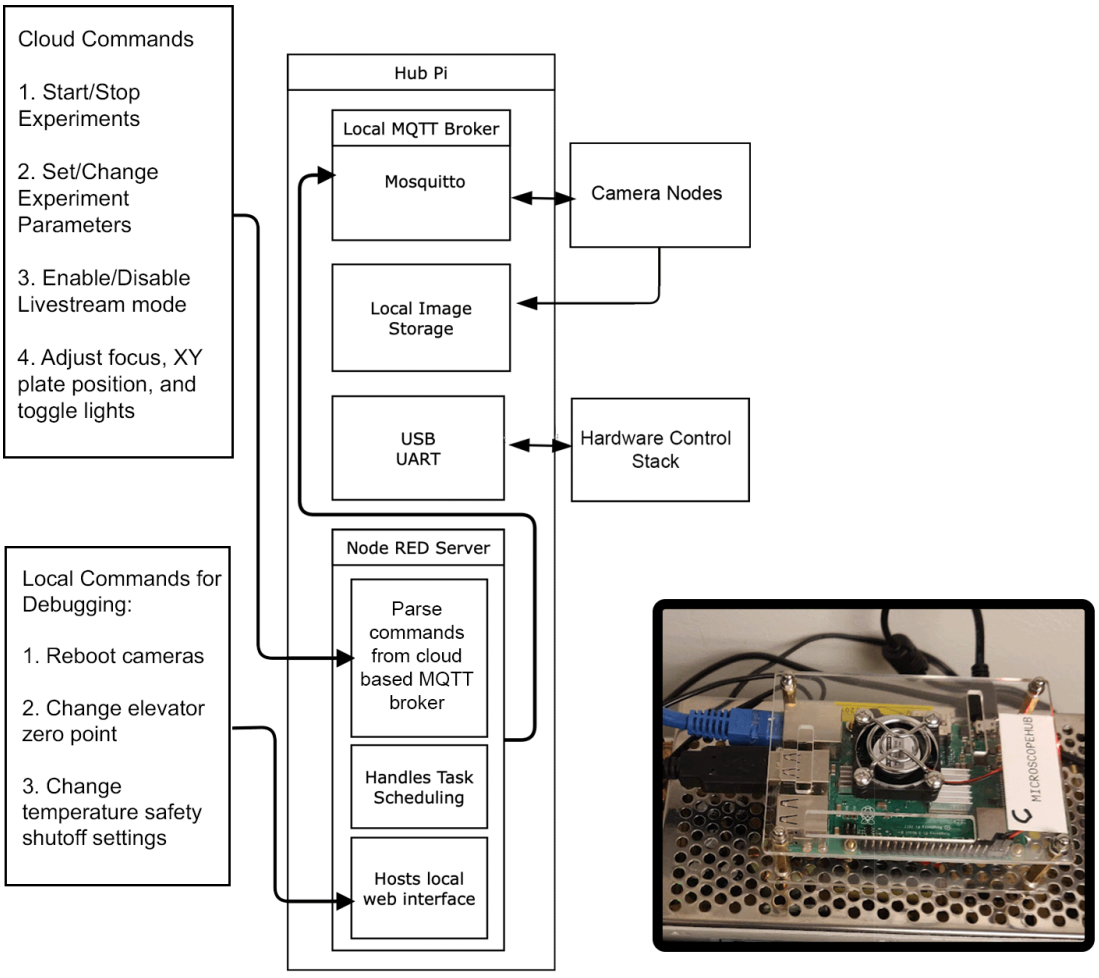

Figure 6.2: Hub Module Architecture: Hub modules take commands from the command console website and translate them into actions on the local hardware. The Hub module also serves as a local data repository, holding all images for a given experiment before uploading them to the cloud. This local repository behavior allows the system to continue capturing data in the event of an internet outage. The system is fully capable of running using a Local Area Network and will upload results when internet is restored. A locally accessible debug interface allows modification of key safety parameters that would not need to be adjusted through the main user interface

6.2.2 Motors, Lights, and Relay Control Stack

A hub module can be outfitted with boards for motorized focus control and viewfinding, sample illumination, and system power management. The boards also handle environment sensing to detect error conditions and prevent hardware malfunctions from harming the samples. The control stack is shown in figure 6.3. The control stack is based on an Arduino Uno, the uno form factor is very popular and clones of this board are available for very low cost. Many add-ons exist for the uno as stackable "shields" which allow for easy expansion of the board's capabilities. The Arduino is connected to the hub module through a USB UART.

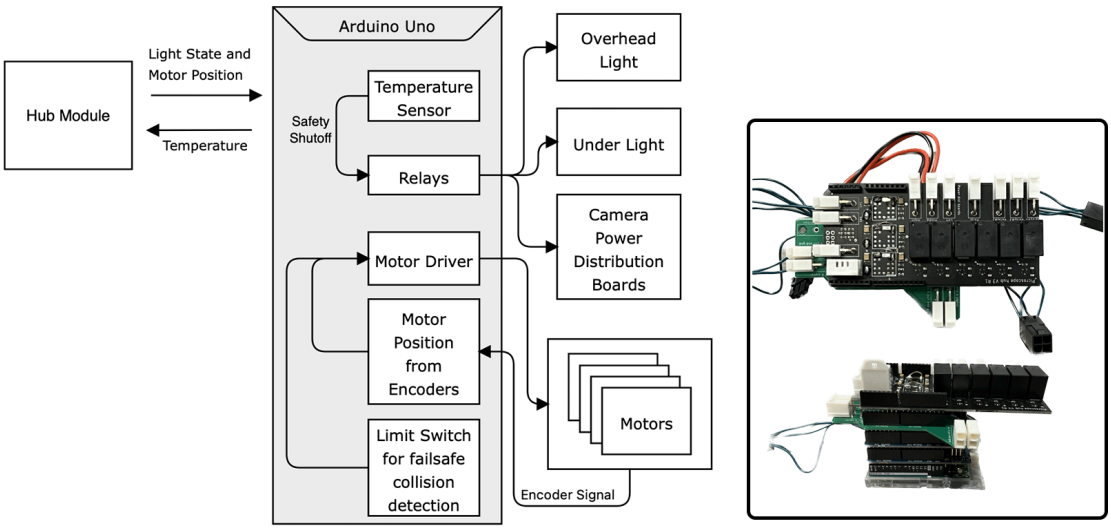

Figure 6.3: Low Level Hardware Control Stack: The arduino based control stack receives commands from the hub module through USB UART and controls the motors, lights, and relays. It also reads from sensors and transmits that data back to the hub module.

6.2.3 Camera Modules

A given module has a user defined alphanumeric id which is defined on the boot partition of the SD card containing the system firmware. This id is used when sending commands, a unit only responds to commands that address its id or

all units of its type. Figure 6.4 shows the behavior of this module.

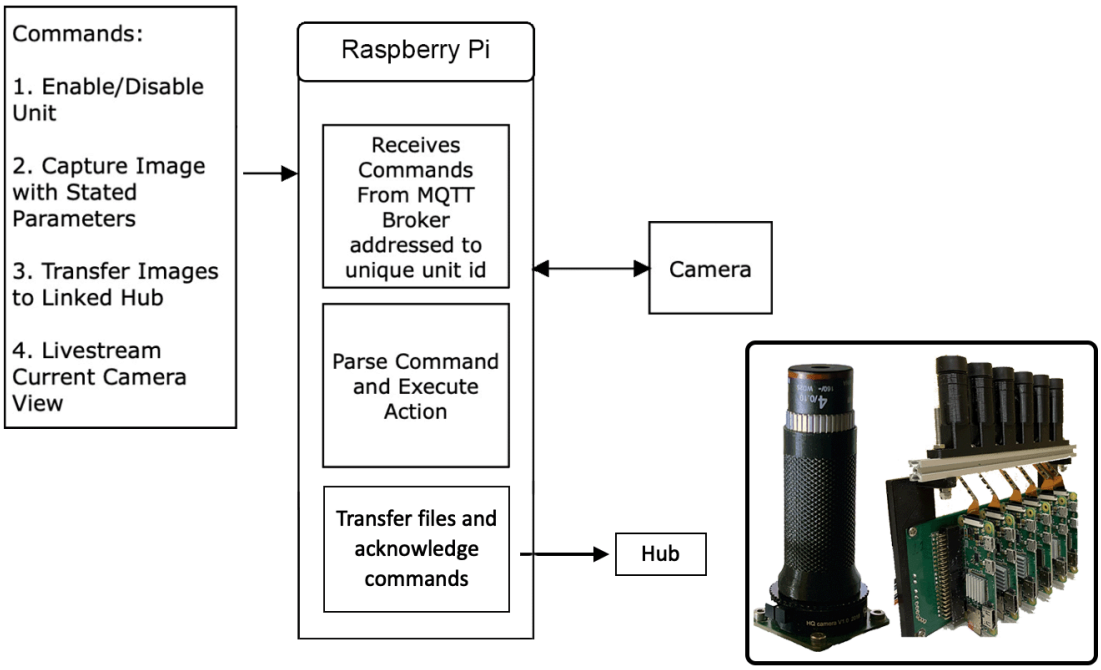

Figure 6.4: Camera Module Architecture The camera module receives commands, captures data from the image sensor, and sends the data to its linked hub.

6.2.4 Inter Module Interaction

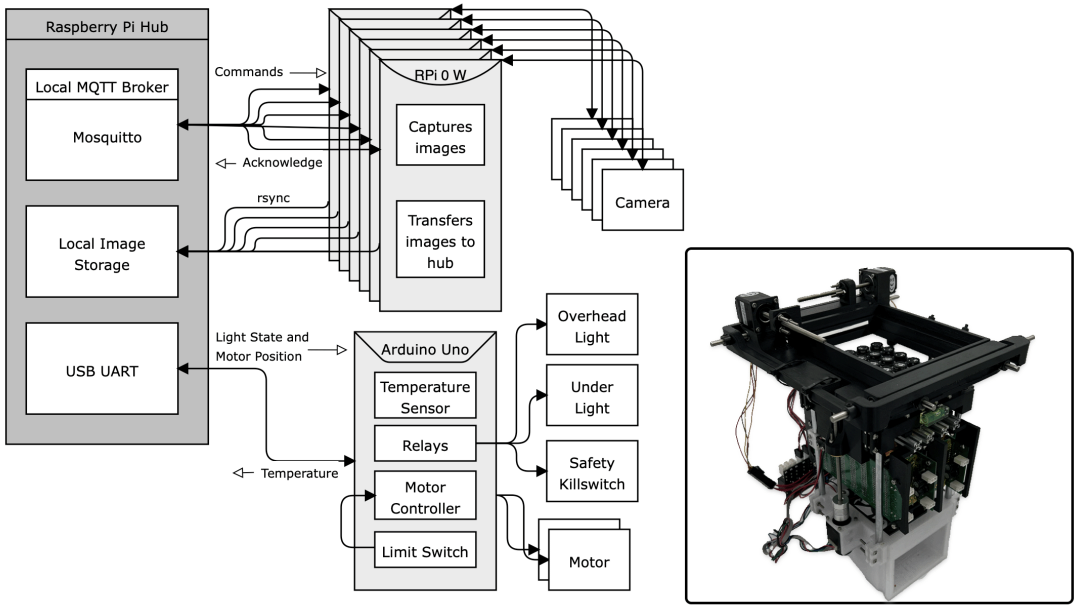

Figure 6.5: Interaction between locally connected modules: Flow of commands and data between hub pi, camera nodes, and control stack.

The Hub module is responsible for coordinating the actions of the camera modules. During the capture of a new timepoint, the hub first tells the camera units to create a directory with a timestamp. After handling elevator position change, the hub tells the camera units to capture an image. When the z-stack is complete, the hub tells the camera units to initialiaze a file transfer to the hub. In this structure, the hub acts as the local repository of images and is responsible for uploading them to the s3 object store when a connection is available. This structure allows the system to continue functioning with only local networking in the event of an internet outage. However, bandwidth limitations mean that the hub module commanding 24 cameras to all transfer their data at once causes major slowdowns. The transfers actually complete much faster if queued and started one at a time. However, a queue structure leads to the possibility of a camera

unit becoming unresponsive and blocking the queue. To address this, we use a custom queuing protocol that initiates file transfers individually on each pi zero W and continues to the next pi when the current transfer finishes or a timeout condition is reached. The protocol is detailed in figure 6.6. This queuing system results in higher throughput than starting all transfers in parallel and the queue is not disrupted in the case of non-responsive camera units.

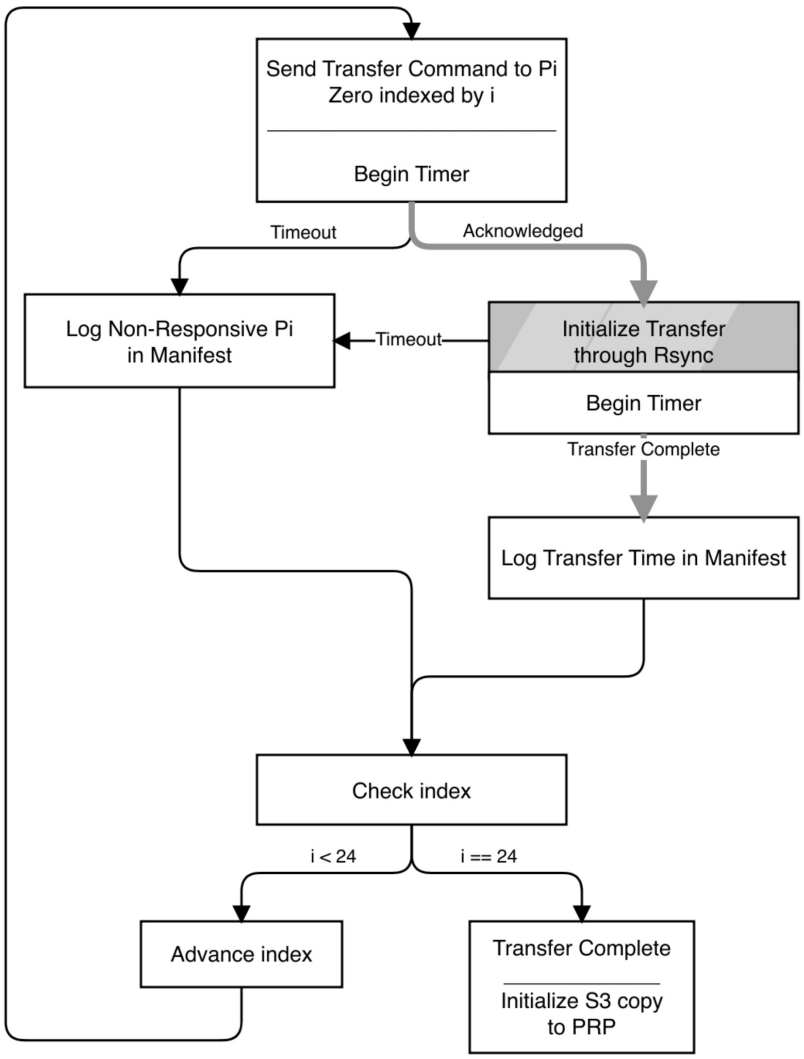

Figure 6.6: File Transfer Queuing Protocol: White boxes with black arrows represent actions taken by the Pi Zeros, Grey Box and arrows indicate messages and actions taken by camera modules, Black arrows and Boxes indicate messages and actions taken by the Hub Pi

6.3 Interaction with Control Console and S3

Figure 6.7 shows the interaction structure surrounding a Picroscop type oenCArM device. User interaction begins through the control console website (figure 4.2) where users can view live feeds from the device and launch longitudinal imaging

studies. Metadata regarding launched studies is automatically added to a private git repository where members of our research group can read them. The device receives commands sent through the console website and sends back status data to be displayed on the website. This status data alerts users to hardware issues and provides reassurance when everything is operating as expected. During a longitudinal imaging study, a Picroscope device uploads image data to an s3 object store.

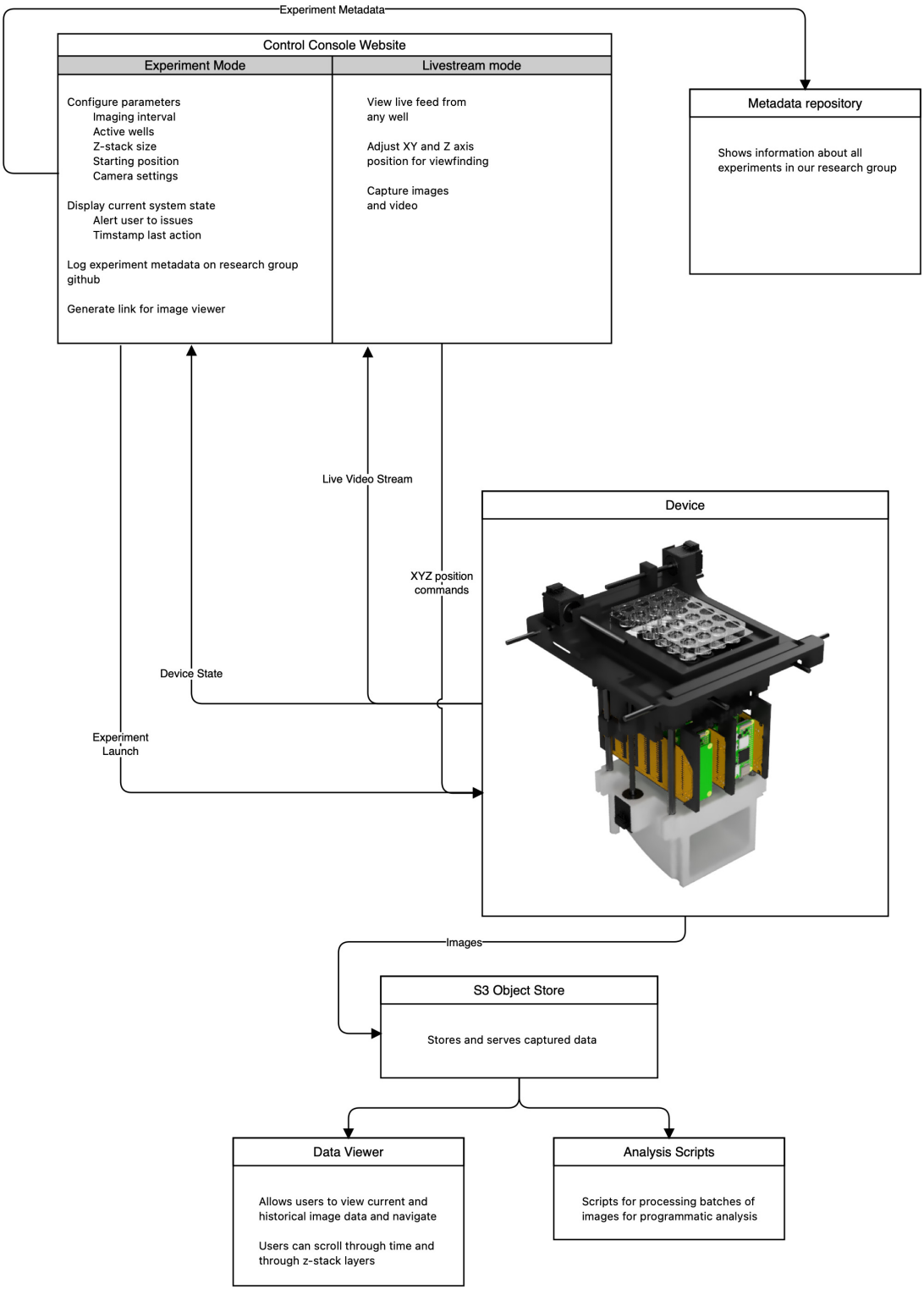

Figure 6.7: Interaction Between Device and IoT system

Chapter 7

Applications 1: Live Imaging of Model Organisms

7.1 Background

7.1.1 Model Organisms

Neuroscientists need ways to study the nervous system. Experiments with human subjects can be ethically fraught and are always logistically challenging. Working with human tissue samples is one way to go but that comes with a different set of challenges, including the need for specialized equipment and expertise [Jones et al., 2016].

For this reason, a lot of research is done using "Model Organisms". Model organisms are species with characteristics that make them ideal for studying specific aspects of biology. Xenopus tropicalis, Planaria, and Zebrafish are three commonly used model organisms that have become essential tools in neuroscience research. Xenopus tropicalis, a species of frog, has been used for decades to study embryonic development due to its large eggs and transparent embryos

[Exner and Willsey, 2021]. In recent years, Xenopus tropicalis has also emerged as a valuable model organism for studying neural development and function. Its ability to regenerate its spinal cord and its amenability to genetic manipulation make it an excellent model for investigating neural regeneration and plasticity [Exner and Willsey, 2021]. Planaria, a species of flatworm, can regenerate their entire body from small fragments, including their nervous system. This unique ability has made them an important model organism for studying neural regeneration and the molecular mechanisms that underlie it [Pagán, 2017]. Zebrafish, a small freshwater fish, is a popular model organism for studying neural development and behavior. Zebrafish embryos are transparent, allowing researchers to visualize and manipulate neural circuits as they develop [Rinkwitz et al., 2011].

Figure 7.1 shows a picroscope with sample images from each of the aforementioned model organisms. In this chapter we will look more closely at the results of model organism experiments using the picroscope.

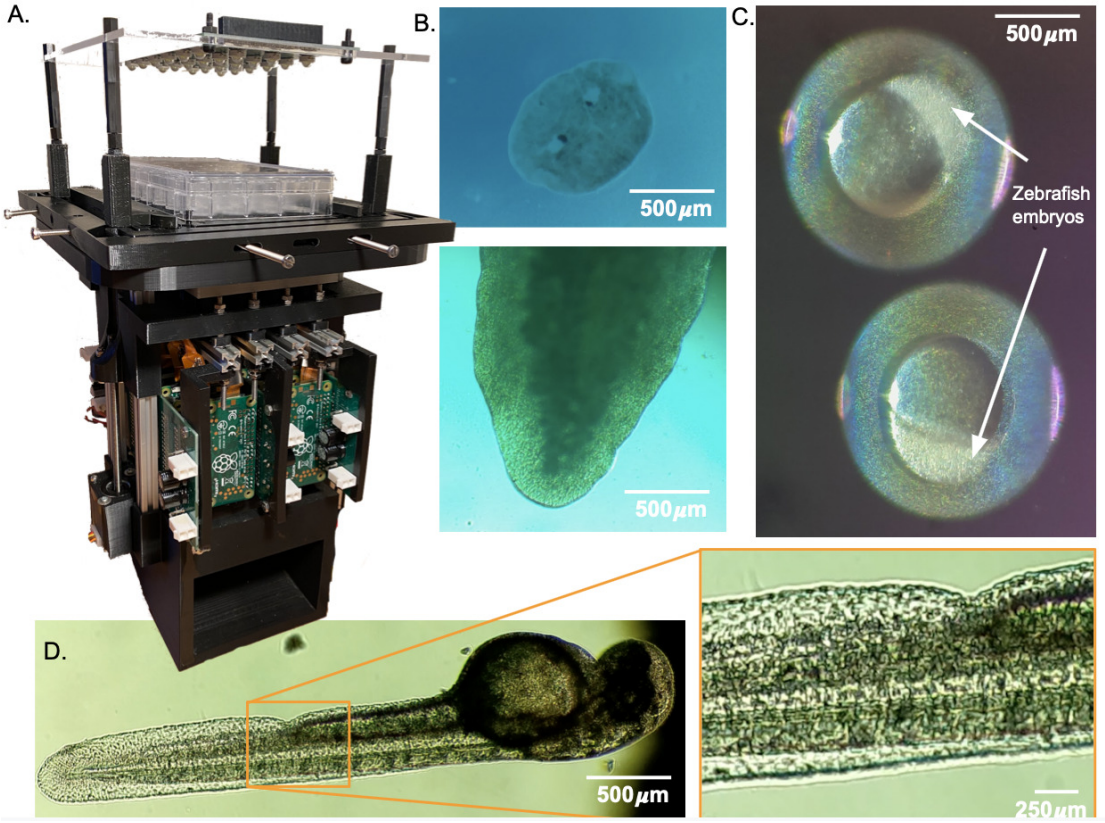

Figure 7.1: Samples Imaged with Picroscope System **b-d** Applications of the Picroscope to longitudinal imaging of developmental biology and regeneration. **b** Regeneration of planaria worms *Dugesia tigrina*. **c** Zebrafish embryonic development at oblong stage. **d**.Zebrafish embryo at 48 hours post fertilization. In complement see Supplementary Video 1.

7.2 Longitudinal imaging of *Xenopus tropicalis* embryonic development

We imaged *Xenopus tropicalis* embryos over a 28 hour time period. Four embryos were placed in each well of a 24-well plate. The embryos were grown in simple saline solution and the experiment took place at room temperature. Imaging was performed hourly, allowing us to view the development of the embryos over a 28 hour period. The images were taken using the Picroscope and the results

are shown in figure 7.2. This simple experiment demonstrated that the Picroscope can be used for longitudinal sequential imaging and tracking of biological systems.

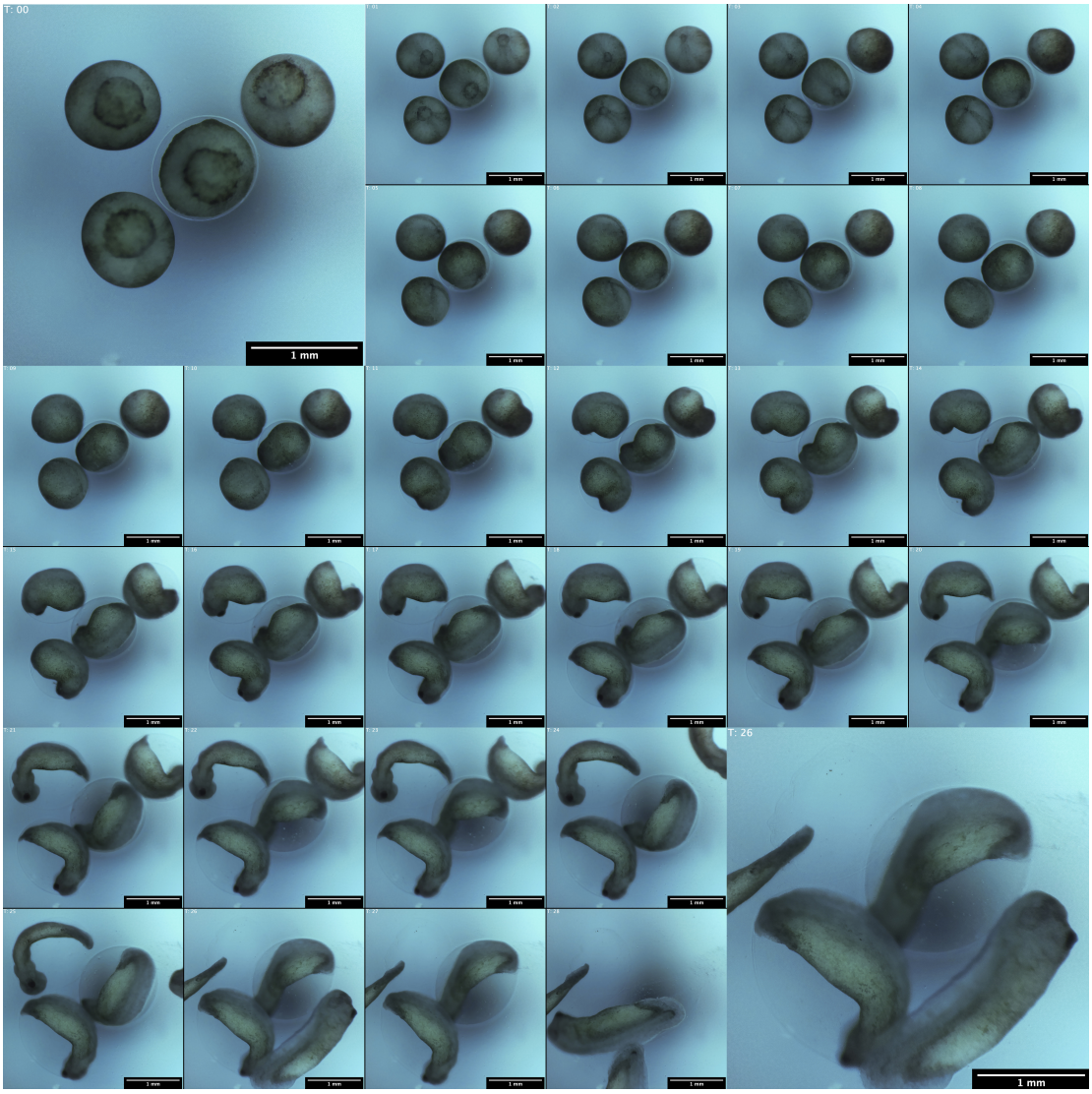

Figure 7.2: Longitudinal imaging of *Xenopus tropicalis* development. Images of a representative well in which 4 frog embryos developed over a 28 hours period. Images were taken hourly.

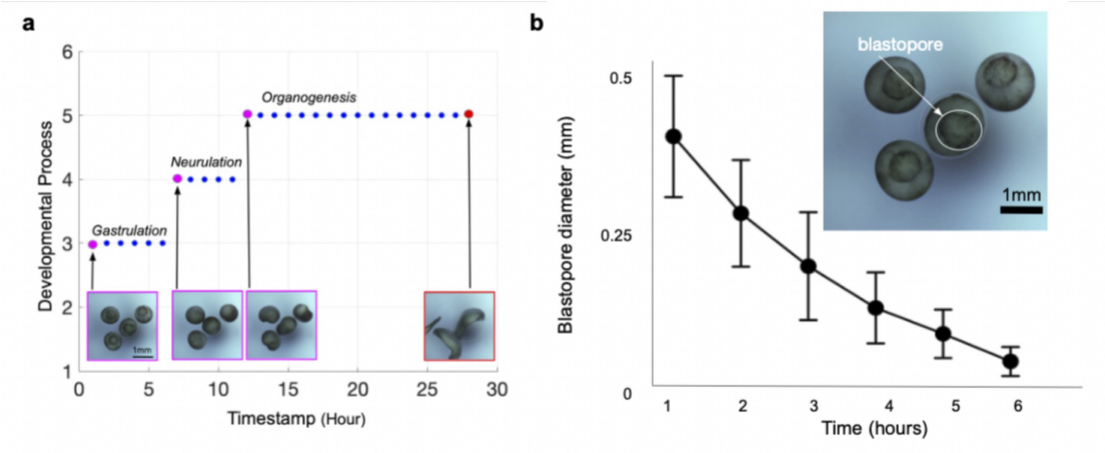

Figure 7.3: Longitudinal imaging allows the tracking of individual developmental processes: a The images shown in figure 7.2 were taken hourly over a 28 hours period and encompass 3 developmental stages: Gastrulation, neurulation and organogenesis. Y-Axis represents the stages of frog embryonic development: 1 = Fertilization , 2 = Cleavage, 3 = Gastrulation, 4 = Neurulation, 5 = Organogenesis, 6 = Metamorphosis. X-Axis represents the timepoint at which it occurs. Each dot in the plot represents a timepoint in which the images were taken. Magenta = the beginning of each developmental process. Red = the end of the experiment at 28 hours. Blue = intermediate timepoints. **b** Diameter of the blastopore is reduced over time from gastrulation to neurulation. Top right panel shows an example of an individual blastopore. A total of 27 embryos were considered for the analysis. Error bars represent Standard Deviation.

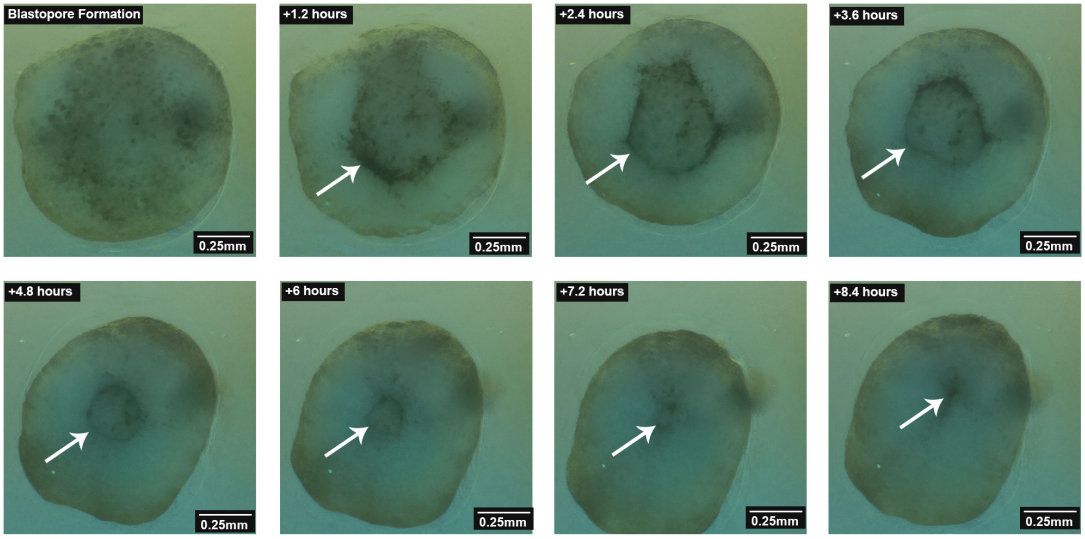

Figure 7.4: Blastopore Closure Selected images during blastopore closure, these are samples from every 5 timesteps during this stage.

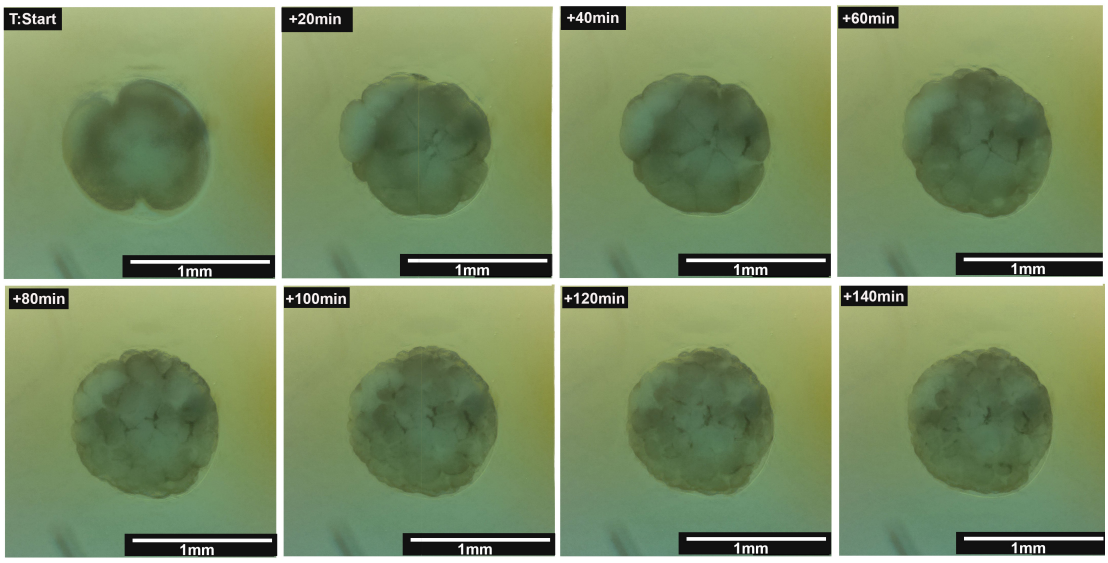

Figure 7.5: Early Cell Divisions The first captured images in our data set show cell divisions as the embryo becomes more complex and individual cells shrink in size.

7.3 Live whole organism imaging: Zebrafish

A picroscope was used in an educational project for AP biology students at a local high school. These students were taking remote classes and did not have access to in-person lab facilities. The students used the Picroscope to measure survival and behavioral changes of zebrafish under the influence of varying concentrations of exogenous chemicals including caffeine and ammonia. This program is discussed in greater detail in chapter 11.

Figure 7.6: Live Imaging of Zebrafish larval zebrafish imaged using a Picroscope device for an educational experiment.

Chapter 8

Applications 2: Cerebral Organoids

8.1 Background

Recent advances in stem cell manipulation have brought about research into "organoids", or stem-cell derived 3D tissue cultures that replicate aspects of complex biological structures. [Kim et al., 2020]. Organoids have opened new doors for in-vitro research on early development of human organs. [Di Lullo and Kriegstein, 2017]

8.1.1 Cerebral Organoids

The promise and limitations of using Human Brain patterned Organoids is reviewed in [Di Lullo and Kriegstein, 2017]. Cerebral Organoids are self organized 3d structures of stem cell derived neurons. They are opening up new avenues of study into human brain development and neurological disorders. There exist a number of different protocols for growing them and results often vary. However

there is still great promise in their use. One application is the creation of patient derived organoids to potentially find genetic triggers for conditions caused by structural issues in the brain.

Organoids developed from the same cell lines under the same conditions often produce tissues with differing structures and cellular identities. Sometimes particular characteristics are observed in a crop of organoids grown together, implying unknown batch effects. More studies with larger numbers of organoids would be useful in assessing their true functionality as models for aspects of brain development. To that end, having a system that can assist in automating the growth and monitoring of these organoids would be quite useful.

8.1.2 Imaging Organoids

[Rios and Clevers, 2018] Lays out current common approaches for imaging fixed and live organoid cultures. Non-invasive methods for capturing 3D images.

For fixed organoids immunolabeling and clearing methods have allowed scientists to see many more 3d structural details within the samples. The authors reference an experiment in which 3D imaging of murine breast organoids revealed that they differentiate into every constituent cell type of breast tissue along with the structural "cellular architecture". They go on to say that 3D volume imaging is likely to become a crucial part of organoid architecture analysis. Longitudinal image studies of live organoids are of interest for observing dynamic processes as high resolution. This is a challenge due to the harmful effects of sustained high intensity light on biological tissue cultures. For longitudinal studies it is best to use a technology that doesn't interfere with the growth and health of the sample. To this end Light-sheet microscopy is a desirable technology as it is capable of caputuring high resultion image data with minimal light exposure. This is because

the light-sheet illuminates only the focal slice of the sample.

The importance of longitudinal image studies are apparant in applications where scientists want to observe many samples at once, possibly to determine the effects particular environmental factors can have on the sample. The authors cite studies in which human colorectal cancer organoids were used to model the sequence of genetic alterations that lead to malignant behavior. This was done by using CRISPR to modify different DNA sequences in several parallel cultures. Having a non obtrusive lognitudinal imaging platform would allow for experiements like this to scale into the thousands of parallel organoids with minimal increases in the human intervention needed to monitor them.

8.2 In-incubator imaging of human embryonic stem cells and cerebral organoids

While many biological systems including zebrafish, planaria and frogs develop at room temperature and atmospheric gas concentrations, mammalian models require special conditions requiring an incubator enclosure.

Mammalian models include 2D monolayer cell cultures, as well as 3D organoid models of development and organogenesis [Mostajo-Radji et al., 2020].

They have been used to assess molecular features and effects of drugs for a variety of phenotypes including cell proliferation,[Abe-Fukasawa et al., 2018, Zhao et al., 2009] morphology [Almassalha et al., 2016, Martin et al., 2014] and activity [Dempsey et al., 2016, Honarnejad et al., 2013], among others.

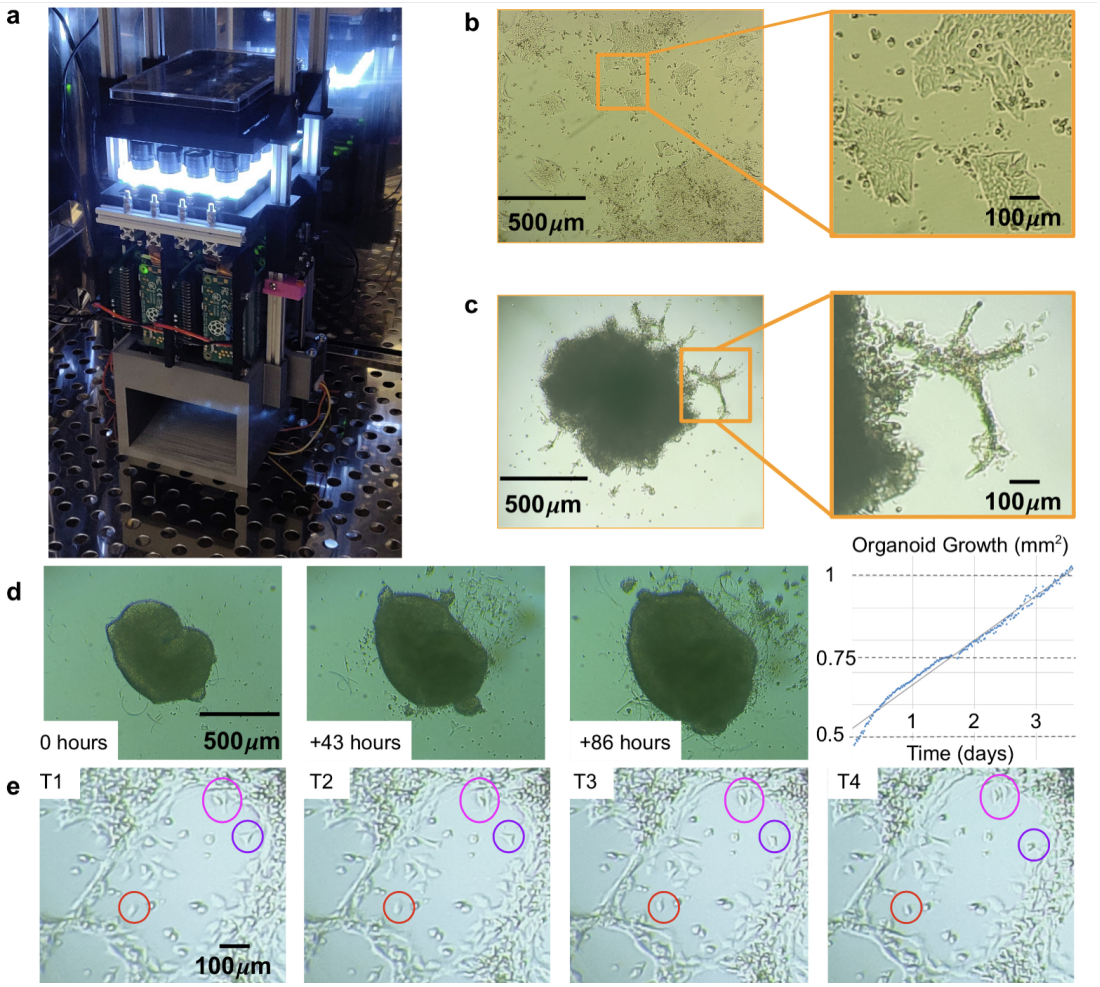

Figure 8.1: In-incubator imaging of mammalian cell and cortical organoid models. **a** The Picroscope inside a standard tissue culture incubator. **b** Imaging of human embryonic stem cells as a model of 2D-monolayer cell cultures. **c** Longitudinal imaging of human cortical organoids embedded in Matrigel. Zoomed images show cellular outgrowths originating in the organoids. **d** Tracking of cortical organoid development over 86 hours. Images were taken hourly. On left. Images of the tracked organoid at timepoints 0, 43 and 86. On right. Measurement of organoid area at each time point analyzed. **e** Manual Longitudinal tracking of individual cells in embedded cortical organoids over 40 minutes. Images were taken every 10 minutes. Magenta = example of cell division, Red = example of cell migration, Purple = example of morphological changes.

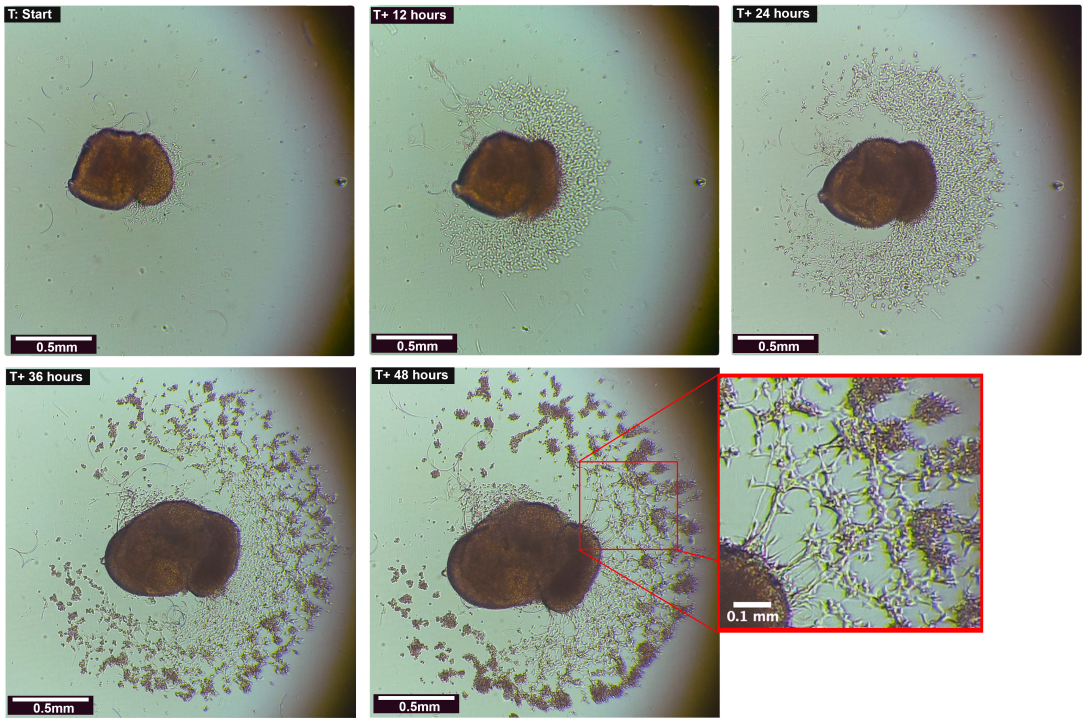

Figure 8.2: Human Cortical Organoid with Outgrowths: Organoids were plated on laminin coated 24 well plates and allowed to adhere to the surface. Outgrowths and cellular migration were restricted to the 2D plane of the plate's surface and captured/monitored over the course of 21 days. Significant morphological changes occurred within the first 48 hours after imaging began.

8.3 Conclusion

To date, few 3D printed microscopes are designed to function inside incubators[Kim et al., 2012, Kim et al., 2016b]. We have run the Picroscope in the incubator for three weeks. This makes the Picroscope compatible with screens in 3D mammalian models including organoids [Renner et al., 2020, Schuster et al., 2020]. We have shown a proof of principle of this function by performing longitudinal imaging of human cortical organoids and analyzing the behavior and movement of individual cells (Figure 8.1). Deploying electronics and 3D printed materials

inside tissue culture incubators presents some unique challenges. The temperature and humidity conditions can cause electronics to fail and cause certain plastics to offgas toxins[Park et al., 2020]. Plastics can also be prone to deformation in these conditions. Additionally, it is important that any device used inside an incubator does not interfere with the conditions required for cell culture. (figure 8.3)

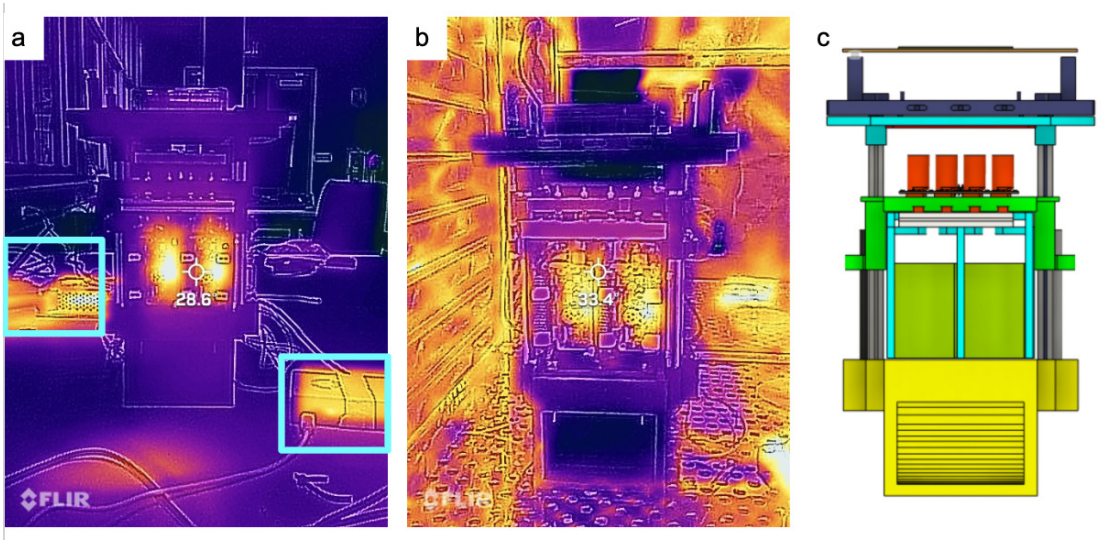

Figure 8.3: Thermal Characteristics of the Picroscope : a. The Picroscope on a lab bench. The two blue boxes indicate components that will not be placed in the incubator. b. The Picroscope during operation inside of an incubator. The temperature of the 24 well plate (1) is not affected by the heatsource (2) c. CAD rendering of the Picroscope (3)indicates the cell plate holder

A common solution for protecting electronics and preventing offgassing is to use inert protective coatings e.g., Parylene C. This requires expensive clean room equipment. Instead we print all of the components with Polylactic acid (PLA), a non-toxic and biodegradable material, to prevent deformation we print using 100% infill and reinforce vulnerable elements with aluminum MakerBeam profiles. We coat all electronic components with Corona Super Dope Coating to protect the electronics from the conditions (heat and humidity) of an incubator.

We tested the functionality of the Picroscope inside a standard tissue culture

incubator by imaging 2D-monolayers of human embryonic stem cells (hESCs) (Figures 8.1a-b). To demonstrate the capacity of our system to perform longitudinal imaging across the z-axis, we imaged human cortical organoids embedded in Matrigel (Figure 8.1c). Using this system we could monitor and measure the growth of the organoids over 86 hours (Figure 8.1d). Tracking of individual cells within organoid outgrowths allowed us observe their migration patterns and behavior (Figure 8.1e). Altogether, we show the feasibility of using our system for longitudinal imaging of mammalian cell and organoid models.

Chapter 9

Integration with Autoculture

Parts of this Chapter were previously published in the Journal Scientific Reports [Seiler et al., 2022]

9.1 Background

9.1.1 Microfluidics

Microfluidics is a field of science and engineering that deals with the study and manipulation of small volumes of fluids, typically in the range of microliters to picoliters, using microfabrication techniques [Whitesides, 2006]. Microfluidic devices consist of microchannels etched into a substrate, typically made of glass, they have found uses in applications ranging from medical diagnostics [Whitesides, 2006] to soft robotics [Filippi et al., 2022].

9.1.2 Microfluidic Lab-on-a-Chip Platforms

A Microfluidic lab-on-a-chip platform is a device that uses microfluidics to move small amounts of fluids to automate biological experiments [Azizipour et al., 2020].

Systems like these can be capable of precise control over the microenvironment surrounding the cells, including the delivery of nutrients and growth factors. This can help to optimize cell growth, and maintain sample health. They can also enable scientists to run experimental screening of many cell culture conditions at once, provided potentially significant reductions in the time and labor typically required for cell culture experiments.

9.1.3 Autoculture

A recent publication presented the "Autoculture" system [Seiler et al., 2022], a microfluidic cell culture automation platform. This platform was used to automate feeding of cerebral organoids and was found to reduce biomarkers of stress, potentially paving the way towards massive parallel experimentation with cerebral organoids.

9.2 Using Autoculture and Picroscope Together

The Picroscope is built to accommodate other modules. A Picroscope device was used in experiments alongside an Autoculture unit to monitor samples being grown and provide real-time feedback from within an incubator. Figure 9.1 shows a 3D render of the autoculture fluidic chip mounted on a picroscope with lines attached. Figure 9.2 shows the system set up inside an incubator to run an experiment.

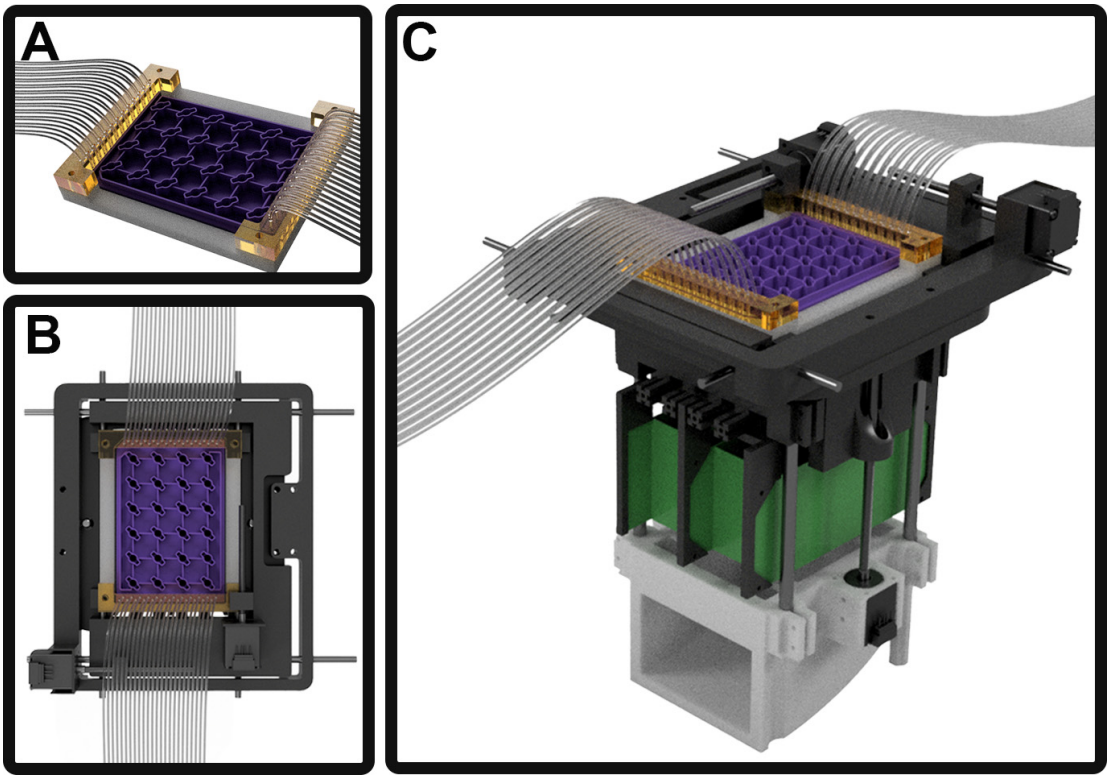

Figure 9.1: CAD renders of Autoculture fluidic chip on Picroscope A: Autoculture chip with microfluidic lines attached, B: Plate mounted on XY translation stage, C: Full Picroscope with attached Autoculture chip

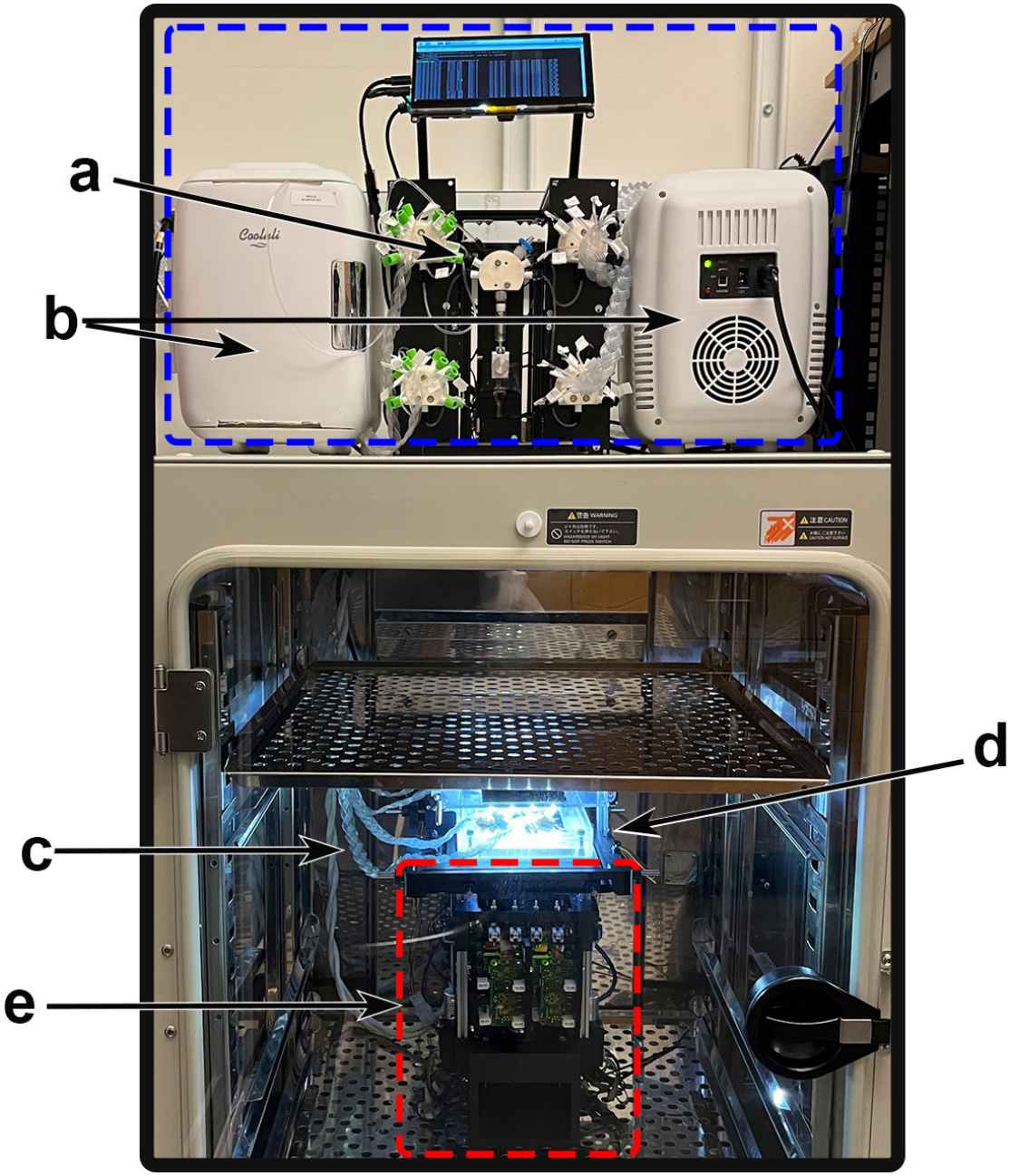

Figure 9.2: Experiment setup for Autoculture and Picroscopea: Autoculture pump system, b: refrigerated fluid storage, c: microfluidic lines attached to (d) the autoculture chip, e: picroscope electronics

With these two devices working in parallel, the Picroscope gathers image data and the cell culture is automatically fed and waste is removed for the entire

duration of the experiment. With imaging and feeding/waste being automated, this lowers the risk of contamination since there is less human interaction with the cell culture.

9.3 Autoculture reduces glycolytic stress in cerebral cortex organoids

A Picroscope paired with an Autoculture system was used in an experiment to monitor a set of organoids over the course of 18 days. The results of this experiment helped to validate the Autoculture system as a viable tool for cell culture automation. [Seiler et al., 2022]

9.3.1 Culture of Cerebral Organoids

The growth of cerebral organoids on *Autoculture* was compared to that of orbital shaker conditions in an 18-day experiment. Human pluripotent stem cells were aggregated to form organoids and maintained under standard conditions for the first 12 days during neural induction. The batch was split, and 12 organoids were loaded onto an *Autoculture* microfluidic chip while the remainder were maintained in a 6-well plate on an orbital shaker as controls.. The automated organoids were fed 70 μL every hour for six days, while the controls were fed 2 mL every other day. In automation, the well plate does not need to be periodically removed from the incubator for feeding; therefore, this system is well-suited for longitudinal monitoring of organoid development. In this study, organoids in the *Autoculture* well plate were monitored once per hour using a Picroscope system

9.3.2 Live Imaging

Figure 9.3A shows the automated, microfluidic culture plate inside an incubator placed on a remote-controlled, IoT-enabled, multi-well automated imaging system. The imaging system was designed to monitor biological experiments in a 24-well plate format, using one dedicated camera for each well. To account for the three-dimensional development of the organoids during the entire experiment, we captured z-stack image data covering the entire three-dimensional tissue. A computer vision algorithm was used to detect the features in focus at each focal plane, generate a composite image maximizing the in-focus features in the entire organoid, and compute the projected area. Figure 9.3B shows 12 cerebral cortex organoid cultures (day 12), loaded in individual wells of the microfluidic chip and fed in parallel on the *Autoculture* platform for the experiment. Figure 9.3C and D show the growth of "Culture 4" over six successive days. Robust organoid growth was observed for the organoids in the *Autoculture* wells and was consistent with the size increase observed for the organoids grown under control conditions. Compared to controls, automated organoids did develop a less-dense perimeter, suggesting that the reduction in velocities and shear forces may accommodate growth and migration that would otherwise be cleaved.

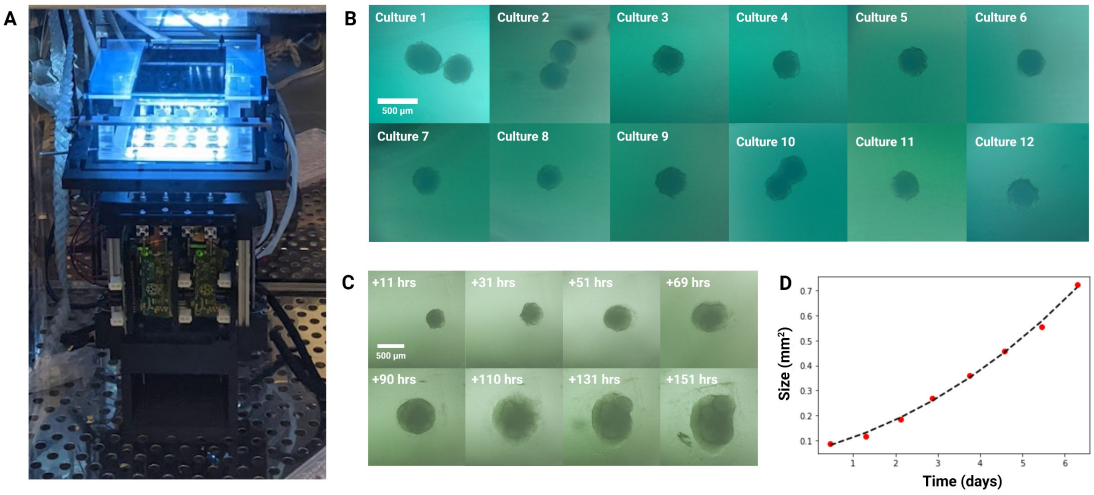

Figure 9.3: Longitudinal monitoring of organoid development. **(A)** The *Autoculture* microfluidic chip sits on a remote-controlled, IoT-enabled, 24-well automated imaging system. **(B)** Bright-field images of twelve individual 12-day-old cerebral cortex cultures at day 1 of automated feeding. **(C)** Longitudinal imaging of "Culture 4" during the experiment. **(D)** Projected area expansion of "Culture 4" during the experiment.

In testing imaging devices with the autoculture system, We noticed that the lighting conditions visibly changed when fluid conditions were modified by the autoculture's microfluidics. This led to the idea that these changes in lighting might be used as sensor feedback to detect issues like clogged lines, or low flow rates. The feasability of sensing changes in fluid from openCArM camera units is explored in chapter 10.

Chapter 10

Optical Detection of Fluid Level in Culture Plates

10.1 Background

The automation of cell culture procedures has the potential to greatly increase the throughput and consistency of cell culture based experiments [Doulgkeroglou et al., 2020]. Manipulation of fluids of is a key feature for any automated culture platform. Systems must have the ability to deliver or move precise quantities of fluids. To automate movement of fluids, some systems use a "lab-on-a-chip" approach [Figeys and Pinto, 2000], utilizing microfluidic channels to transport fluids. Other systems use robot manipulators to deliver measured quantities of fluids with micro-pipettes [Doulgkeroglou et al., 2020, Fleischer et al., 2018, Steffens et al., 2017]. Regardless of mechanism behind the delivery of fluids, being able to detect the presence and volume of fluids within provides key error detection and correction functionality that open loop methods lack.

Surface level measurement within a container of known volume is a simple

way to determine fluid volume. This can be done with electrically active probes dipped into a fluid being measured [Singh et al., 2019]. These probes can be effective but direct contact with the fluid can be problematic for cell culture applications wherein any potential contamination vector increases the risk of failure [Lincoln and Gabridge, 1998]. Non-contact sensing is preferable for sensitive applications. Optical fluid sensing methods take advantage of how fluids interact with light. Several optical approaches for measuring fluids in culture plates exist. One method uses computer vision with well placed light sources and sensors placed at specific angles to measure ray deflection [Jain et al., 2021]. This method uses reflectance of the fluid surface, which makes it usable no matter the solid mass contents of the well. However, the angular requirements of the sensor electronics makes tight packing of independent sensing elements infeasible, making parallel measurements within a plate complex or impossible. Another published method involves imaging the distortions in a printed grid to visualize changes in refraction related to fluid level [Litt, 1989]. While this approach can be used in parallel on many wells at once, it is highly affected by occlusion resulting from material in the plate and can be affected by ambient lighting conditions.

Here we propose a method for non-contact optical detection of fluid level using a CMOS camera sensor and an LED. We detail the principles at work and show a 3D printed device that can be used to perform measurements in 24 well culture plates. Similar to the approach shown in [Litt, 1989], this method relies on the lens-like properties of fluids and the resulting changes of an image viewed through them. Instead of viewing a grid, we detect the apparent size of an overhead light source. Changes in the apparent distance of the light source correlate to changes in fluid level. A bright overhead light source can shine through some samples, making this approach usable in scenarios with solid occlusion that would disrupt

the viewing of a grid. Additionally, the electronics required are set up directly inline with the sample wells, allowing electronics to be packed into a grid allowing parallel sensing of many wells at once.

10.2 Methods

10.2.1 Operating Principle

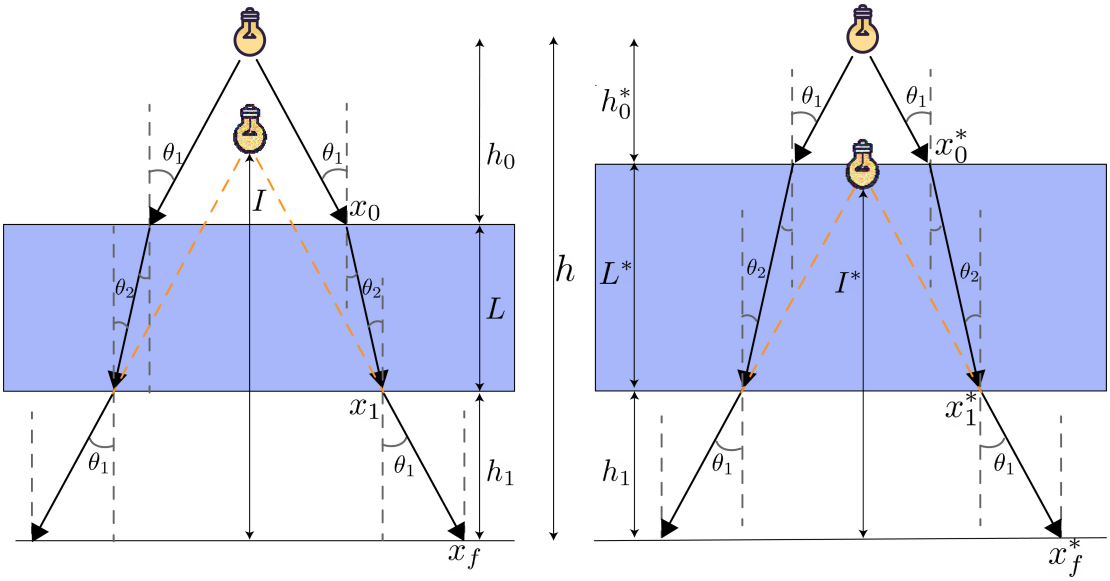

Figure 10.1: Apparent distance of the light source changes based on fluid depth for fluids with index of refraction greater than air (relationship is inverted if index is less than air). Refraction angles can be determined with Snell's law with known indices of refraction of the 2 media ($n_1 sin(\theta_1) = n_2 sin(\theta_2)$). In the case of second transition back into the original medium, the relationship $\theta_3 = \theta_1$ can be derived, hence the labeling of the third angle as θ_1 in this diagram. L = fluid depth, I = apparant distance of object. h_0 = distance between object and top of fluid, h_1 = distance between bottom of fluid and measurement plane.

The measurement principle behind this system relies on the lensing effects of fluids with different indices of refraction. In figure 10.1 the diagrams represent how the apparent distance of the light source changes based on fluid depth. In the

case of a fluid with a index of refraction greater than air (like water), the light source will appear closer as the fluid level increases.

To derive a function relating the fluid depth to the apparent distance of the light source, we define the following constants.

$$C_0 = h - h_1$$

$$C_1 = \tan\theta_1$$

$$C_2 = \tan\theta_2$$

These can be considered constants because our light source sends rays in all directions below it, so any angle θ_1 can be chosen so long as it results in a ray that intersects the fluid, and from this chosen angle θ_2 can be derived via Snell's Law. In terms of these constants the resulting transfer function is:

$$I = \frac{L(-C_1 + C_2) + h_1 C_1 + C_0 C_1}{C_0}$$

This function relates the apparent distance of the image I to the fluid level L and is a first degree polynomial. The full derivation can be found in appendix section A.2. This function is a useful approximation that ignores several factors including refraction caused by the plate material and refraction from the meniscus geometry of the fluid surface, our data show that accurate results can be obtained with this approximation in most scenarios. Meniscus has a substantial effect on measurement in two extremes, an almost empty well, and an almost full well. These meniscus effects are further explored in section 10.3

The polynomial can be characterized analytically so long as we can determine how the image distance relates to size on the camera sensor. This can be determined

by taking a picture of a ruled measurement calibration slide at several known distances. It can also be characterized by a simple calibration step, being that the relationship is linear, a 2 point calibration would theoretically be sufficient, but for greater accuracy a 5 point calibration would be more prudent. Once this polynomial is characterized, image data is sufficient for capturing fluid level

10.2.2 Hardware

To test this approach, we designed a 3D printable rig that holds a raspberry pi camera and a white LED. Figure 10.2 shows 3D renders of the parts comprising the measurement device and figure 10.3 shows the experimental setup.

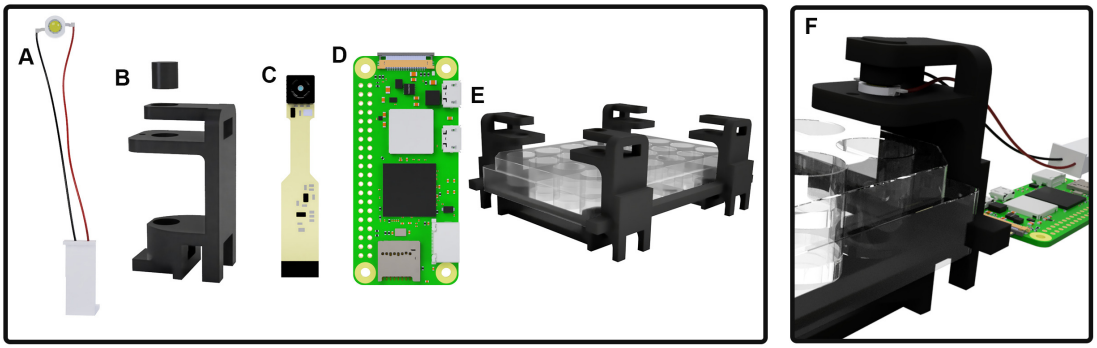

Figure 10.2: 3D renders of measurement rig A: a 3W white LED, B: 3D printed enclosure with a plug to hold the light in place, C: Raspberry Pi Spy Camera, D: Raspberry Pi Zero W, E: rigid plate holder, F: experimental setup. Rendered using Fusion360, real setup shown in figure 10.3

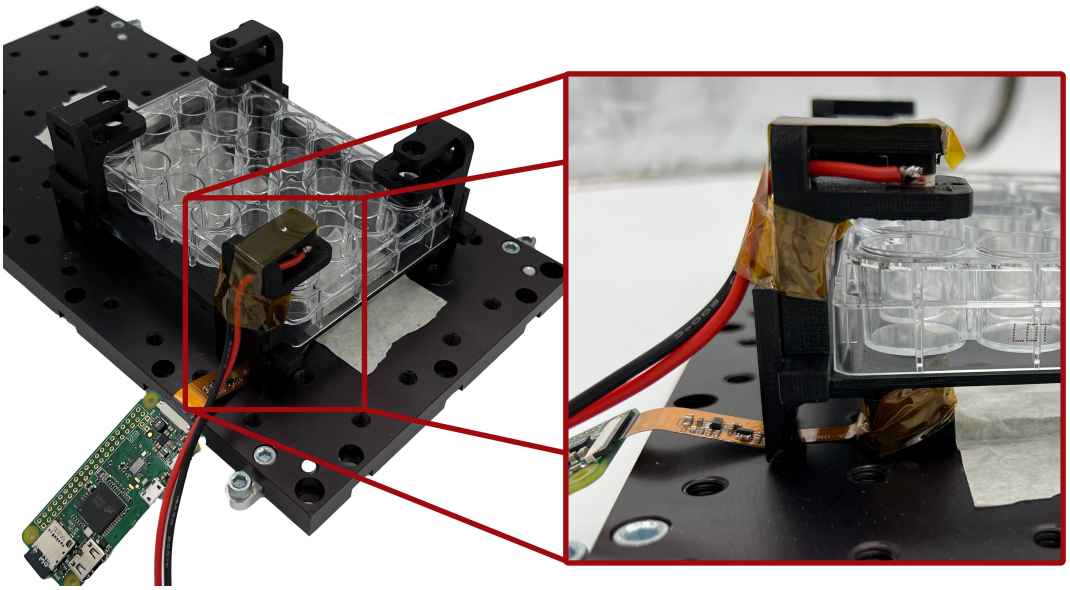

Figure 10.3: Experimental setup with 24 Well plate

10.2.3 Analysis Pipeline

Using openCV [Bradski, 2000], a free and open-source machine vision toolkit, we can capture and measure the size of spot light image. This can be done on static images or on videos including live feeds. We do this by detecting the central contour in the image and fitting an ellipse to it. The result can be calculated fast and is robust to occlusion and noise. In order to do this On the raspberry pi zero we run a video stream using the open-source RPi Cam Web Interface [silvanmelchior, 2023]. The python code for this image analysis is lightweight and can be run internally on the raspberry pi or on an external system. For external system use, the code grabs frames from the MJPEG stream generated by the camera web interface.

Figure 10.4 details the process through which a data point is obtained. Once an ellipse is fit to the central contour of the image, we filter the output by accepting the average value of a rolling buffer when the standard deviation of that buffer

falls below a threshold value. This is to compensate for the disturbance of the fluid surface when new fluid is added or if the plate is shaken. By only accepting reads when the reading has stabilized, we avoid wildly fluctuating erroneous readings any time the fluid is disturbed.

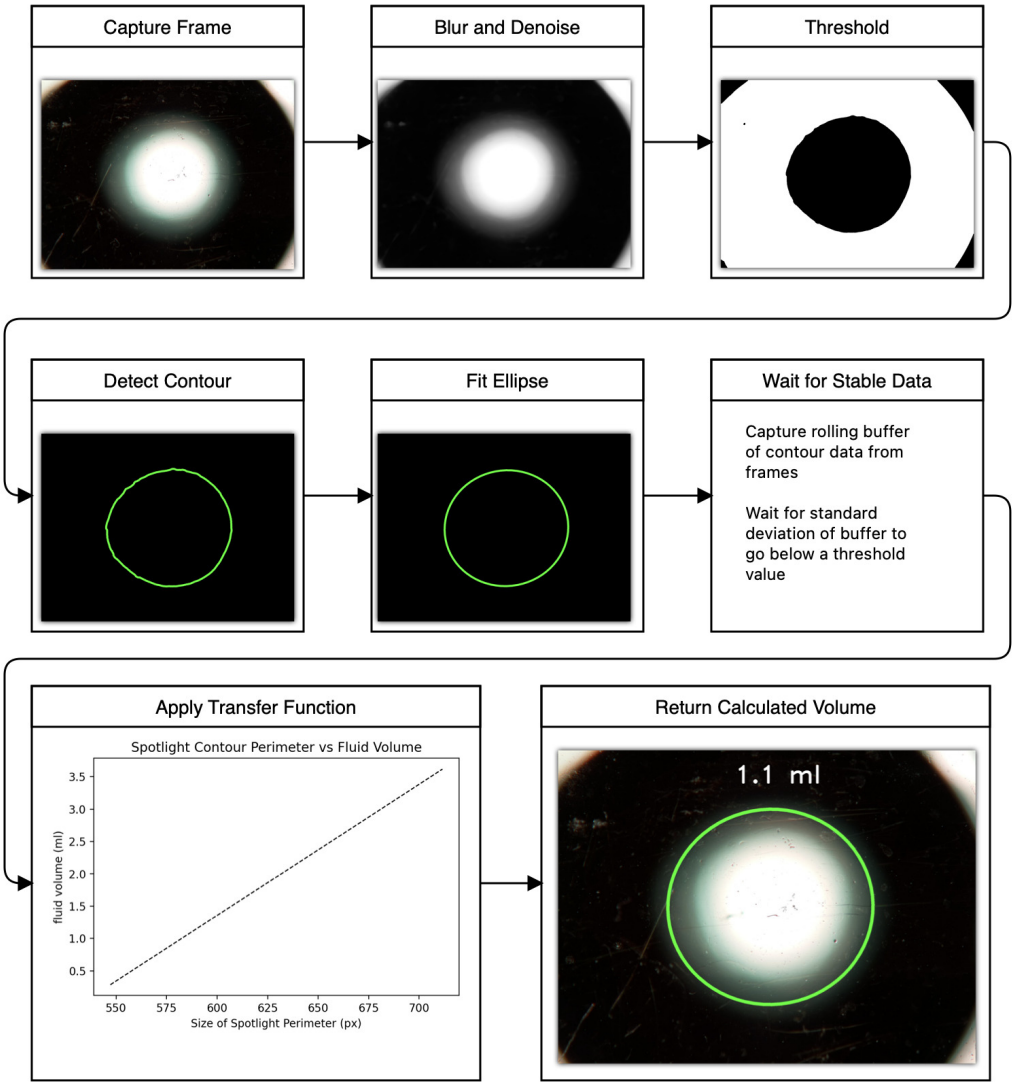

Figure 10.4: Flowchart representing detection process pipeline

10.3 Results

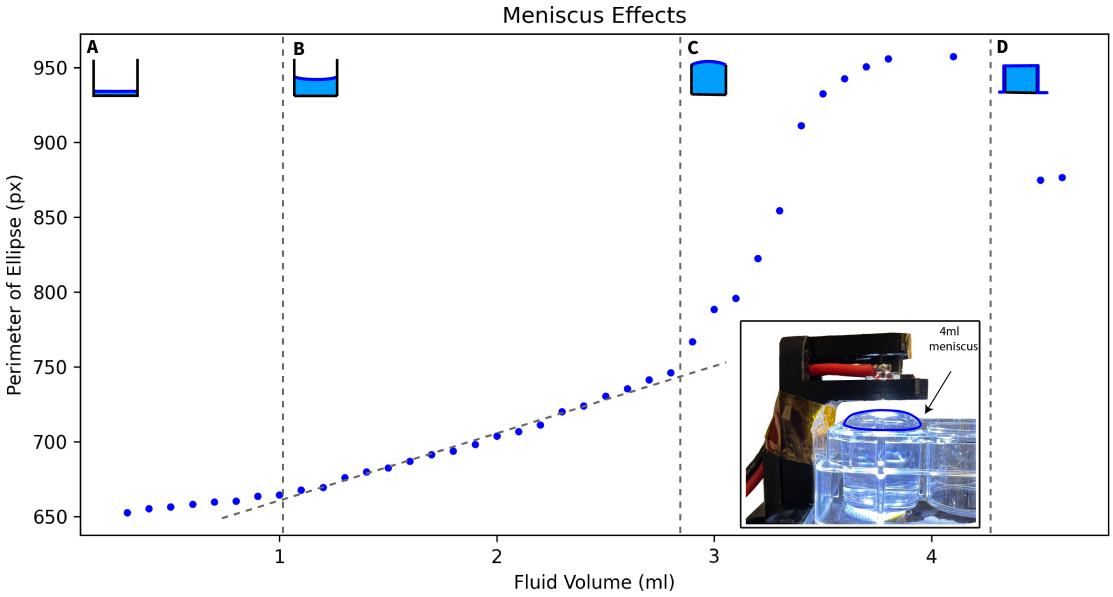

Figure 10.5: Contour ellipse perimeter as a function of fluid volume. Region A shows behavior before meniscus has reached stable geometry. Region B has stable meniscus and shows linear response as predicted in section 10.2.1, Region C shows when the well begins to get full, the surface tension causes Meniscus Inversion. Region D is where fluid has spilled over the edge of the well, flattening the meniscus.

The plot shown in figure 10.5 shows the output of our sensing system for from the first possible reading to the overflowing of the well. Figure 10.8 shows why the first possible reading from a previously dry well occurs around 0.4ml. When the fluid level is very low in a well, the geometry of the meniscus cannot fully form. The center of the meniscus will rise more slowly before the full geometry of the meniscus is formed, this is because of the fluid volume held in the meniscus edges. Therefore, before the full formation of the meniscus, the overhead light image viewed from the center of the meniscus grows more slowly up until point A shown in figure 10.5. As the well starts to get full, a new distortion of the meniscus geometry occurs due to the surface tension of the fluid. The image grows

substantially faster due to the magnifying properties of the convex meniscus, this phenomenon begins at point B. Finally, when the well overflows, the meniscus flattens resulting in a final level of unchanging magnification beginning at point C.

The region between points A and B are where this sensing process will be most generalizable, as the relationship between the spotlight image contour size and the fluid level is highly linear.

10.3.1 Calibration

Deriving an effective transfer function for this system can be done by fitting a curve to a set of calibration points. Deciding on the best fit curve is a question of trade offs. The phenomenon we are measuring is linear within the range of volumes that have a stable meniscus geometry. A simple 2 point linear fit with points from the linear region, generates outputs with average error below 100μl within the linear range. Outside this range, the estimation error increases substantially.

In order to represent the entire curve, we need a high order polynomial fit. Using a least squares approximation method, we can fit polynomials to any subset of points we choose. Considering the phenomena shown in figure 10.5, the curve we are attempting to characterize has 3 distinct regions. Calibration points should be selected to include points from each of these regions. Precision measurements of well volume inside the meniscus inversion region is unlikely to be very accurate, as disruptions in surface tension can cause overflow to occur at different points. Therefore for calibration it should be sufficient to model the linear region occurring at the start of meniscus inversion. This is adequate to detect that the fluid level is greater than the capacity of the well. Since the other 2 regions are linear, we can adequately fit a curve with 2 data points selected from each region. Comparisons of different order curve fits can be seen in figure 10.6

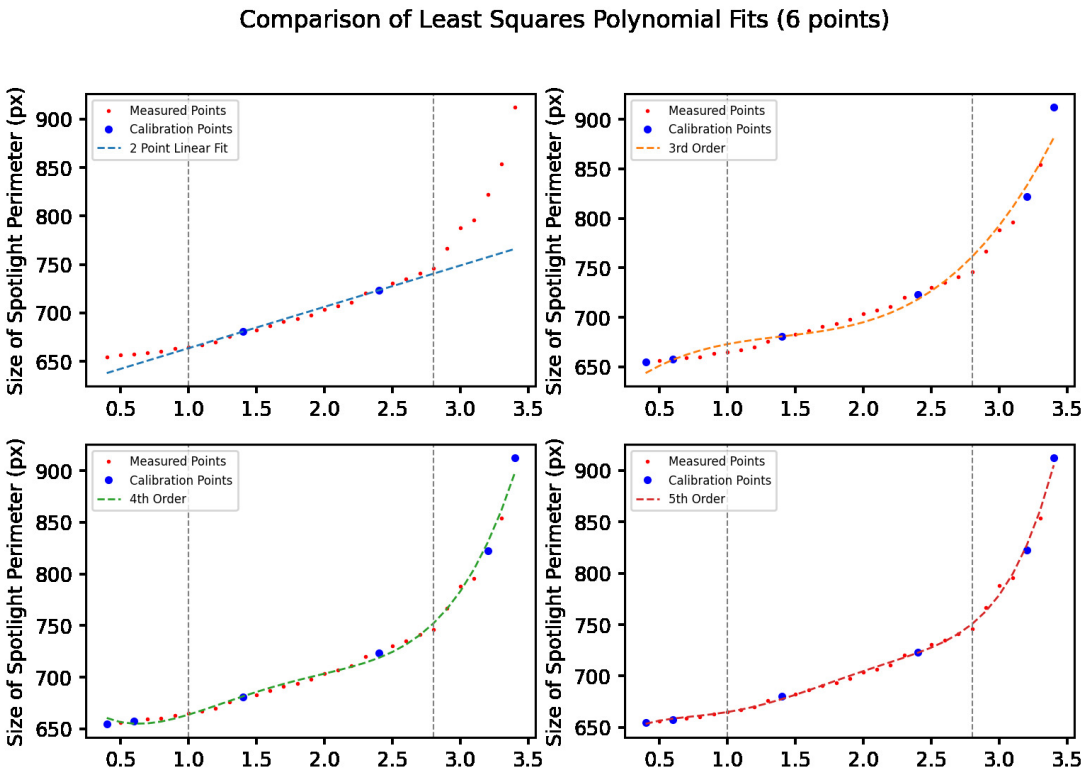

Figure 10.6: Curve comparisons Comparing 2 point linear fit with 6 point least square polynomial fits of different orders

Generalizability of transfer function

To evaluate the consistency of this measurement principle, data was captured in 2 different wells during 2 different runs. The resulting error magnitudes are shown in figure 10.7

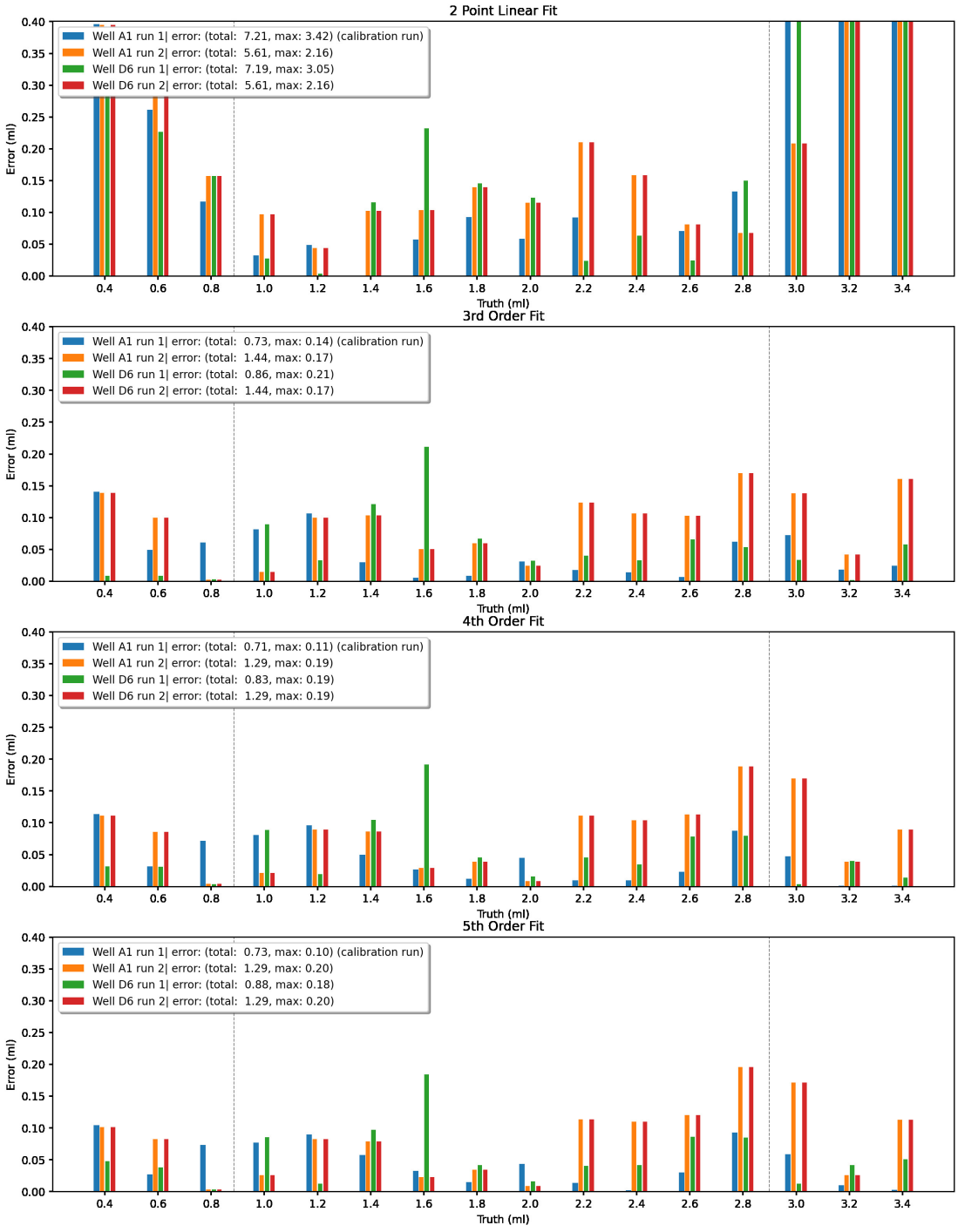

Figure 10.7: Error Comparison Comparing errors across 4 runs for various polynomial fits

As expected, the error from the 2 point linear fit is substantial outside the

central linear range, but within this range, the measurement error can be reasonable depending on the precision needs of the user. Having the option of a simple 2 point calibration for certain uses is an advantage. The other polynomial fits use the 6 points shown in the curve in figure 10.6. It is interesting to note that the 4th order curve fit performs better than the 5th order fit. Most datapoints shown fall within $100\mu l$ error with occasional outlier measurements with a maximum error of $190\mu l$. Knowing this measurement precision means that volumetric fluid dosing measured with this particular implementation of this principle should be tolerant to errors up to $190\mu l$.

10.3.2 Dry Well

When a well is completely dry, droplets hold their shape rather than forming a layer along the bottom. Once 0.5ml have been placed in the dry well, a layer adheres to the bottom and the measurement starts to work. This is shown in figure 10.8 The well can also be moistened beforehand with a small amount of water, doing so disrupts the formation of droplets and allows the measurements to work at smaller fluid volumes.

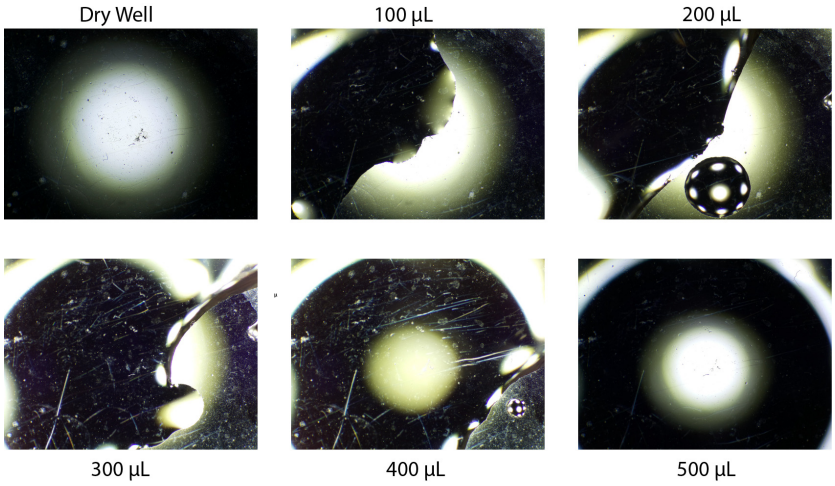

Figure 10.8: Limitations with dry wells before a fluid film has formed across the dry bottom of the well, measurements have no significance

10.4 Conclusion

By leveraging the availability of low cost camera hardware and open source machine vision tools, devices that use computer vision for sensing tasks are likely to become more ubiquitous. The proliferation of cheap mass-produced camera sensors is an opportunity for designers to consider many new methods of measurement.

The device shown here serves as a simple proof of concept for the use of this fluid level measurement principle. For practical purposes, this should be deployed with many cameras in parallel, each monitoring a single well. Previous work has been published laying out the design and use of a 24 well parallel microscope system using similar camera hardware and LEDs, this system is called the "Picroscope" [Ly et al., 2021, Baudin et al., 2021]. The Picroscope is also built to be compatible with a microfluidic cell culture feeding platform [Seiler et al., 2022]. Applying this principle to this system can enable feedback control for fluid contents of the wells in this and other microfluidic "lab-on-a-chip" type systems.

It would also be possible to use this principle without the overhead LED being

permanently affixed above the culture plate. In applications using pipette robots, LEDs could be attached to the end effector, if the arm positions the LED at a known position, spot measurements can be taken and used to detect potential dosing errors or losses due to evaporation.

The principle can also be applied to much larger containers where fluid level measurements are important. Fluid storage containers exist for many applications and while approaches for measuring level in large containers exist, few of those applications are applicable to small volume containers like culture plates. The approach presented here may be broadly applicable to many fields. Furthermore, with different light frequency selections, this principle could be applied to fluids that are opaque in the visible light spectrum but transparent to infrared.

This proposed fluid level sensing method is a simple, reliable, and accurate approach that has been validated for cell culture plates and has potential for uses in other applications.

Chapter 11

OpenCArM Enables Remote Project Based Learning for Biology Classes

Parts of this Chapter were previously published in the journal Heliyon [Baudin et al., 2022]

11.1 Background

11.1.1 Project-Based Learning

Project-based learning (PBL) is an effective approach for teaching complex STEM concepts [Bradforth et al., 2015, Waldrop et al., 2015], particularly for students from backgrounds typically underrepresented in STEM professions[Ferreira et al., 2019, Freishtat, 2014, Hrabowski III, 2011, Bravo-Mosquera et al., 2019]. In PBL, students have the chance to learn in a hands-on matter, investigating deeper questions and discovering truth for themselves

[Ferreira et al., 2019, Serpa et al., 2018, Bravo-Mosquera et al., 2019]. Despite the benefits of PBL, three significant barriers stand in the way of its broad implementation into STEM laboratory courses: 1) high local infrastructural cost required to perform complex PBL projects, 2) limited teacher training, and 3) potential exposure to hazardous materials [Ferreira et al., 2019, Aksela and Haatainen, 2019]. The additional challenges of remote learning further compound these barriers. The lack of an effective replacement for in-person lab activities has caused sub-par learning experiences for students. Finding a way to provide students with the experience of practical project-based lab work is essential if we expect remote classes to work as well as in-person ones.

11.1.2 Remote Lab Experiments

Several systems have been proposed to address this issue by facilitating at-home PBL. Different initiatives and companies have created do-it-yourself (DIY) kits that students can use to perform simple experiments [Rybnicky et al., 2022, Pisarcik, 2021, Marzullo and Gage, 2012, Beattie et al., 2020b]. While intriguing, these kits require the acquisition and shipping of individual kits to each student, group of students, or school [Hanzlick-Burton et al., 2020, McDonnell et al., 2022] and are therefore not scalable, nor can they easily reach isolated communities. Another approach involves creating experiment protocols involving common household items [Al-Soufi et al., 2020, Schultz et al., 2020]. This approach in limited in terms of what experiments can be run and assumes access to a common set of objects. And then there is the simulation approach, wherein students interact with a video game that attempts to replicate the results of a real experiment [Balamuralithara and Woods, 2009a, Dinc et al., 2021]. While clever, these solutions only enable students to explore a few canned options with a predetermined

"right answer," denying them the true experience of scientific experimentation and discovery.

The Internet of Things (IoT) has transformed many fields of society and research, including agriculture [Kour and Arora, 2020], healthcare [Dang et al., 2019] and wildlife conservation [Perera et al., 2019]. Yet, the adoption of IoT in the classroom has been minimal [López-Vargas et al., 2021]. When applied to the remote operation of lab equipment, IoT can be used to facilitate educational lab experiences. Early work using internet-connected single camera microscopes used photophobic organism samples and enabled remote control of light stimulation to create interactive experiments [Kumar et al., 2014, Hossain et al., 2016]. The activities enabled by these devices are short and generally designed to fit in the time frame of a single class session. Programs like this provide a proof of principle for the usability of IoT technologies in education. However, these technologies are not designed to be adaptable for context-informed PBL and running experiments requiring multiple conditions over longer multi-day periods. One recent study used an IoT system in a longer-term experiment. Students remotely monitored soil moisture while evaluating the effects of ground cover on plant seedlings [Tsybulsky and Sinai, 2022]. However, this project was not fully remote and required students to make measurements in person at the site of the experiment, and must therefore be confined to a defined geographical location.

In the world of education, remote lab systems have a history of use as a classroom tool alongside fully simulated lab systems [Gustavsson et al., 2007, Alves et al., 2011, Blazquez-Merino et al., 2019]. Simulated labs have been used as a replacement for, or supplement to, traditional educational lab experience [Balamuralithara and Woods, 2009b, Scheckler, 2003] with the aim of introducing students without access to the necessary experimental equipment and environment

to the experience of the scientific process. However, simulations can never provide students with the experience of actually discovering something new. By contrast, Remote lab experimentation allows students to manipulate live experiments running on real lab equipment from their classrooms, home computers, or their mobile phones. This removes the stale predictability of fully simulated experimentation, giving students a chance to experience the actual scientific process of discovery. Remote microscopy is an important aspect of many of these remote lab experiments [Jones et al., 2003, Wallace et al., 2008, Hossain et al., 2016].

We have developed a framework for facilitating PBL using openCArM based remote-controlled internet-connected microscopes. Through this approach, one lab facility can host an experiment for many students around the world simultaneously. Experiments on this platform can be run on long timescales and with materials that are typically unavailable to high school classrooms. This allows students to perform novel research projects rather than just repeating standard classroom experiments. To investigate the impact of this program, we designed and ran four user studies with students worldwide. All experiments were hosted in Santa Cruz and San Francisco, California, with observations and decisions made remotely by the students using their personal computers and cellphones. In surveys gathered after the experiments, students reported increased excitement for science and a greater desire to pursue a career in STEM. This framework represents a novel, scalable, and effective PBL approach that has the potential to democratize biology and STEM education around the world.

11.2 A Curriculum Roadmap For Remote PBL

We defined a roadmap for designing a curriculum program using a remote microscopy system to facilitate project-based experimental biology. The roadmap

is aimed at research groups interested in using their lab to facilitate a remote PBL program. The program is designed as a supplement to existing biology courses, and facilitators would be researchers from the lab that wish to participate in educational collaboration with a teacher's class. In the weeks leading up to the remote experiment, the facilitators teach supplemental lessons on various scientific topics. The lessons build on the student's current knowledge and prepare them to design their biological experiment. After the experiment, students analyze their findings and present a conclusion to the class. A broad outline of this framework is shown in Figure 11.1.

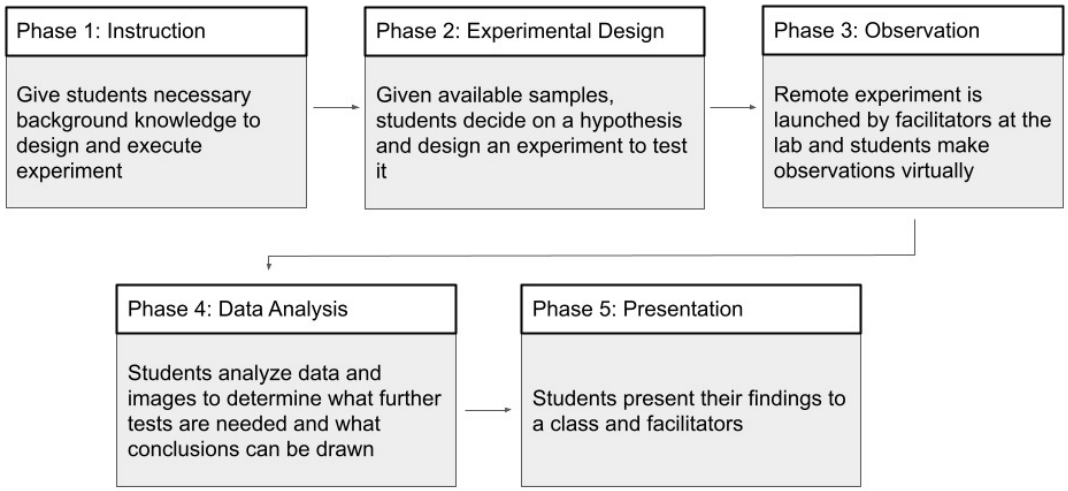

Figure 11.1: Program Roadmap: We developed a program structure with five phases for remote project based supplemental learning.

Phase 1: Instruction Modules

The first phase of this remote experimental biology course is to provide students with the instruction to support them through designing their experiments, collecting and analyzing data, and coming to scientifically supported conclusions. This is

done through a series of lectures and activities in the weeks leading up to the experiment.

Rather than replicating the content the students are already learning in class, facilitators should aim to show students relevant topics from the perspective of a researcher, with a focus on how to approach a subject from an experimental design standpoint.

Phase 2: Experiment Design

After facilitators have run lessons presenting the necessary background knowledge, it is time to design the experiment. A good experiment for our platform is one where the sample requires no maintenance after setup, and the observations of interest are all visual. Facilitators introduce the available biological samples and then guide students through defining a testable question and designing an experiment to address that question. The students will then create a proposal outlining their question, experimental design, and hypothesis to be tested. An example activity to help students propose their hypotheses and design their experiment can be found in Supplemental Note 3. In the example proposal, students are given the experimental question "how do certain drugs affect cancer cell growth?". They then define a hypothesis for their specific drug, determine the dependent variables, independent variables, and controls, and plan out the materials and methods needed to conduct the experiment. With this proposal, the project facilitators will prepare the appropriate samples and set up the remote imaging device. After the setup, the experiment is launched.

Phase 3: Observation

Next, students make observations as the experiment runs in real-time. The most substantial hurdle to conducting a successful remote biology course is providing students with the experience of real-time observations of an experiment that does not have a predetermined outcome. This is the essence of doing science, so this issue must be faced. Once the experiment is launched, the device is set up in such a way as to allow students to make observations from their own cell phones or computers at any time, and they may do so on nights or weekends when there is no facilitator to help them interpret what they are seeing happening in the biological system. These real-time observations are analogous to looking directly through a microscope. Students should capture and log their observations for later use, i.e. keep an elementary lab notebook.

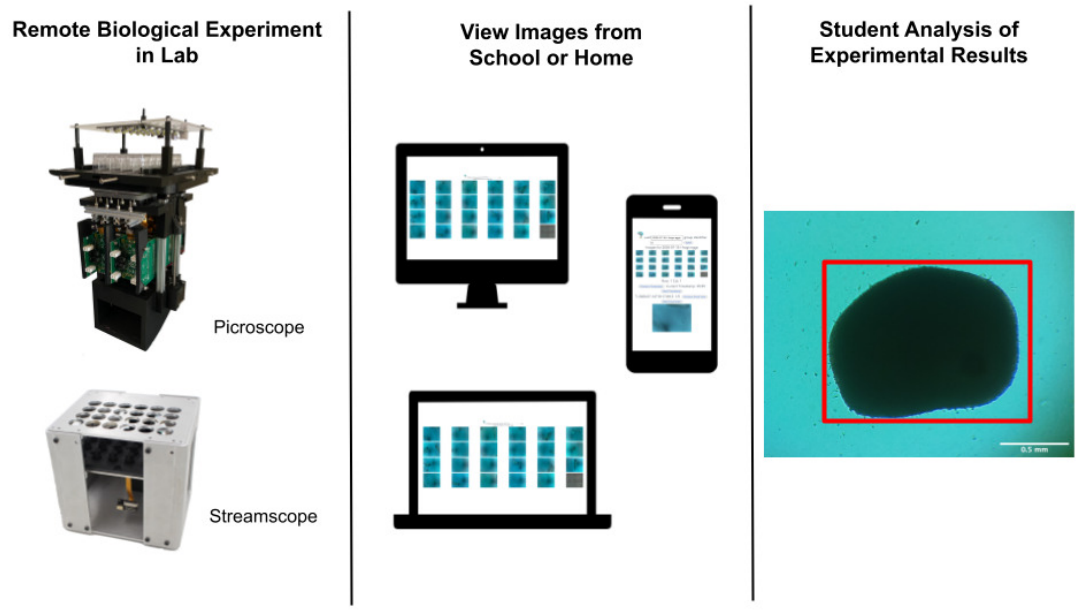

Figure 11.2: Remote experiment workflow. Data is recorded in the remote lab using the Picroscope or Streamscope, viewed from personal devices, and analyzed by the students.

Phase 4: Data Analysis

Finally, the students compile their observations and analyze their data. In addition to live monitoring, time-stamped historical data is also accessible. This allows students to revisit earlier time points to make direct measurements for comparative analysis or make additional observations. Data analysis and the related computer skills required for this are a critical component of modern scientific research that is typically under-emphasized in early college biology coursework [Emery et al., 2021]. By providing students with simple-to-use analysis tools, students are empowered to look closer at what is occurring and draw more interesting conclusions. For an image-based experiment, this can be accomplished with software that allows students to annotate timestamped images in the data set such that features can be visually tracked over time, and students can note observations on them (Figure 11.2).

Phase 5: Presentation

When the experiment has concluded and the data has been analyzed, the students present their findings. They should offer a scientific conclusion based on the data and then defend their analysis against questions asked by the instructors and their peers. Presentations can come in many forms, including live slide show presentations, video production, or written reports. An example of a scientific presentation outline is provided in Supplemental Note 5. This mirrors how new science is reported by professionals working in the field and challenges the students to consider the most effective ways to communicate science.

11.3 Results

11.3.1 Remote PBL Program is Adaptable and Scalable

We ran four experiments with different user groups to evaluate the flexibility of our framework and possible experiments we can run. These experiments allowed us to iterate on the technology, obtaining user feedback and adapting the technique accordingly. We coordinated with local teachers to ensure that the projects related to real-world problems of interest to the students. These experiments were hosted in San Francisco, CA, while students interfaced with them in near real-time from their homes. Experiment details can be found in Table 11.1.

Study 1: Alisal High School (proof of concept, single drug)

As caffeine consumption is higher in student groups compared to the general population [Mahoney et al., 2019], we focused our first study on the effects of caffeine exposure on organism development. Students in the AP Biology course at Alisal High School in Salinas, CA observed the effects of three different caffeine concentrations in developing zebrafish embryos. Observations included effects in the whole body, such as movement and twitching, and effects on specific organs, such as the heart. This was our first user study and was important in determining the feasibility of the program with a relatively simple experimental condition

Study 2: Alisal High School (multiple drugs)

A second user study with a new cohort of AP Biology students also from Alisal High School focused on the effects of common byproducts of agricultural activities. We focused on three chemicals: 1) ammonium nitrate, a chemical commonly used in fertilizers [Chien et al., 2011], 2) nicotine, which has historically been used as

a pesticide and is the chemical basis of several modern neonicotinoid pesticides [Jacobson, 1989, Jeschke and Nauen, 2008], and 3) caffeine, a contaminant found in cultures of several plants and crops [John Hendel et al., 2006]. The students observed the effects of these chemicals in the developing zebrafish embryo. Descriptions of their observations unveiled novel discoveries, such as a delay in fin development in zebrafish exposed to ammonium nitrate (Figure 11.3). Measuring the effects of multiple drugs increased the complexity involved and helped to evaluate any pain points that may arise with more complex experiments. We found our framework suitable for facilitating this more complicated experiment.

Study 3: Five Countries (simultaneous multinational access)

While there are variable degrees of Internet reliability throughout the United States, availabillity of high speed internet is relatively high compared to the rest of the world [Tang and Ho, 2019]. To understand if places with less reliable internet could adopt IoT-enabled PBL, we performed a user study with 20 students in five countries: Brazil, Bolivia, Spain, Mexico, and Peru. The study complemented an online outreach activity by a United States-based non-profit organization Science Clubs International, which targets high school and early college students in the named countries. The students used remote microscopy to perform biocompatibility studies of custom-made gold and graphene nanoparticles and determine the optimal concentration of such particles to be used in the bioengineering context. This study demonstrated the flexibility of our program and showed that it can simultaneously serve students in different places around the world with varying levels of connection reliability.

Study 4: Bolivia (scalability to large user group with limited internet access)

In our fourth user study, we focused on scalability. We performed a user study complementing a pharmacology college-level course in Bolivia. This course had over 130 students enrolled across four cities in the country: Santa Cruz de la Sierra, La Paz, El Alto, and Cochabamba. Bolivia has the slowest Internet connection in South America, which makes remote education challenging. Indeed, the government and the education sector have often turned to television and radio as means to conduct large-scale remote education in situations such as the COVID-19 pandemic [Torrico et al., 2021]. In this study, the students tested the toxic effects of chlorine dioxide in animal physiology. Chlorine dioxide is a type of industrial bleach that became highly popular in Latin America during the COVID-19 pandemic, as several politicians promoted its use to prevent SARS-CoV-2 infection [Mostajo-Radji, 2021]. This experiment demonstrated that the system performs well with many more users than were involved in our previous studies. The ability for students to view prior data compensated for any temporary gaps in internet coverage experienced by the users.

Experiment Theme	**Biological Sample**	**Experiment Condition**	**Number of Users**	**Geographical Area**	**Distance from the experiment**
Effects of caffeine on development	Zebrafish embryos	Caffeine	12	Salinas, CA, USA	170 Km.
Effects of agriculture byproducts on development and physiology	Zebrafish embryos	Ammonium nitrate, nicotine and caffeine	20	Salinas, CA, USA	170 Km.
Biocompatibility of nanoparticles	Zebrafish embryos	Gold and Graphene Nanoparticles	20	Bolivia, Mexico, Peru, Brazil, and Spain	Up to 9,700 Km.
Toxicity of chlorine dioxide	Zebrafish embryos	Chlorine dioxide	131	Bolivia: Santa Cruz de la Sierra, Cochabamba, La Paz, and El Alto	Up to 8,700 Km.

Table 11.1: Summary of user studies performed.

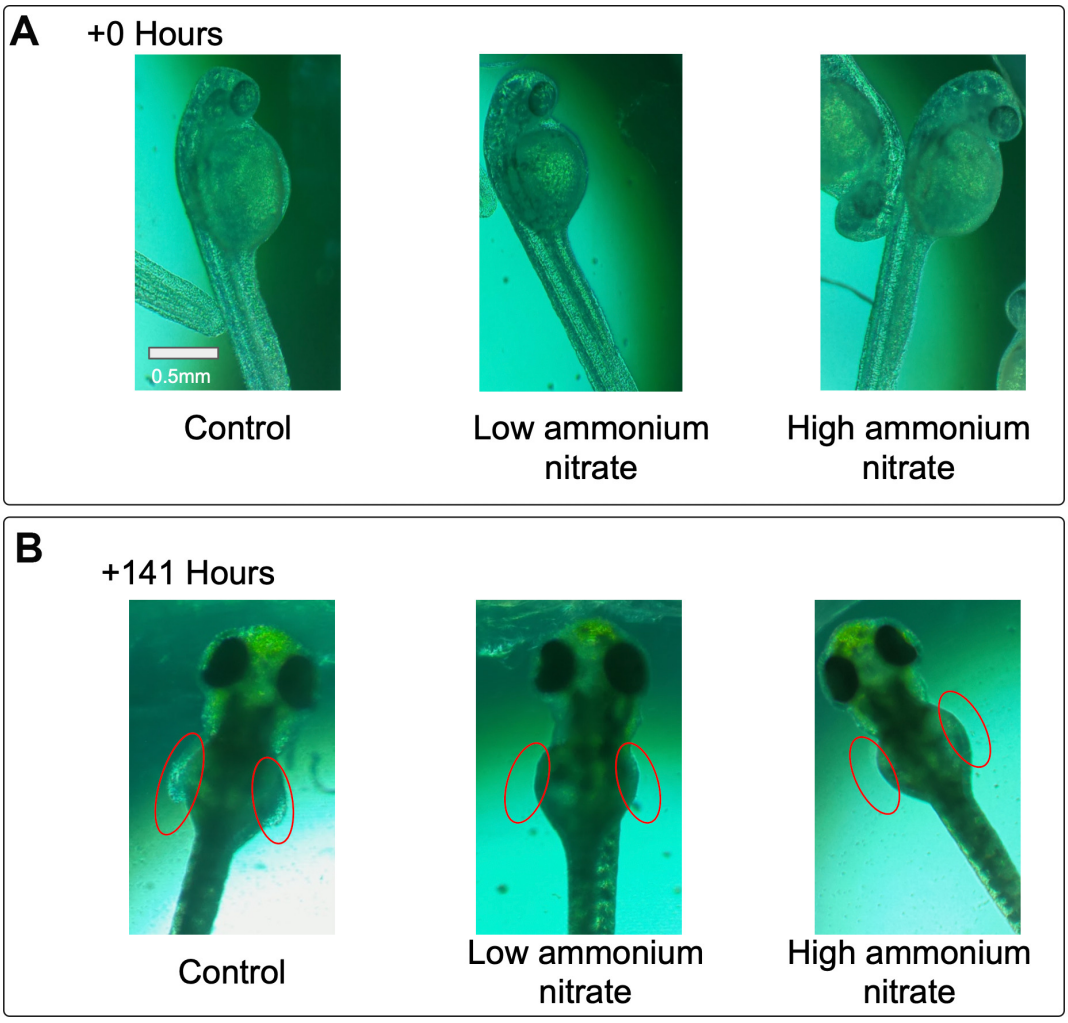

Figure 11.3: Context-informed PBL using whole organisms. Students tracked the effects of chemicals, such as ammonium nitrate, in the development of zebrafish embryos. Representative images over a 141 hours show that ammonium nitrate affects fin development. A) Example of zebrafish embryos at the beginning of the experiment. B) Example of zebrafish embryos after 141 hours show a delay in fin development in low and high concentrations of ammonium nitrate.

11.4 Conclusion

Education technology 'megaprojects' such as the "One Laptop per Child" project [Cristia et al., 2017] and "EdX" [Ch and Popuri, 2013] have shown that access to

technology alone is ineffective at helping underrepresented students [Freire, 2019, Warschauer et al., 2011]. Therefore, novel approaches that can integrate scalable technologies with proven successful teaching methodologies are needed to target students effectively [Sandrone et al., 2021].

We used IoT-enabled microscopy to complement high school and college biology courses for student populations in the United States, Bolivia, Brazil, Spain, Colombia, and Mexico. Our framework allows for the instruction of the students in their native language using PBL and was adapted to a variety of real-world projects, such as caffeine consumption in students, agriculture chemical exposure, and pharmacology.

A unique aspect of this remote PBL paradigm is that it allows students to run experiments using materials that would otherwise be inaccessible due to their hazardous potential or the difficulty of transporting them to remote locations. For example, the AP Biology and college general biology curricula include content on mammalian cellular biology [Byrd, 2007]. Yet, experiments in those courses have been limited in scope, focusing on microbiology or plant biology [Flores, 2013]. Students are usually not exposed to experimental mammalian cell and tissue culture until upper division college courses [Barrera and Hurst-Kennedy, 2019]. Given the differences in cellular biology between life kingdoms, there is a disconnect between theory and practice in high school and lower-level college biology courses. We addressed this disconnect by creating a context-informed project centered on the culture of neuroblastoma cells and the effects of various drugs on those cells. These "clinical trials in a dish" expose students to many facets of scientific work and introduce them to career paths in STEM that may have been unknown to them, including biochemistry, analytical chemistry, and bioinformatics. Most surveyed students self-reported that this program positively impacted their interest

in science and pursuing scientific careers, and we expect that this will be important for increasing diversity in STEM.

Chapter 12

Discussion

12.1 Impact of Picroscope on the research landscape

The combination of 3D printed technology and open-source software has significantly increased the accessibility of academic and teaching laboratories to biomedical equipment [Pearce, 2012]. Thermocyclers, for example, were once an expensive commodity unattainable for many laboratories around the world [Mendoza-Gallegos et al., 2018, Carosso et al., 2019]. Now, low cost thermocyclers have been shown to perform as well as high-end commercially available equipment [Kwon et al., 2016]. Inexpensive thermocyclers can be used in a variety of previously unimaginable contexts, including conservation studies in the Amazon [Byagathvalli et al., 2019], diagnostics of Ebola, Zika and SARS-CoV-2 [Byagathvalli et al., 2019, González-González et al., 2020], teaching high school students in the developing world [Ferreira et al., 2019]and epigenetic studies onboard the International Space Station [Boguraev et al., 2017].

Simultaneous imaging of biological systems is crucial for drug discovery, ge-

netic screening, and high-throughput phenotyping of biological processes and disease [Abe-Fukasawa et al., 2018, Zhao et al., 2009, Martin et al., 2014]. This technique typically requires expensive multicamera and robotic equipment, making it inaccessible to most. While the need for a low cost solution has long been appreciated [Hossain et al., 2016], few solutions have been proposed. Currently, the low cost solutions can be grouped in two categories: 1) those that use of gantry systems that move an individual camera through multiple wells, performing "semi-simultaneous" imaging [Bohm, 2018, Merces et al., 2021, Gürkan and Gürkan, 2019] or 2) those that use acquisition of large fields of view encompassing multiple wells (usually with limited resolution per well, followed by post-processing of images [Klimaj et al., 2020, Kim et al., 2012]. Neither of these solutions is optimal to perform true simultaneous imaging of biological replicates across multiple conditions. To overcome these limitations, the Picroscope performs an automated image capture of a standard 24 wells cell culture plate using 24 individual objectives. The images are then transferred to a remote computer or server (using the Picroscope's internet connection), where they can be viewed and/or processed with minimal intervention.

Commercial electronic systems for simultaneous imaging of biological samples are typically designed to image cells plated in monolayers [Ruckdäschel et al., 2017]. Yet, significant attention has been given to longitudinal imaging-based screens using whole organisms. These have included zebrafish [Early et al., 2018, Tsuji et al., 2014], worms [Lemieux et al., 2011], and plants [Schreiber et al., 2008]. Many times, the results of the screens are based on single plane images or in maximal projections obtained from external microscopes [Lemieux et al., 2011, Schreiber et al., 2008]. The Picroscope was designed to overcome these limitations and image along the z-axis. This is accomplished with

fine adjustment by two stepper motors that lift the elevator unit that holds all 24 camera objectives.

12.2 Limitations

12.2.1 Documentation

OpenCArM provides a lot of functionality but involves many different interconnected systems both within the hardware itself and the data storage and analysis pipelines. There is a level of complexity to this structure that can make it difficult for an interested user starting from scratch. Strong documentation is often what makes or breaks an open source project. While openCArM based systems like the Picroscope have detailed build guides and CAD models available (A.3) A consolidated documentation wiki would greatly improve the experience for designers wishing use openCArM in their systems.

12.2.2 Hardware Dependencies

All current versions of openCArM systems use the Raspberry Pi platform. However, other hardware platforms exist that can interface with camera hardware. These include linux-based single-board-computers like the Nvidia Jetson or the Beaglebone Black, as well as lower level devices like ESP32 based microcontrollers. OpenCArM's current hardware requirement is a limitation and publishing examples of the framework operating on alternate hardware would expand the possible use cases.

12.3 Future Directions

12.3.1 Parallel Fluorescence Imaging

Besides the test slide shown in figure 3.5, the fluorescence module was also tested with a 2D culture of mouse stem cells and fibroblasts. The cells were plated in a 24 well plate and imaged using the fluorescence module. The results are shown in figure 12.1, showing clear differentiation between the fluorescent and non fluorescent cells validates the key functionality of this unit.

Six-well Form Factor

The footprint of the fluorescence module described in section 3.2.2 makes it possible to pack six of them together in the same spacing as a standard 6 well cell culture plate. Enabling an openCArM variant capable of parallel monitoring with fluorescence. This is shown in figure 12.1.

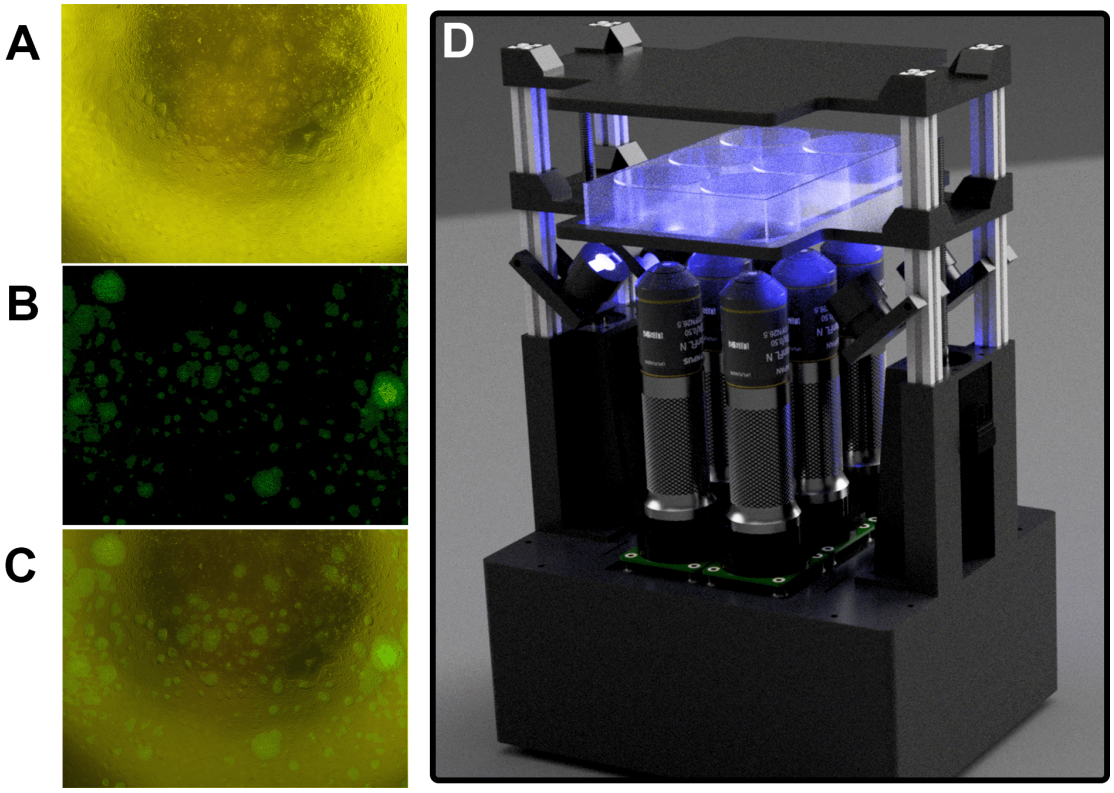

Figure 12.1: openCArM fluorescence functionality looking forward A-C. 2D culture of GFP positive mouse stem cells and non fluorescent fibroblasts. A shows brightfield, B shows green fluorescence, and C shows fluorescence overlaid on top of brightfield to visually differentiate between fibroblasts and stem cells. D: The fluorescence camera unit fits into the form factor of a standard 6 well cell culture plate. Allowing for the future implementation of a device to perform parallel GFP imaging.

12.3.2 Documentation

The openCArM github repository (A.3) has a growing set of documentation. We are currently recruiting interested people to help with the streamlining and maintenance of this knowledge base and are committed to supporting this community effort going forward.

12.3.3 Integrating with other Braingeneers projects

The interaction model provided by the Shadows Database and Control Console has utility beyond imaging systems. Currently we are working on adding remote interaction functionality to other devices in our research group. The BraingeneersPy library (A.3) is an collaboratively built python library provided wrappers that simplify integration of existing systems with the Shadows database and messaging system used by openCArM systems. Furthermore, the fluorescence functionality demonstrated by the unit shown in section 3.2.2 is being integrated into another cell culture automation platform developed within our group with different computer hardware necessitating software specially adapted for this application.

The use of this software with these other systems will require changes and be documented. Providing a model for how openCArM can be adapted for different hardware.

With this system we have provided a low cost solution (costing 88$ per well)[Ly et al., 2021] for biologists to work remotely with greater ease. The result is a sensor-per-well parallel imaging system capable of brightfield microscopy that can be deployed inside a standard CO2 incubator. By having one camera per well, we have an array of microscopes available to researchers allowing them to remotely monitor the development of the biological samples over a long period of time.

Having access to this system allows researchers to easily monitor long term morphological changes in their cell cultures without needing to interfere with their incubator environments. Using Picroscopes also allows for seamless collaboration between researchers at different institutions, allowing them to easily compare cultures as they grow. We envision deployment of many of these systems at once in our lab and collaborator's labs to help push us into an interconnected open source bio-lab of the future.

12.4 Conclusion

We have demonstrated the use of openCArM based systems on a multitude of applications and shown that the design paradigm it enables is a practical and scalable way of building low cost, open source, and modular microscope systems. We have shown that these systems can be used for a variety of applications including remote microscopy, remote PBL, and fluid level sensing in cell culture plates. Furthermore, we have shown that openCArM based microscope systems can be made to be deployed inside a standard CO2 incubator, allowing for low impact longitudinal remote of biological samples over long time scales. We envision deployment of many of these systems in our lab and collaborator's labs will help push us towards an interconnected open source bio-lab of the future.

Appendix A

Appendix

A.1 Fluorescence Camera Module: tube lens position calculation

section text comes from the design notes of Seth Nicholson who worked with me on this project

Given that a standard eyepiece is $14 - 26$ mm, with 17 mm being a common value, and the diagonal of the Pi HQ camera being 7.9 mm, we calculate the magnification as follows:

$$M = \frac{\text{Sensor Diagonal}}{\text{Field Number}} = \frac{7.9}{17} = 0.465$$

If we assume that we are setting the distance between the tube lens and the objective to be 10 mm, then we can calculate the desired focal length of the tube lens using the steps below:

$$f_t = \frac{M}{M-1}p = \frac{0.465}{0.485-1}(10-150) = 121.7$$

Choosing the closest available tube lens, with a focal length of 125 , we confirm that this slightly different f_t value still produces an effective field number between 14 mm and 26 mm.

$$M = \frac{f}{f-p} = \frac{125}{125+140} = 0.472$$

Field Number $= \frac{7.9}{0.472} = 16.75$ Now, we determine q using the equation below:

$$M = \frac{q}{p} \rightarrow q = Mp = 0.472 \times 140 = 66.0 \text{ mm}$$

The total back focal length of the system is just q plus the chosen 10 mm distance between the tube lens and the objective, or 76 mm.

A.2 Fluid Level Measurement: Derivation of Image Distance function

Labeled values are in reference to items in figure 10.1 in chapter 10

$$h = h_0 + L + h_1$$

since h_0 varies with L but h is constant we reframe h_0 as

$$h_0 = (h - h_1) - L$$

$h - h_1$ is constant and we will now label it as C_0

$$C_0 = h - h_1$$

$$x_0 = (C_0 - L)\tan\theta_1$$

$$C_1 = \tan\theta_1$$

$$x_1 = x_0 + L\tan\theta_2$$

$$C_2 = \tan\theta_2$$

$$x_f = x_1 + h_1 C_1$$

$$x_f = (C_0 - L)C_1 + LC_2 + h_1 C_1$$

$$x_f = C_0 C_1 - LC_1 + LC_2 + h_1 C_1$$

$$x_f = L(-C_1 + C_2) + h_1 C_1 + C_0 C_1$$

$$\tan(\theta_1) = \frac{x_f}{I}$$

$$I = \frac{x_f}{C_0}$$

$$I = \frac{L(-C_1 + C_2) + h_1 C_1 + C_0 C_1}{C_0}$$

A.3 Github Repositories

1. Main openCArM repository containing Embedded device firmwares for Picroscope and other openCArM systems openCArM

2. Shadows Database as described in section 5.2 Braingeneers-Shadows-Database

3. Datahub console as described in section 5.3 Braingeneers-Datahub

4. Control Console as described in section 4.5.1 Picroscope-Device-Control-Console

5. Livestream containers are described in section 4.5.2 Raspberry-Pi-Livestream-Tunnel

6. Picroscope CAD files and build guide picroscope-supplement

Bibliography

[Abas et al., 2018] Abas, K., Obraczka, K., and Miller, L. (2018). Solar-powered, wireless smart camera network: An IoT solution for outdoor video monitoring. *Computer Communications*, 118:217–233. Publisher: Elsevier.

[Abate et al., 2012] Abate, P., Di Cosmo, R., Treinen, R., and Zacchiroli, S. (2012). Dependency solving: A separate concern in component evolution management. *Journal of Systems and Software*, 85(10):2228–2240.

[Abe-Fukasawa et al., 2018] Abe-Fukasawa, N., Otsuka, K., Aihara, A., Itasaki, N., and Nishino, T. (2018). Novel 3D liquid cell culture method for anchorage-independent cell growth, cell imaging and automated drug screening. *Scientific reports*, 8(1):1–12. Publisher: Nature Publishing Group.

[Abrahamsson et al., 2013] Abrahamsson, P., Helmer, S., Phaphoom, N., Nicolodi, L., Preda, N., Miori, L., Angriman, M., Rikkilä, J., Wang, X., Hamily, K., and others (2013). Affordable and energy-efficient cloud computing clusters: The bolzano raspberry pi cloud cluster experiment. In *2013 IEEE 5th International Conference on Cloud Computing Technology and Science*, volume 2, pages 170–175. IEEE.

[Aidukas et al., 2019a] Aidukas, T., Eckert, R., Harvey, A. R., Waller, L., and Konda, P. C. (2019a). Low-cost, sub-micron resolution, wide-field computational microscopy using opensource hardware. *Scientific reports*, 9(1):1–12. Publisher: Nature Publishing Group.

[Aidukas et al., 2019b] Aidukas, T., Konda, P. C., Taylor, J. M., and Harvey, A. R. (2019b). Multi-camera Fourier Ptychographic Microscopy. In *Imaging and Applied Optics 2019 (COSI, IS, MATH, pcAOP) (2019), paper CW3A.4*, page CW3A.4. Optica Publishing Group.

[Aksela and Haatainen, 2019] Aksela, M. and Haatainen, O. (2019). Project-based learning (pbl) in practise: Active teachers' views of its' advantages and challenges. *Integrated Education for the Real World*.

[Al-Soufi et al., 2020] Al-Soufi, W., Carrazana-Garcia, J., and Novo, M. (2020). When the kitchen turns into a physical chemistry lab. *Journal of Chemical Education*, 97(9):3090–3096.

[Alessandri et al., 2017] Alessandri, K., Andrique, L., Feyeux, M., Bikfalvi, A., Nassoy, P., and Recher, G. (2017). All-in-one 3D printed microscopy chamber for multidimensional imaging, the UniverSlide. *Scientific reports*, 7(1):1–10. Publisher: Nature Publishing Group.

[Almassalha et al., 2016] Almassalha, L. M., Bauer, G. M., Chandler, J. E., Gladstein, S., Cherkezyan, L., Stypula-Cyrus, Y., Weinberg, S., Zhang, D., Ruhoff, P. T., Roy, H. K., and others (2016). Label-free imaging of the native, living cellular nanoarchitecture using partial-wave spectroscopic microscopy. *Proceedings of the National Academy of Sciences*, 113(42):E6372–E6381. Publisher: National Acad Sciences.

[Alves et al., 2011] Alves, G. R., Marques, M. A., Viegas, C., Lobo, M. C. C., Barral, R. G., Couto, R. J., Jacob, F. L., Ramos, C. A., Vilão, G. M., Covita, D. S., Alves, J., Guimarães, P. S., and Gustavsson, I. (2011). Using VISIR in a large undergraduate course: Preliminary assessment results. In *2011 IEEE Global Engineering Education Conference (EDUCON)*, pages 1125–1132.

[Ambrose et al., 2020] Ambrose, B., Baxter, J., Cully, J., Willmott, M., Bateman, B. C., Steele, E., Cadby, A. J., Shewring, J., Aaldering, M., and Craggs, T. D. (2020). Democratizing Single-Molecule FRET: An Open-Source Microscope for Measuring Precise Distances and Biomolecular Dynamics. *Biophysical Journal*, 118(3):614a. Publisher: Elsevier.

[Araque et al., 2001] Araque, A., Carmignoto, G., and Haydon, P. G. (2001). Dynamic Signaling Between Astrocytes and Neurons. *Annual Review of Physiology*, 63(1):795–813. _eprint: https://doi.org/10.1146/annurev.physiol.63.1.795.

[Azizipour et al., 2020] Azizipour, N., Avazpour, R., Rosenzweig, D. H., Sawan, M., and Ajji, A. (2020). Evolution of Biochip Technology: A Review from Lab-on-a-Chip to Organ-on-a-Chip. *Micromachines*, 11(6):599. Number: 6 Publisher: Multidisciplinary Digital Publishing Institute.

[Baden et al., 2015] Baden, T., Chagas, A. M., Gage, G., Marzullo, T., Prieto-Godino, L. L., and Euler, T. (2015). Open Labware: 3-D printing your own lab equipment. *PLoS biology*, 13(3):e1002086. Publisher: Public Library of Science.

[Baker, 2016a] Baker, M. (2016a). 1,500 scientists lift the lid on reproducibility. *Nature*, 533(7604):452–454. Number: 7604 Publisher: Nature Publishing Group.

[Baker, 2016b] Baker, M. (2016b). Biotech giant publishes failures to confirm high-profile science. *Nature*, 530(7589):141–141.

[Balamuralithara and Woods, 2009a] Balamuralithara, B. and Woods, P. C. (2009a). Virtual laboratories in engineering education: The simulation lab and remote lab. *Computer Applications in Engineering Education*, 17(1):108–118.

[Balamuralithara and Woods, 2009b] Balamuralithara, B. and Woods, P. C. (2009b). Virtual laboratories in engineering education: The simulation lab and remote lab. *Computer Applications in Engineering Education*, 17(1):108–118.

[Barber and Mostajo-Radji, 2020] Barber, K. and Mostajo-Radji, M. A. (2020). Youth Networks' Advances Toward the Sustainable Development Goals During the COVID-19 Pandemic. *Front. Sociol. 5: 589539. doi: 10.3389/fsoc.*

[Barrera and Hurst-Kennedy, 2019] Barrera, A. and Hurst-Kennedy, J. (2019). An inquiry-based laboratory curriculum investigating cell viability using mammalian cell culture and fluorescence microscopy. *Proceedings of the Association for Biology Laboratory Education*, 40:22.

[Baudin et al., 2021] Baudin, P. V., Ly, V. T., Pansodtee, P., Jung, E. A., Currie, R., Hoffman, R., Willsey, H. R., Pollen, A. A., Nowakowski, T. J., Haussler, D., and others (2021). Low cost cloud based remote microscopy for biological sciences. *Internet of Things*, page 100454. Publisher: Elsevier.

[Baudin et al., 2022] Baudin, P. V., Sacksteder, R. E., Worthington, A. K., Voitiuk, K., Ly, V. T., Hoffman, R. N., Elliott, M. A. T., Parks, D. F., Ward, R., Torres-Montoya, S., Amend, F., Montellano Duran, N., Vargas, P. A., Martinez, G., Ramirez, S. M., Alvarado-Arnez, L. E., Ehrlich, D., Rosen, Y. M., Breevoort, A., Schouten, T., Kurniawan, S., Haussler, D., Teodorescu, M., and Mostajo-Radji, M. A. (2022). Cloud-controlled microscopy enables remote project-based biology education in underserved Latinx communities. *Heliyon*, 8(11):e11596.

[Baudin and Teodorescu, 2023] Baudin, P. V. and Teodorescu, M. (2023). A computer vision based optical method for measuring fluid level in cell culture plates. arXiv:2303.14233 [eess].

[Beattie et al., 2020a] Beattie, R., Hippenmeyer, S., and Pauler, F. M. (2020a). SCOPES: Sparking Curiosity Through Open-Source Platforms in Education and Science. *Frontiers in Education*, 5:48.

[Beattie et al., 2020b] Beattie, R., Hippenmeyer, S., and Pauler, F. M. (2020b). Scopes: sparking curiosity through open-source platforms in education and science. In *Frontiers in Education*, volume 5, page 48. Frontiers Media SA.

[Blazquez-Merino et al., 2019] Blazquez-Merino, M., Macho-Aroca, A., Baizán-Álvarez, P., Garcia-Loro, F., San Cristobal, E., Diez, G., and Castro, M. (2019). Use of VISIR Remote Lab in Secondary School: Didactic Experience and Outcomes. In Auer, M. E. and Langmann, R., editors, *Smart Industry & Smart Education*, Lecture Notes in Networks and Systems, pages 69–79, Cham. Springer International Publishing.

[Boguraev et al., 2017] Boguraev, A.-S., Christensen, H. C., Bonneau, A. R., Pezza, J. A., Nichols, N. M., Giraldez, A. J., Gray, M. M., Wagner, B. M., Aken, J. T., Foley, K. D., and others (2017). Successful amplification of DNA aboard the International Space Station. *NPJ microgravity*, 3(1):1–4. Publisher: Nature Publishing Group.

[Bohm, 2018] Bohm, A. (2018). An inexpensive system for imaging the contents of multi-well plates. *Acta Crystallographica Section F: Structural Biology Communications*, 74(12):797–802. Publisher: International Union of Crystallography.

[Bradforth et al., 2015] Bradforth, S. E., Miller, E. R., Dichtel, W. R., Leibovich, A. K., Feig, A. L., Martin, J. D., Bjorkman, K. S., Schultz, Z. D., and Smith, T. L. (2015). University learning: Improve undergraduate science education. *Nature*, 523(7560):282–284.

[Bradski, 2000] Bradski, G. (2000). The OpenCV Library. *Dr. Dobb's Journal of Software Tools*.

[Bravo-Mosquera et al., 2019] Bravo-Mosquera, P. D., Cisneros-Insuasti, N. D., Mosquera-Rivadeneira, F., and Avendaño-Uribe, B. (2019). Stem learning based on aircraft design: an interdisciplinary strategy developed to science clubs colombia. *Ciencia y Poder Aéreo*, 14(1):204–227.

[Brown et al., 2019] Brown, J. W., Bauer, A., Polinkovsky, M. E., Bhumkar, A., Hunter, D. J., Gaus, K., Sierecki, E., and Gambin, Y. (2019). Single-molecule detection on a portable 3D-printed microscope. *Nature communications*, 10(1):1–7. Publisher: Nature Publishing Group.

[Byagathvalli et al., 2019] Byagathvalli, G., Pomerantz, A., Sinha, S., Standeven, J., and Bhamla, M. S. (2019). A 3D-printed hand-powered centrifuge for molecular biology. *PLoS biology*, 17(5):e3000251. Publisher: Public Library of Science San Francisco, CA USA.

[Byrd, 2007] Byrd, S. (2007). Advanced Placement and International Baccalaureate: Do They Deserve Gold Star Status?. *Thomas B. Fordham Institute*. Publisher: ERIC.

[Cai et al., 2020] Cai, F., Wang, T., Lu, W., and Zhang, X. (2020). High-resolution mobile bio-microscope with smartphone telephoto camera lens. *Optik*, 207:164449. Publisher: Elsevier.

[Carosso et al., 2019] Carosso, G. A., Ferreira, L. M., and Mostajo-Radji, M. A. (2019). Scientists as non-state actors of public diplomacy. *Nature human behaviour*, 3(11):1129–1130. Publisher: Nature Publishing Group.

[Ch and Popuri, 2013] Ch, S. K. and Popuri, S. (2013). Impact of online education: A study on online learning platforms and edX. In *2013 IEEE International Conference in MOOC, Innovation and Technology in Education (MITE)*, pages 366–370.

[Chaczko and Braun, 2017] Chaczko, Z. and Braun, R. (2017). Learning data engineering: Creating IoT apps using the node-RED and the RPI technologies. In *2017 16th International Conference on Information Technology Based Higher Education and Training (ITHET)*, pages 1–8, Ohrid, Macedonia. IEEE.

[Chan et al., 2019] Chan, A. C. S., Kim, J., Pan, A., Xu, H., Nojima, D., Hale, C., Wang, S., and Yang, C. (2019). Parallel Fourier ptychographic microscopy for high-throughput screening with 96 cameras (96 Eyes). *Scientific Reports*, 9(1):11114.

[Chan and Yang, 2020] Chan, C. S. and Yang, C. (2020). Parallel imaging acquisition and restoration methods and systems.

[Chien et al., 2011] Chien, S. H., Gearhart, M. M., and Villagarcía, S. (2011). Comparison of ammonium sulfate with other nitrogen and sulfur fertilizers in increasing crop production and minimizing environmental impact: a review. *Soil Science*, 176(7):327–335.

[Coakley et al., 2014] Coakley, M. F., Hurt, D. E., Weber, N., Mtingwa, M., Fincher, E. C., Alekseyev, V., Chen, D. T., Yun, A., Gizaw, M., Swan, J., and others (2014). The NIH 3D print exchange: a public resource for bioscientific and biomedical 3D prints. *3D printing and additive manufacturing*, 1(3):137–140. Publisher: Mary Ann Liebert, Inc. 140 Huguenot Street, 3rd Floor New Rochelle, NY 10801 USA.

[Collins et al., 2020] Collins, J. T., Knapper, J., Stirling, J., Mduda, J., Mkindi, C., Mayagaya, V., Mwakajinga, G. A., Nyakyi, P. T., Sanga, V. L., Carbery, D., White, L., Dale, S., Lim, Z. J., Baumberg, J. J., Cicuta, P., McDermott, S., Vodenicharski, B., and Bowman, R. (2020). Robotic microscopy for everyone: the OpenFlexure microscope. *Biomedical Optics Express*, 11(5):2447–2460. Publisher: Optica Publishing Group.

[Cox et al., 2014] Cox, S. J., Cox, J. T., Boardman, R. P., Johnston, S. J., Scott, M., and O'brien, N. S. (2014). Iridis-pi: a low-cost, compact demonstration cluster. *Cluster Computing*, 17(2):349–358. Publisher: Springer.

[Cristia et al., 2017] Cristia, J., Ibarrarán, P., Cueto, S., Santiago, A., and Severín, E. (2017). Technology and Child Development: Evidence from the One Laptop per Child Program. *American Economic Journal: Applied Economics*, 9(3):295–320.

[Cybulski et al., 2014] Cybulski, J. S., Clements, J., and Prakash, M. (2014). Foldscope: origami-based paper microscope. *PloS one*, 9(6):e98781. Publisher: Public Library of Science.

[Dang et al., 2019] Dang, L. M., Piran, M. J., Han, D., Min, K., and Moon, H. (2019). A survey on internet of things and cloud computing for healthcare. *Electronics*, 8(7):768.

[Dempsey et al., 2016] Dempsey, G. T., Chaudhary, K. W., Atwater, N., Nguyen, C., Brown, B. S., McNeish, J. D., Cohen, A. E., and Kralj, J. M. (2016). Cardiotoxicity screening with simultaneous optogenetic pacing, voltage imaging and calcium imaging. *Journal of pharmacological and toxicological methods*, 81:240–250. Publisher: Elsevier.

[Di Lullo and Kriegstein, 2017] Di Lullo, E. and Kriegstein, A. R. (2017). The use of brain organoids to investigate neural development and disease. *Nature Reviews Neuroscience*, 18(10):573–584.

[Diederich et al., 2020] Diederich, B., Lachmann, R., Carlstedt, S., Marsikova, B., Wang, H., Uwurukundo, X., Mosig, A. S., and Heintzmann, R. (2020). A versatile and customizable low-cost 3D-printed open standard for microscopic imaging. *Nature Communications*, 11(1):5979. Number: 1 Publisher: Nature Publishing Group.

[Dinc et al., 2021] Dinc, F., De, A., Goins, A., Halic, T., Massey, M., and Yarberry, F. (2021). Archem: Augmented reality based chemistry lab simulation for teaching and assessment. In *2021 19th International Conference on Information Technology Based Higher Education and Training (ITHET)*, pages 1–7. IEEE.

[Doulgkeroglou et al., 2020] Doulgkeroglou, M.-N., Di Nubila, A., Niessing, B., König, N., Schmitt, R. H., Damen, J., Szilvassy, S. J., Chang, W., Csontos, L., Louis, S., Kugelmeier, P., Ronfard, V., Bayon, Y., and Zeugolis, D. I. (2020). Automation, Monitoring, and Standardization of Cell Product Manufacturing. *Frontiers in Bioengineering and Biotechnology*, 8.

[Dörr et al., 2016] Dörr, M., Fibinger, M. P., Last, D., Schmidt, S., Santos-Aberturas, J., Böttcher, D., Hummel, A., Vickers, C., Voss, M., and Bornscheuer, U. T. (2016). Fully automatized high-throughput enzyme library screening using a robotic platform. *Biotechnology and Bioengineering*, 113(7):1421–1432. _eprint: https://onlinelibrary.wiley.com/doi/pdf/10.1002/bit.25925.

[Early et al., 2018] Early, J. J., Cole, K. L., Williamson, J. M., Swire, M., Kamadurai, H., Muskavitch, M., and Lyons, D. A. (2018). An automated high-resolution in vivo screen in zebrafish to identify chemical regulators of myelination. *Elife*, 7:e35136. Publisher: eLife Sciences Publications Limited.

[Emery et al., 2021] Emery, N. C., Crispo, E., Supp, S. R., Farrell, K. J., Kerkhoff, A. J., Bledsoe, E. K., O'Donnell, K. L., McCall, A. C., and Aiello-Lammens, M. E. (2021). Data Science in Undergraduate Life Science Education: A Need for Instructor Skills Training. *BioScience*, 71(12):1274–1287. Publisher: Oxford University Press.

[Exner and Willsey, 2021] Exner, C. R. T. and Willsey, H. R. (2021). Xenopus leads the way: Frogs as a pioneering model to understand the human brain. *genesis*, 59(1-2):e23405. _eprint: https://onlinelibrary.wiley.com/doi/pdf/10.1002/dvg.23405.

[Ezzyat et al., 2017] Ezzyat, Y., Kragel, J. E., Burke, J. F., Levy, D. F., Lyalenko, A., Wanda, P., O'Sullivan, L., Hurley, K. B., Busygin, S., Pedisich, I., Sperling, M. R., Worrell, G. A., Kucewicz, M. T., Davis, K. A., Lucas, T. H., Inman, C. S., Lega, B. C., Jobst, B. C., Sheth, S. A., Zaghloul, K., Jutras, M. J., Stein, J. M., Das, S. R., Gorniak, R., Rizzuto, D. S., and Kahana, M. J. (2017). Direct Brain Stimulation Modulates Encoding States and Memory Performance in Humans. *Current Biology*, 27(9):1251–1258.

[Fan et al., 2014] Fan, J., Han, F., and Liu, H. (2014). Challenges of big data analysis. *National science review*, 1(2):293–314. Publisher: Oxford University Press.

[Fenno et al., 2011] Fenno, L., Yizhar, O., and Deisseroth, K. (2011). The Development and Application of Optogenetics. *Annual Review of Neuroscience*, 34(1):389–412. _eprint: https://doi.org/10.1146/annurev-neuro-061010-113817.

[Ferreira et al., 2019] Ferreira, L. M., Carosso, G. A., Duran, N. M., Bohorquez-Massud, S. V., Vaca-Diez, G., Rivera-Betancourt, L. I., Rodriguez, Y., Ordonez, D. G., Alatriste-Gonzalez, D. K., Vacaflores, A., and others (2019). Effective participatory science education in a diverse Latin American population. *Palgrave Communications*, 5(1):1–18. Publisher: Palgrave.

[Figeys and Pinto, 2000] Figeys, D. and Pinto, D. (2000). Lab-on-a-Chip: A Revolution in Biological and Medical Sciences. *Analytical Chemistry*, 72(9):330 A–335 A.

[Filippi et al., 2022] Filippi, M., Yasa, O., Kamm, R. D., Raman, R., and Katzschmann, R. K. (2022). Will microfluidics enable functionally integrated biohybrid robots? *Proceedings of the National Academy of Sciences*, 119(35):e2200741119. Publisher: Proceedings of the National Academy of Sciences.

[Fleischer et al., 2018] Fleischer, H., Baumann, D., Joshi, S., Chu, X., Roddelkopf, T., Klos, M., and Thurow, K. (2018). Analytical Measurements and Efficient Process Generation Using a Dual–Arm Robot Equipped with Electronic Pipettes. *Energies*, 11(10):2567. Number: 10 Publisher: Multidisciplinary Digital Publishing Institute.

[Flores, 2013] Flores, N. M. (2013). *Engaging Learners Through Inquiry-Based Instruction to Promote Evidence-Based Writing in Advanced Placement Biology*. PhD Thesis.

[Forster et al., 2004] Forster, B., Van De Ville, D., Berent, J., Sage, D., and Unser, M. (2004). Extended Depth-of-Focus for Multi-Channel Microscopy Images: A Complex Wavelet Approach. In *Proceedings of the Second IEEE International Symposium on Biomedical Imaging: From Nano to Macro (ISBI'04)*, pages 660–663, Arlington VA, USA.

[Foundation and Contributors, 2022] Foundation, o. and Contributors (2022). NodeRED. *Online]. http://nodered. org. Accessed September*, 22:2022.

[Freire, 2019] Freire, F. D. (2019). *Work-based Learning Through the Multidisciplinary Design of edX MOOCS for Latin America and the Caribbean*. PhD Thesis, Teachers College, Columbia University.

[Freishtat, 2014] Freishtat, R. (2014). An evaluation of course evaluations. *ScienceOpen Research*.

[Frigault et al., 2009] Frigault, M. M., Lacoste, J., Swift, J. L., and Brown, C. M. (2009). Live-cell microscopy - tips and tools. *Journal of Cell Science*, 122(6):753–767.

[Godin et al., 2014] Godin, A. G., Lounis, B., and Cognet, L. (2014). Super-resolution microscopy approaches for live cell imaging. *Biophysical journal*, 107(8):1777–1784. Publisher: Elsevier.

[González-González et al., 2020] González-González, E., Trujillo-de Santiago, G., Lara-Mayorga, I. M., Martinez-Chapa, S. O., and Alvarez, M. M. (2020). Portable and accurate diagnostics for COVID-19: Combined use of the miniPCR thermocycler and a well-plate reader for SARS-CoV-2 virus detection. *PloS one*, 15(8):e0237418. Publisher: Public Library of Science San Francisco, CA USA.

[Grieves, 2015] Grieves, M. (2015). Digital Twin: Manufacturing Excellence through Virtual Factory Replication.

[Gross et al., 2014] Gross, B. C., Erkal, J. L., Lockwood, S. Y., Chen, C., and Spence, D. M. (2014). Evaluation of 3D printing and its potential impact on biotechnology and the chemical sciences. *ACS Publications*.

[Gustavsson et al., 2007] Gustavsson, I., Zackrisson, J., Håkansson, L., Claesson, I., and Lagö, T. L. (2007). The VISIR project – an Open Source Software Initiative for Distributed Online Laboratories.

[Gürkan and Gürkan, 2019] Gürkan, G. and Gürkan, K. (2019). Incu-stream 1.0: an open-hardware live-cell imaging system based on inverted bright-field microscopy and automated mechanical scanning for real-time and long-term imaging of microplates in incubator. *IEEE Access*, 7:58764–58779. Publisher: IEEE.

[Hanzlick-Burton et al., 2020] Hanzlick-Burton, C., Ciric, J., Diaz-Rios, M., Colgan III, W., and Gage, G. J. (2020). Developing and Implementing Low-Cost Remote Laboratories for Undergraduate Biology and Neuroscience Courses. *Journal of Undergraduate Neuroscience Education*, 19(1):A118. Publisher: Faculty for Undergraduate Neuroscience.

[Hart, 2013] Hart, C. (2013). Product Focus: Screening Robotics and Automation. *Journal of Biomolecular Screening*, 18(3):361–363. Publisher: SAGE Publications Sage CA: Los Angeles, CA.

[Health, 2021] Health, C. f. D. a. R. (2021). Repetitive Transcranial Magnetic Stimulation (rTMS) Systems - Class II Special Controls Guidance for Industry and FDA Staff. *FDA*. Publisher: FDA.

[Hernández Vera et al., 2016] Hernández Vera, R., Schwan, E., Fatsis-Kavalopoulos, N., and Kreuger, J. (2016). A modular and affordable time-lapse imaging and incubation system based on 3D-printed parts, a smartphone, and off-the-shelf electronics. *PLoS One*, 11(12):e0167583. Publisher: Public Library of Science San Francisco, CA USA.

[Hochberg et al., 2012] Hochberg, L. R., Bacher, D., Jarosiewicz, B., Masse, N. Y., Simeral, J. D., Vogel, J., Haddadin, S., Liu, J., Cash, S. S., van der Smagt, P.,

and Donoghue, J. P. (2012). Reach and grasp by people with tetraplegia using a neurally controlled robotic arm. *Nature*, 485(7398):372–375. Number: 7398 Publisher: Nature Publishing Group.

[Hochberg et al., 2006] Hochberg, L. R., Serruya, M. D., Friehs, G. M., Mukand, J. A., Saleh, M., Caplan, A. H., Branner, A., Chen, D., Penn, R. D., and Donoghue, J. P. (2006). Neuronal ensemble control of prosthetic devices by a human with tetraplegia. *Nature*, 442(7099):164–171. Number: 7099 Publisher: Nature Publishing Group.

[Honarnejad et al., 2013] Honarnejad, K., Kirsch, A. K., Daschner, A., Szybinska, A., Kuznicki, J., and Herms, J. (2013). FRET-based calcium imaging: a tool for high-throughput/content phenotypic drug screening in Alzheimer disease. *Journal of biomolecular screening*, 18(10):1309–1320. Publisher: SAGE Publications Sage CA: Los Angeles, CA.

[Hossain et al., 2016] Hossain, Z., Bumbacher, E. W., Chung, A. M., Kim, H., Litton, C., Walter, A. D., Pradhan, S. N., Jona, K., Blikstein, P., and Riedel-Kruse, I. H. (2016). Interactive and scalable biology cloud experimentation for scientific inquiry and education. *Nature biotechnology*, 34(12):1293–1298. Publisher: Nature Publishing Group.

[Hrabowski III, 2011] Hrabowski III, F. A. (2011). Boosting minorities in science.

[Jacobson, 1989] Jacobson, M. (1989). Botanical pesticides: past, present, and future. ACS Publications.

[Jain et al., 2021] Jain, U., Gauthier, A., and van der Meer, D. (2021). Total-internal-reflection deflectometry for measuring small deflections of a fluid surface. *Experiments in Fluids*, 62(11):235.

[Jeschke and Nauen, 2008] Jeschke, P. and Nauen, R. (2008). Neonicotinoids—from zero to hero in insecticide chemistry. *Pest Management Science: formerly Pesticide Science*, 64(11):1084–1098. Publisher: Wiley Online Library.

[John Hendel et al., 2006] John Hendel, E. T., Lu, Z., and Chapman, R. (2006). Biodegradation of caffeine in agricultural soil. *Canadian Journal of Soil Science*, 86(3):533–544.

[Jones et al., 2003] Jones, M. G., Andre, T., Superfine, R., and Taylor, R. (2003). Learning at the nanoscale: The impact of students' use of remote microscopy on concepts of viruses, scale, and microscopy. *Journal of Research in Science Teaching: The Official Journal of the National Association for Research in Science Teaching*, 40(3):303–322. Publisher: Wiley Online Library.

[Jones et al., 2016] Jones, R. S. G., da Silva, A. B., Whittaker, R. G., Woodhall, G. L., and Cunningham, M. O. (2016). Human brain slices for epilepsy research: Pitfalls, solutions and future challenges. *Journal of Neuroscience Methods*, 260:221–232.

[Khan et al., 2021] Khan, I., Prabhakar, A., Delepine, C., Tsang, H., Pham, V., and Sur, M. (2021). A low-cost 3D printed microfluidic bioreactor and imaging chamber for live-organoid imaging. *Biomicrofluidics*, 15(2):024105. Publisher: AIP Publishing LLC.

[Kim et al., 2016a] Kim, H., Gerber, L. C., Chiu, D., Lee, S. A., Cira, N. J., Xia, S. Y., and Riedel-Kruse, I. H. (2016a). LudusScope: accessible interactive smartphone microscopy for life-science education. *PloS one*, 11(10):e0162602. Publisher: Public Library of Science San Francisco, CA USA.

[Kim et al., 2016b] Kim, J., Henley, B. M., Kim, C. H., Lester, H. A., and Yang, C. (2016b). Incubator embedded cell culture imaging system (EmSight) based on Fourier ptychographic microscopy. *Biomedical optics express*, 7(8):3097–3110. Publisher: Optical Society of America.

[Kim et al., 2020] Kim, J., Koo, B.-K., and Knoblich, J. A. (2020). Human organoids: model systems for human biology and medicine. *Nature Reviews Molecular Cell Biology*, 21(10):571–584. Publisher: Nature Publishing Group.

[Kim et al., 2012] Kim, S. B., Koo, K.-i., Bae, H., Dokmeci, M. R., Hamilton, G. A., Bahinski, A., Kim, S. M., Ingber, D. E., and Khademhosseini, A. (2012). A mini-microscope for in situ monitoring of cells. *Lab on a Chip*, 12(20):3976–3982. Publisher: Royal Society of Chemistry.

[Klimaj et al., 2020] Klimaj, S. D., Licon Munoz, Y., Del Toro, K., and Hines, W. C. (2020). A high-throughput imaging and quantification pipeline for the EVOS imaging platform. *Plos one*, 15(8):e0236397. Publisher: Public Library of Science San Francisco, CA USA.

[Kour and Arora, 2020] Kour, V. P. and Arora, S. (2020). Recent developments of the internet of things in agriculture: a survey. *Ieee Access*, 8:129924–129957.

[Kumar et al., 2014] Kumar, D., Singanamala, H., Achuthan, K., Srivastava, S., Nair, B., and Diwakar, S. (2014). Implementing a remote-triggered light microscope: Enabling lab access via value virtual labs. In *Proceedings of the 2014 International Conference on Interdisciplinary Advances in Applied Computing*, pages 1–6.

[Kurtzer et al., 2017] Kurtzer, G. M., Sochat, V., and Bauer, M. W. (2017). Singularity: Scientific containers for mobility of compute. *PLOS ONE*, 12(5):e0177459. Publisher: Public Library of Science.

[Kuscu and Unluturk, 2021] Kuscu, M. and Unluturk, B. D. (2021). Internet of Bio-Nano Things: A Review of Applications, Enabling Technologies and Key Challenges. arXiv:2112.09249 [cs].

[Kwon et al., 2016] Kwon, H.-S., Park, H.-C., Lee, K., An, S., Oh, Y.-L., Ahn, E.-R., Jung, J. Y., and Lim, S.-K. (2016). Performance of MiniPCR TM mini8, a portable thermal cycler. *Analytical Science and Technology*, 29(2):79–84. Publisher: The Korean Society of Analytical Science.

[Lasi et al., 2014] Lasi, H., Fettke, P., Kemper, H.-G., Feld, T., and Hoffmann, M. (2014). Industry 4.0. *Business & Information Systems Engineering*, 6(4):239–242.

[Lemieux et al., 2011] Lemieux, G. A., Liu, J., Mayer, N., Bainton, R. J., Ashrafi, K., and Werb, Z. (2011). A whole-organism screen identifies new regulators of fat storage. *Nature chemical biology*, 7(4):206–213. Publisher: Nature Publishing Group.

[Lima et al., 2019] Lima, D. B. C., da Silva Lima, R. M. B., de Farias Medeiros, D., Pereira, R. I. S., de Souza, C. P., and Baiocchi, O. (2019). A Performance Evaluation of Raspberry Pi Zero W Based Gateway Running MQTT Broker for IoT. In *2019 IEEE 10th Annual Information Technology, Electronics and Mobile Communication Conference (IEMCON)*, pages 0076–0081. IEEE.

[Lincoln and Gabridge, 1998] Lincoln, C. K. and Gabridge, M. G. (1998). Chapter 4 Cell Culture Contamination: Sources, Consequences, Prevention, and Elimination. In Mather, J. P. and Barnes, D., editors, *Methods in Cell Biology*, volume 57 of *Animal Cell Culture Methods*, pages 49–65. Academic Press.

[Lippi and Da Rin, 2019] Lippi, G. and Da Rin, G. (2019). Advantages and limitations of total laboratory automation: a personal overview. *Clinical Chemistry and Laboratory Medicine (CCLM)*, 57(6):802–811.

[Litt, 1989] Litt, G. J. (1989). Visualization device.

[López-Vargas et al., 2021] López-Vargas, A., Ledezma, A., Bott, J., and Sanchis, A. (2021). Iot for global development to achieve the united nations sustainable development goals: The new scenario after the covid-19 pandemic. *Ieee Access*, 9:124711–124726.

[Ly et al., 2021] Ly, V. T., Baudin, P. V., Pansodtee, P., Jung, E. A., Voitiuk, K., Rosen, Y. M., Willsey, H. R., Mantalas, G. L., Seiler, S. T., Selberg, J. A., and others (2021). Picroscope: low-cost system for simultaneous longitudinal biological imaging. *Communications biology*, 4(1):1–11. Publisher: Nature Publishing Group.

[Mahoney et al., 2019] Mahoney, C. R., Giles, G. E., Marriott, B. P., Judelson, D. A., Glickman, E. L., Geiselman, P. J., and Lieberman, H. R. (2019). Intake of caffeine from all sources and reasons for use by college students. *Clinical nutrition*, 38(2):668–675.

[Maia Chagas et al., 2017] Maia Chagas, A., Prieto-Godino, L. L., Arrenberg, A. B., and Baden, T. (2017). The €100 lab: A 3D-printable open-source platform for fluorescence microscopy, optogenetics, and accurate temperature control during behaviour of zebrafish, Drosophila, and Caenorhabditis elegans. *PLOS Biology*, 15(7):e2002702.

[Martin et al., 2014] Martin, H. L., Adams, M., Higgins, J., Bond, J., Morrison, E. E., Bell, S. M., Warriner, S., Nelson, A., and Tomlinson, D. C. (2014). High-content, high-throughput screening for the identification of cytotoxic compounds based on cell morphology and cell proliferation markers. *PloS one*, 9(2):e88338. Publisher: Public Library of Science.

[Marzullo and Gage, 2012] Marzullo, T. C. and Gage, G. J. (2012). The spikerbox: a low cost, open-source bioamplifier for increasing public participation in neuroscience inquiry. *PloS one*, 7(3):e30837.

[May, 2019] May, M. (2019). A DIY approach to automating your lab. *Nature*, 569(7757):587–588. Bandiera_abtest: a Cg_type: Technology Feature Number: 7757 Publisher: Nature Publishing Group Subject_term: Biotechnology, Microscopy.

[Maynard et al., 1997] Maynard, E. M., Nordhausen, C. T., and Normann, R. A. (1997). The Utah Intracortical Electrode Array: A recording structure for potential brain-computer interfaces. *Electroencephalography and Clinical Neurophysiology*, 102(3):228–239.

[McDermott et al., 2022] McDermott, S., Ayazi, F., Collins, J., Knapper, J., Stirling, J., Bowman, R., and Cicuta, P. (2022). Multi-modal microscopy imaging with the OpenFlexure Delta Stage. *Optics Express*, 30(15):26377–26395. Publisher: Optica Publishing Group.

[McDonnell et al., 2022] McDonnell, L., Moore, A., Micou, M., Day, C., Grossman, E., and Meaders, C. (2022). Crispr in your kitchen: an at-home crispr kit to edit genes in saccharomyces cerevisiae used during a remote lab course. *Journal of microbiology & biology education*, 23(1):e00321–21.

[Mendoza-Gallegos et al., 2018] Mendoza-Gallegos, R. A., Rios, A., and Garcia-Cordero, J. L. (2018). An affordable and portable thermocycler for real-time PCR made of 3D-printed parts and off-the-shelf electronics. *Analytical chemistry*, 90(9):5563–5568. Publisher: ACS Publications.

[Meng et al., 2020] Meng, Q., Harrington, K., Stirling, J., and Bowman, R. (2020). The OpenFlexure Block Stage: sub-100 nm fibre alignment with a monolithic plastic flexure stage. *Optics Express*, 28(4):4763–4772. Publisher: Optica Publishing Group.

[Merces et al., 2021] Merces, G. O., Kennedy, C., Lenoci, B., Reynaud, E. G., Burke, N., and Pickering, M. (2021). The incubot: A 3D printer-based microscope for long-term live cell imaging within a tissue culture incubator. *HardwareX*, 9:e00189. Publisher: Elsevier.

[Merkel, 2014] Merkel, D. (2014). Docker: Lightweight Linux Containers for Consistent Development and Deployment. *Linux J.*, 2014(239). Place: Houston, TX Publisher: Belltown Media.

[Meyer, 2012] Meyer, M. (2012). Build your own lab: Do-it-yourself biology and the rise of citizen biotech-economies. *Journal of Peer Production*, 2(online):4–p.

[Miles and Lee, 2018] Miles, B. and Lee, P. L. (2018). Achieving Reproducibility and Closed-Loop Automation in Biological Experimentation with an IoT-Enabled Lab of the Future. *SLAS TECHNOLOGY: Translating Life Sciences Innovation*, 23(5):432–439.

[Miller et al., 2010] Miller, A. R., Davis, G. L., Oden, Z. M., Razavi, M. R., Fateh, A., Ghazanfari, M., Abdolrahimi, F., Poorazar, S., Sakhaie, F., Olsen, R. J., and others (2010). Portable, battery-operated, low-cost, bright field and fluorescence microscope. *PloS one*, 5(8):e11890. Publisher: Public Library of Science.

[Mostajo-Radji, 2021] Mostajo-Radji, M. A. (2021). Pseudoscience in the times of crisis: how and why chlorine dioxide consumption became popular in latin america during the covid-19 pandemic. *Frontiers in Political Science*, page 25.

[Mostajo-Radji et al., 2020] Mostajo-Radji, M. A., Schmitz, M. T., Montoya, S. T., and Pollen, A. A. (2020). Reverse engineering human brain evolution using organoid models. *Brain research*, 1729:146582. Publisher: Elsevier.

[Muguruma and Sasai, 2012] Muguruma, K. and Sasai, Y. (2012). In vitro recapitulation of neural development using embryonic stem cells: From neurogenesis to histogenesis. *Development, Growth & Differentiation*, 54(3):349–357. _eprint: https://onlinelibrary.wiley.com/doi/pdf/10.1111/j.1440-169X.2012.01329.x.

[Muhammad et al., 2018] Muhammad, K., Hamza, R., Ahmad, J., Lloret, J., Wang, H., and Baik, S. W. (2018). Secure surveillance framework for IoT systems using probabilistic image encryption. *IEEE Transactions on Industrial Informatics*, 14(8):3679–3689. Publisher: IEEE.

[Myers et al., 2020] Myers, K. R., Tham, W. Y., Yin, Y., Cohodes, N., Thursby, J. G., Thursby, M. C., Schiffer, P., Walsh, J. T., Lakhani, K. R., and Wang, D. (2020). Unequal effects of the COVID-19 pandemic on scientists. *Nature human behaviour*, 4(9):880–883. Publisher: Nature Publishing Group.

[Ollion et al., 2013] Ollion, J., Cochennec, J., Loll, F., Escudé, C., and Boudier, T. (2013). TANGO: a generic tool for high-throughput 3D image analysis for studying nuclear organization. *Bioinformatics*, 29(14):1840–1841. Publisher: Oxford University Press.

[Ornes, 2016] Ornes, S. (2016). Core Concept: The Internet of Things and the explosion of interconnectivity. *Proceedings of the National Academy of Sciences*, 113(40):11059–11060.

[Pagán, 2017] Pagán, O. R. (2017). Planaria: an animal model that integrates development, regeneration and pharmacology. *International Journal of Developmental Biology*, 61(8-9):519–529. Number: 8-9 Publisher: UPV/EHU Press.

[Park et al., 2020] Park, J., Kwon, O.-h., Yoon, C., and Park, M. (2020). Estimates of particulate matter inhalation doses during three-dimensional printing: How many particles can penetrate into our body? *Indoor air*. Publisher: Wiley Online Library.

[Parks et al., 2022] Parks, D. F., Voitiuk, K., Geng, J., Elliott, M. A. T., Keefe, M. G., Jung, E. A., Robbins, A., Baudin, P. V., Ly, V. T., Hawthorne, N., Yong, D., Sanso, S. E., Rezaee, N., Sevetson, J. L., Seiler, S. T., Currie, R., Pollen, A. A., Hengen, K. B., Nowakowski, T. J., Mostajo-Radji, M. A., Salama, S. R., Teodorescu, M., and Haussler, D. (2022). IoT cloud laboratory: Internet of Things architecture for cellular biology. *Internet of Things*, 20:100618.

[Patel and Devaki, 2019] Patel, A. and Devaki, P. (2019). Survey on NodeMCU and Raspberry pi: IoT. *International Research Journal of Engineering and Technology (IRJET)*, 6(4):5101–5105.

[Pearce, 2012] Pearce, J. M. (2012). Building research equipment with free, open-source hardware. *Science*, 337(6100):1303–1304. Publisher: American Association for the Advancement of Science.

[Perera et al., 2019] Perera, C., Rana, O., Goossens, B., and Orozco-ter Wengel, P. (2019). Internet of things for efficient wildlife conservation: challenges and opportunities.

[Pisarcik, 2021] Pisarcik, K. (2021). Crispr in a box™ and the journey toward inspiring new scientists. *Delaware Journal of Public Health*, 7(5):42.

[Plageras et al., 2016] Plageras, A. P., Psannis, K. E., Ishibashi, Y., and Kim, B.-G. (2016). IoT-based surveillance system for ubiquitous healthcare. In *IECON 2016-42nd Annual Conference of the IEEE Industrial Electronics Society*, pages 6226–6230. IEEE.

[Qian et al., 2009] Qian, L., Luo, Z., Du, Y., and Guo, L. (2009). Cloud Computing: An Overview. In Jaatun, M. G., Zhao, G., and Rong, C., editors, *Cloud Computing*, Lecture Notes in Computer Science, pages 626–631, Berlin, Heidelberg. Springer.

[Renner et al., 2020] Renner, H., Grabos, M., Becker, K. J., Kagermeier, T. E., Wu, J., Otto, M., Peischard, S., Zeuschner, D., TsyTsyura, Y., Disse, P., and others (2020). A fully automated high-throughput workflow for 3D-based chemical screening in human midbrain organoids. *Elife*, 9:e52904. Publisher: eLife Sciences Publications Limited.

[Richard et al.,] Richard, B., Julian, S., and The Openflexure Community. The OpenFlexure Microscope Imaging Optics.

[Rinkwitz et al., 2011] Rinkwitz, S., Mourrain, P., and Becker, T. S. (2011). Zebrafish: An integrative system for neurogenomics and neurosciences. *Progress in Neurobiology*, 93(2):231–243.

[Rios and Clevers, 2018] Rios, A. C. and Clevers, H. (2018). Imaging organoids: a bright future ahead. *Nature Methods*, 15(1):24–26.

[Ruckdäschel et al., 2017] Ruckdäschel, S., Michaelis, S., and Wegener, J. (2017). Time Lapse Imaging of Spheroids–zenCELLowl Incubator Microscope. *OMNI Life Science*.

[Rybnicky et al., 2022] Rybnicky, G. A., Dixon, R. A., Kuhn, R. M., Karim, A. S., and Jewett, M. C. (2022). Development of a freeze-dried crispr-cas12 sensor for detecting wolbachia in the secondary science classroom. *ACS synthetic biology*, 11(2):835–842.

[Saffran et al., 2016] Saffran, J., Garcia, G., Souza, M. A., Penna, P. H., Castro, M., Góes, L. F., and Freitas, H. C. (2016). A low-cost energy-efficient Raspberry Pi cluster for data mining algorithms. In *European Conference on Parallel Processing*, pages 788–799. Springer.

[Sandrone et al., 2021] Sandrone, S., Scott, G., Anderson, W. J., and Musunuru, K. (2021). Active learning-based STEM education for in-person and online learning. *Cell*, 184(6):1409–1414. Publisher: Elsevier.

[Santamaria et al., 2019] Santamaria, A. F., Raimondo, P., Tropea, M., De Rango, F., and Aiello, C. (2019). An IoT surveillance system based on a decentralised architecture. *Sensors*, 19(6):1469. Publisher: Multidisciplinary Digital Publishing Institute.

[Sarrafha et al., 2021] Sarrafha, L., Parfitt, G. M., Reyes, R., Goldman, C., Coccia, E., Kareva, T., and Ahfeldt, T. (2021). High-throughput generation of midbrain dopaminergic neuron organoids from reporter human pluripotent stem cells. *STAR protocols*, 2(2):100463. Publisher: Elsevier.

[Savas et al., 2018] Savas, J., Khayatzadeh, R., Civitci, F., Gokdel, Y. D., and Ferhanoglu, O. (2018). Toward fully three-dimensional-printed miniaturized confocal imager. *Optical Engineering*, 57(4):041402. Publisher: International Society for Optics and Photonics.

[Savell et al., 2019] Savell, K. E., Bach, S. V., Zipperly, M. E., Revanna, J. S., Goska, N. A., Tuscher, J. J., Duke, C. G., Sultan, F. A., Burke, J. N., Williams, D., Ianov, L., and Day, J. J. (2019). A Neuron-Optimized CRISPR/dCas9 Activation System for Robust and Specific Gene Regulation. *eNeuro*, 6(1):ENEURO.0495–18.2019.

[Sayre and Riegelman, 2018] Sayre, F. and Riegelman, A. (2018). The reproducibility crisis and academic libraries. *College & Research Libraries*, 79(1):2.

[Scheckler, 2003] Scheckler, R. K. (2003). Virtual labs: a substitute for traditional labs? *International journal of developmental biology*, 47(2-3):231–236. Publisher: UPV/EHU Press.

[Schindelin et al., 2012] Schindelin, J., Arganda-Carreras, I., Frise, E., Kaynig, V., Longair, M., Pietzsch, T., Preibisch, S., Rueden, C., Saalfeld, S., Schmid, B., and others (2012). Fiji: an open-source platform for biological-image analysis. *Nature methods*, 9(7):676–682. Publisher: Nature Publishing Group.

[Schmidt et al., 2008] Schmidt, B. T., Feduska, J. M., Witt, A. M., and Deasy, B. M. (2008). Robotic cell culture system for stem cell assays. *Industrial Robot: An International Journal*, 35(2):116–124.

[Schreiber et al., 2008] Schreiber, K., Ckurshumova, W., Peek, J., and Desveaux, D. (2008). A high-throughput chemical screen for resistance to Pseudomonas syringae in Arabidopsis. *The Plant Journal*, 54(3):522–531. Publisher: Wiley Online Library.

[Schuepbach et al., 2013] Schuepbach, W., Rau, J., Knudsen, K., Volkmann, J., Krack, P., Timmermann, L., Hälbig, T., Hesekamp, H., Navarro, S., Meier, N., Falk, D., Mehdorn, M., Paschen, S., Maarouf, M., Barbe, M., Fink, G.,

Kupsch, A., Gruber, D., Schneider, G.-H., Seigneuret, E., Kistner, A., Chaynes, P., Ory-Magne, F., Brefel Courbon, C., Vesper, J., Schnitzler, A., Wojtecki, L., Houeto, J.-L., Bataille, B., Maltête, D., Damier, P., Raoul, S., Sixel-Doering, F., Hellwig, D., Gharabaghi, A., Krüger, R., Pinsker, M., Amtage, F., Régis, J.-M., Witjas, T., Thobois, S., Mertens, P., Kloss, M., Hartmann, A., Oertel, W., Post, B., Speelman, H., Agid, Y., Schade-Brittinger, C., and Deuschl, G. (2013). Neurostimulation for Parkinson's Disease with Early Motor Complications. *New England Journal of Medicine*, 368(7):610–622. Publisher: Massachusetts Medical Society _eprint: https://doi.org/10.1056/NEJMoa1205158.

[Schultz et al., 2020] Schultz, M., Callahan, D. L., and Miltiadous, A. (2020). Development and use of kitchen chemistry home practical activities during unanticipated campus closures. *Journal of Chemical Education*, 97(9):2678–2684.

[Schulz et al., 2016] Schulz, W., Durant, T., Siddon, A., and Torres, R. (2016). Use of application containers and workflows for genomic data analysis. *Journal of Pathology Informatics*, 7(1):53.

[Schuster et al., 2020] Schuster, B., Junkin, M., Kashaf, S. S., Romero-Calvo, I., Kirby, K., Matthews, J., Weber, C. R., Rzhetsky, A., White, K. P., and Tay, S. (2020). Automated microfluidic platform for dynamic and combinatorial drug screening of tumor organoids. *Nature communications*, 11(1):1–12. Publisher: Nature Publishing Group.

[Seiler et al., 2022] Seiler, S. T., Mantalas, G. L., Selberg, J., Cordero, S., Torres-Montoya, S., Baudin, P. V., Ly, V. T., Amend, F., Tran, L., Hoffman, R. N., Rolandi, M., Green, R. E., Haussler, D., Salama, S. R., and Teodorescu, M. (2022). Modular automated microfluidic cell culture platform reduces glycolytic stress in cerebral cortex organoids. *Scientific Reports*, 12(1):20173. Number: 1 Publisher: Nature Publishing Group.

[Selinummi et al., 2009] Selinummi, J., Ruusuvuori, P., Podolsky, I., Ozinsky, A., Gold, E., Yli-Harja, O., Aderem, A., and Shmulevich, I. (2009). Bright field microscopy as an alternative to whole cell fluorescence in automated analysis of macrophage images. *PloS one*, 4(10):e7497. Publisher: Public Library of Science.

[Serpa et al., 2018] Serpa, S., Ferreira, C. M., Santos, A. I., and Teixeira, R. (2018). Participatory action research in higher education training. *Int'l J. Soc. Sci. Stud.*, 6:1.

[Shiri et al., 2019] Shiri, Z., Simorgh, S., Naderi, S., and Baharvand, H. (2019). Optogenetics in the Era of Cerebral Organoids. *Trends in Biotechnology*, 37(12):1282–1294.

[silvanmelchior, 2023] silvanmelchior (2023). silvanmelchior/RPi_cam_web_interface. original-date: 2014-03-12T21:51:34Z.

[Simeral et al., 2011] Simeral, J. D., Kim, S.-P., Black, M. J., Donoghue, J. P., and Hochberg, L. R. (2011). Neural control of cursor trajectory and click by a human with tetraplegia 1000 days after implant of an intracortical microelectrode array. *Journal of Neural Engineering*, 8(2):025027.

[Singh et al., 2019] Singh, Y., Raghuwanshi, S. K., and Kumar, S. (2019). Review on Liquid-level Measurement and Level Transmitter Using Conventional and Optical Techniques. *IETE Technical Review*, 36(4):329–340. Publisher: Taylor & Francis _eprint: https://doi.org/10.1080/02564602.2018.1471364.

[Sliepen, 2010] Sliepen, G. (2010). The difficulties of a peer-to-peer VPN on the hostile Internet.

[Smarr et al., 2018] Smarr, L., Crittenden, C., DeFanti, T., Graham, J., Mishin, D., Moore, R., Papadopoulos, P., and Würthwein, F. (2018). The pacific research platform: Making high-speed networking a reality for the scientist. In *Proceedings of the Practice and Experience on Advanced Research Computing*, pages 1–8.

[Specht et al., 2017] Specht, E. A., Braselmann, E., and Palmer, A. E. (2017). A critical and comparative review of fluorescent tools for live-cell imaging. *Annual review of physiology*, 79:93–117. Publisher: Annual Reviews.

[Steffens et al., 2017] Steffens, S., Nüßer, L., Seiler, T.-B., Ruchter, N., Schumann, M., Döring, R., Cofalla, C., Ostfeld, A., Salomons, E., Schüttrumpf, H., Hollert, H., and Brinkmann, M. (2017). A versatile and low-cost open source pipetting robot for automation of toxicological and ecotoxicological bioassays. *PLOS ONE*, 12(6):e0179636. Publisher: Public Library of Science.

[Stirling et al., 2021] Stirling, D. R., Swain-Bowden, M. J., Lucas, A. M., Carpenter, A. E., Cimini, B. A., and Goodman, A. (2021). CellProfiler 4: improvements in speed, utility and usability. *BMC Bioinformatics*, 22(1):433.

[Süel, 2011] Süel, G. (2011). Chapter thirteen - Use of Fluorescence Microscopy to Analyze Genetic Circuit Dynamics. In Voigt, C., editor, *Synthetic Biology, Part A*, volume 497 of *Methods in Enzymology*, pages 275–293. Academic Press. ISSN: 0076-6879.

[Tang and Ho, 2019] Tang, T. and Ho, A. T.-K. (2019). A path-dependence perspective on the adoption of internet of things: Evidence from early adopters of smart and connected sensors in the united states. *Government Information Quarterly*, 36(2):321–332.

[Thomson et al., 2022] Thomson, E., Harfouche, M., Kim, K., Konda, P., Seitz, C. W., Cooke, C., Xu, S., Jacobs, W. S., Blazing, R., Chen, Y., Sharma, S., Dunn, T. W., Park, J., Horstmeyer, R. W., and Naumann, E. A. (2022). Gigapixel imaging with a novel multi-camera array microscope. *eLife*, 11:e74988. Publisher: eLife Sciences Publications, Ltd.

[Thorn, 2016] Thorn, K. (2016). A quick guide to light microscopy in cell biology. *Molecular Biology of the Cell*, 27(2):219–222.

[Torrico et al., 2021] Torrico, P. L., Revilla, A. M., and Domínguez, M. M. (2021). Educación y tic. acceso y uso del internet en ixiamas-bolivia. *Luciérnaga Comunicación*, 13(25):99–115.

[Trujillo et al., 2019] Trujillo, C. A., Gao, R., Negraes, P. D., Gu, J., Buchanan, J., Preissl, S., Wang, A., Wu, W., Haddad, G. G., Chaim, I. A., Domissy, A., Vandenberghe, M., Devor, A., Yeo, G. W., Voytek, B., and Muotri, A. R. (2019). Complex Oscillatory Waves Emerging from Cortical Organoids Model Early Human Brain Network Development. *Cell Stem Cell*, 25(4):558–569.e7.

[Tsuji et al., 2014] Tsuji, N., Ninov, N., Delawary, M., Osman, S., Roh, A. S., Gut, P., and Stainier, D. Y. (2014). Whole organism high content screening identifies stimulators of pancreatic beta-cell proliferation. *PloS one*, 9(8):e104112. Publisher: Public Library of Science.

[Tsybulsky and Sinai, 2022] Tsybulsky, D. and Sinai, E. (2022). Iot in project-based biology learning: Students' experiences and skill development. *Journal of Science Education and Technology*, pages 1–12.

[Ventola, 2014] Ventola, C. L. (2014). Medical applications for 3D printing: current and projected uses. *Pharmacy and Therapeutics*, 39(10):704. Publisher: MediMedia, USA.

[Waldrop et al., 2015] Waldrop, M. M. et al. (2015). Why we are teaching science wrong, and how to make it right. *Nature*, 523(7560):272–274.

[Wallace et al., 2008] Wallace, C., Conway, C., Ray, A. M., and Robinson, S. J. (2008). Remote-Access Scanning Electron Microscopy for K-12 Students: The Bugscope Project Nine Years On. *Microscopy and Microanalysis*, 14(S2):858–859.

[Wang et al., 2022] Wang, K., Khoo, K. S., Leong, H. Y., Nagarajan, D., Chew, K. W., Ting, H. Y., Selvarajoo, A., Chang, J.-S., and Show, P. L. (2022). How does the Internet of Things (IoT) help in microalgae biorefinery? *Biotechnology Advances*, 54:107819.

[Wang et al., 2017] Wang, Z., Boddeda, A., Parker, B., Samanipour, R., Ghosh, S., Menard, F., and Kim, K. (2017). A high-resolution minimicroscope system for wireless real-time monitoring. *IEEE Transactions on Biomedical Engineering*, 65(7):1524–1531. Publisher: IEEE.

[Warschauer et al., 2011] Warschauer, M., Cotten, S. R., and Ames, M. G. (2011). One laptop per child Birmingham: Case study of a radical experiment. *International Journal of Learning and Media*, 3(2). Publisher: MIT Press.

[Watada et al., 2019] Watada, J., Roy, A., Kadikar, R., Pham, H., and Xu, B. (2019). Emerging Trends, Techniques and Open Issues of Containerization: A Review. *IEEE Access*, 7:152443–152472. Conference Name: IEEE Access.

[Whitesides, 2006] Whitesides, G. M. (2006). The origins and the future of microfluidics. *Nature*, 442(7101):368–373. Number: 7101 Publisher: Nature Publishing Group.

[Willis, 2018] Willis, S. (2018). The maker revolution. *Computer*, 51(3):62–65. Publisher: IEEE.

[Wincott et al., 2021] Wincott, M., Jefferson, A., Dobbie, I. M., Booth, M. J., Davis, I., and Parton, R. M. (2021). Democratising "Microscopi": a 3D printed automated XYZT fluorescence imaging system for teaching, outreach and fieldwork. *Wellcome Open Research*, 6. Publisher: The Wellcome Trust.

[Yao et al., 2020] Yao, S., Mills, J. K., Ajamieh, I. A., Li, H., and Zhang, X. (2020). Automatic three-dimensional imaging for blastomere identification in early-stage embryos based on brightfield microscopy. *Optics and Lasers in Engineering*, 130:106093. Publisher: Elsevier.

[Zamani et al., 2020] Zamani, N. S., Mohammed, M., Al-Zubaidi, S., and Yusuf, E. (2020). Design and Development of Portable Digital Microscope platform using Iot Technology. In *2020 16th IEEE International Colloquium on Signal Processing & Its Applications (CSPA)*, pages 80–83. IEEE.

[Zamxaka et al., 2004] Zamxaka, M., Pironcheva, G., and Muyima, N. (2004). Microbiological and physico-chemical assessment of the quality of domestic water sources in selected rural communities of the Eastern Cape Province, South Africa. *Water Sa*, 30(3):333–340.

[Zhang et al., 2013] Zhang, C., Anzalone, N. C., Faria, R. P., and Pearce, J. M. (2013). Open-source 3D-printable optics equipment. *PloS one*, 8(3):e59840. Publisher: Public Library of Science.

[Zhang et al., 2015] Zhang, Y. S., Ribas, J., Nadhman, A., Aleman, J., Selimovic, S., Lesher-Perez, S. C., Wang, T., Manoharan, V., Shin, S.-R., Damilano, A., and others (2015). A cost-effective fluorescence mini-microscope for biomedical applications. *Lab on a Chip*, 15(18):3661–3669. Publisher: Royal Society of Chemistry.

[Zhao et al., 2009] Zhao, H., Tang, C., Cui, K., Ang, B.-T., and Wong, S. T. (2009). A screening platform for glioma growth and invasion using bioluminescence imaging. *Journal of neurosurgery*, 111(2):238–246. Publisher: American Association of Neurological Surgeons.